Therapeutic targeting of Hairy and Enhancer of Split 1 (HES1) transcriptional programs in T-cell Acute Lymphoblastic Leukemia

Stephanie A. Schnell

Submitted in partial fulfillment of the
requirements for the degree of
Doctor of Philosophy
under the Executive Committee
of the Graduate School of Arts and Sciences

COLUMBIA UNIVERSITY
2015

ABSTRACT
Therapeutic targeting of Hairy and Enhancer of Split 1 (HES1) transcriptional programs in T-cell Acute Lymphoblastic Leukemia

Stephanie Schnell

T-cell acute lymphoblastic leukemia (T-ALL) is an aggressive hematological tumor resulting from the malignant transformation of immature T-cell progenitors. Originally associated with a dismal prognosis, the outcome of T-ALL patients has improved remarkably over the last two decades as a result of the introduction of intensified chemotherapy protocols. However, these treatments are associated with significant acute and long-term toxicities, and the treatment of patients presenting with primary resistant disease or those relapsing after a transient response remains challenging. Oncogenic activation of NOTCH1 signaling plays a central role in the pathogenesis of T-cell acute lymphoblastic leukemia (T-ALL), with mutations on this signaling pathway affecting more than 60% of patients at diagnosis. However the transcriptional regulatory circuitries driving T-cell transformation downstream of NOTCH1 remain incompletely understood. Here we identify HES1, a transcriptional repressor controlled by NOTCH1 as a critical mediator of NOTCH1 induced leukemogenesis strictly required for tumor cell survival. Mechanistically, we demonstrate that HES1 inhibits leukemia cell death by repressing *BBC3,* the gene encoding the PUMA BH3-only proapototic factor. Finally, we identify perhexiline, a small molecule inhibitor of mitochondrial carnitine palmitoyltransferase-1, as a HES1-signature antagonist drug with robust antileukemic activity against NOTCH1 induced leukemias *in vitro* and *in vivo*.

TABLE OF CONTENTS

LIST OF FIGURES

CHAPTER 1

CHAPTER 2

No Figures

CHAPTER 3

CHAPTER 4

CHAPTER 5

CHAPTER 6

LIST OF TABLES

ACKNOWLEDGMENTS

First and foremost, I would like to thank Dr. Adolfo Ferrando for his mentorship throughout the course of this thesis project. His guidance, as well as his enthusiasm and commitment to science, has been instrumental in my development as a scientist. I would like to thank my thesis committee, Dr. Jan Kitajewski, Dr. Ulf Klein, and Dr. Shan Zha for their constructive insights and discussions throughout the development and execution of this project. Also, thanks to Dr. Iannis Aifantis for participating as my outside reader for my thesis defense.

I would like to thank Kenta Yamamoto from the Zha lab for teaching and performing the southern blot analysis of the NOTCH1-induced T-ALL mouse tumors. Thank you to the Gu Lab, especially Omid Tavan for gifting the p53 plasmids used in the luciferase assays and the advice on the PUMA antibody used for western blot.

I have to thank the Ferrando lab, both current and past members, for your continual support in the development of different aspects of the project. Luyao Xu was critical for the mice experiments, thanks for your continual patience and assistance in the mouse breeding, procedures, and tissue collections. Thank you to Alberto Ambesi and Yue Qin for the bioinformatics analysis and the willingness to help when I came across more questions. Giusy Della Gatta, thank you for the guidance in the ChIP experiments, especially the moral support after having tested more than twenty antibodies. Thank you to Laura Belver in helping me with the cloning strategy of the *BBC3* promoter and in editing my thesis. Marta Sanchez was very helpful in the experimental set up of the perhexiline drug treatments, thank you. Thank you to Daniel and Arianne for our morning coffee sessions, they truly kept me going through the rougher periods. Also, thank you to Guisy, Ana, and Lucile for always bringing a smile to my face.

Thank you to the Columbia MD/PhD program for giving me this incredible opportunity to learn from the top scientists and for supporting my thesis project. A special thank you to Patrice Spitalnik for not only being a mentor but a friend these last six years. Jeffrey Brandt, thank you for making my life easier and filling it with musical theater.

Thank you to my parents for your dedication in helping me achieve my goals. To my sisters, Ingrid and Jenny where do I begin? Thank you for a lifetime of adventures, silliness, and laughter. Thank you for always attempting to follow my jargon filled explanations and supporting me every step of the way. Thank you to my second family, my friends, for creating a home for me in the city. This experience would have never been the same without you. And, thank you to Ewan for your endless love, encouragement, and friendship; I can't imagine going through these last years without you by my side.

DEDICATION

"Our greatest weakness lies in giving up. The most certain way to succeed is always to try just one more time."
Thomas A. Edison

This work is dedicated to my parents. You provided me with the love of learning, the example of hard work, the encouragement and confidence to take on any challenge, the endless support in both my successes and failures, and most importantly unconditional love. You are my rock.

Chapter 1: Introduction

"Down to their innate molecular core, cancer cells are hyperactive, survival-endowed, scrappy, fecund, inventive copies of ourselves."

Sidhartha Mukherjee, The Emperor of All Maladies

Opening Statement

The onset of chemotherapy for the treatment of cancer was a consequence from observing the toxic hematopoietic effects in naval troops who were accidentally exposed to mustard gas during WWII. This observation led to the subsequent testing of other gases and the discovery of nitrogen mustard as an antileukemic agent in lymphoma patients due to its DNA damaging properties. Thus, the field of chemotherapy grew from the understanding that cancer cells can be targeted by blocking the pathways involved in cell growth and replication (DeVita and Chu 2008). Now, 75 years later, scientists have a greater scope of the genetic and molecular mechanisms involved in the transformation of a normal cell into a malignant cell and a diverse selection of chemotherapeutics. However, the field still requires a deeper understanding of the mechanisms driving malignancy as not all patients respond to treatment and many face severe short and long-term consequences from toxic effects of chemotherapy.

The focus of this thesis is to elucidate the molecular pathways involved in the pathogenesis of T cell acute lymphoblastic leukemia (T-ALL), a hematological malignancy, and to apply that knowledge into the identification of new potential therapies for the treatment of this disease. Chapter 1 will describe the clinical presentation and the current standard of treatment for T cell acute lymphoblastic leukemia. This will be followed by an overview of normal T cell development and the established genetic and molecular mechanisms driving the transformation of T cell progenitors. Chapter 2-5 will describe the transcriptional and cellular effects of the

NOTCH1-HES1 pathway in the maintenance of T-ALL, the identification of a novel antileukemic drug, and the materials and methods used during experimentation.

I. T-cell Acute Lymphoblastic Leukemia

Acute lymphoblastic leukemia (ALL) is an aggressive hematological disorder characterized by the malignant transformation of either B-cell or T-cell lymphoid progenitors. ALL is the most frequently diagnosed childhood malignancy, with the highest incidence occurring between 2 to 5 years of age. T cell acute lymphoblastic leukemia (T-ALL) accounts for 10-15% of childhood ALL and 25% of adult ALLs and is characteristically more prevalent in males than females (Rubnitz, Camitta et al. 1999, Ferrando, Neuberg et al. 2002, Pui, Relling et al. 2004). T-ALL patients typically present with large tumor burdens at diagnosis including high peripheral white blood cell counts, diffuse infiltration of the bone marrow by T-cell lymphoblasts, mediastinal masses with pleural effusions, and frequent infiltration of the central nervous system (Pui, Relling et al. 2004). Prior to the 1950's diagnosis of ALL was universally fatal; however, the introduction of intensified chemotherapy has gradually improved the outcome of T-ALL patients so that over 75% of children and 40-50% of adults with this disease achieve long term and durable remissions (Pui, Robison et al. 2008).

Patients diagnosed with T-ALL currently undergo a two-phase treatment plan involving 2-3 years of chemotherapy. Although there is variation in the specific protocols used to treat patients with T-ALL, there are four components that form the backbone of T-ALL treatment: remission induction, central nervous system (CNS)-directed therapy, intensification (consolidation) therapy, and maintenance treatment (Pui and Evans 2013). The goal of the first phase of treatment, called remission-induction chemotherapy, is to eliminate 99.9% of leukemia cells found in the blood and bone marrow of the patients. This is accomplished over the course of a 4-week treatment with a corticosteroid (prednisone, prednisolone, or dexamethasone), vincristine, L-asparaginase, and sometimes anthracycline. Patients diagnosed with high risk

ALL receive four or more drugs during this phase of treatment (Pui and Evans 2006, Pui, Pei et al. 2010). The response to treatment is assessed via quantitation of minimal residual disease (MRD), remaining leukemia cells, detected by flow cytometry or polymerase-chain-reaction (PCR) (Pui 2001, Pui, Campana et al. 2001). MRD levels less than 0.01% upon completion of remission-induction treatment predict a favorable prognosis, however patients with 1% MRD have a high risk of relapse and are therefore treated with an extended period of remission-induction intensified chemotherapy (Attarbaschi, Mann et al. 2008, Van der Velden, Corral et al. 2009, Conter, Bartram et al. 2010).

After the induction treatment and complete remission resulting in the restoration of normal hematopoiesis, patients are started on post induction treatment. This second phase of treatment, which aims to kill any residual leukemia cells that may eventually proliferate and result in relapse, consists of three steps: consolidation, intensification, and maintenance therapy. Consolidation therapy consisting of high-dose methotrexate and daily mercaptopurine is essential for all patients, but there is much variation in the drug regimen and duration of treatment (Asselin, Devidas et al. 2011, Pui and Evans 2013). The most common intensification treatment involves treatment with aspariganse, vincristine, and dexamethasone with or without anthracycline, mercaptopurine, and methotrexate for the course of 6-10 months (Gaynon, Angiolillo et al. 2010, Silverman, Stevenson et al. 2010). Maintenance therapy consists of daily mercaptopurine and low-dose methotrexate for 2-3 years (Pui and Evans 2006, Moricke, Zimmermann et al. 2010). Variation in specific chemotherapies and length of treatment of this post-induction protocol is common, specifically among high-risk T-ALL patients and low-risk T-ALL patients. During induction and post-induction therapy, patients are also treated with central nervous system (CNS) directed therapy to eliminate residual cells in the CNS and decrease the risk of relapse (Richards, Pui et al. 2013). Lastly, allogeneic hematopoietic stem cell (HSC) transplantation is sometimes used for the treatment of patients who are at high risk for induction failure or disease relapse (Hunault, Harousseau et al. 2004, Thomas, Boiron et al. 2004). HSC

transplantation has the potential to cure patients; however patients have a significant risk for long-term physiological side effects including graft-vs-host disease (GVHD), non-malignant organ and tissue dysfunction, delayed or abnormal immune reconstitution, and secondary cancers (Mohty and Apperley 2010).

T-ALL patients who do not respond to induction chemotherapy treatment or those whose disease relapses have a poor prognosis (Goldberg, Silverman et al. 2003, Oudot, Auclerc et al. 2008). The dismal outcome for those patients highlights the need to focus research efforts in elucidating the molecular pathogenesis of T-ALL in order to search for molecular drug targets and tumor-specific therapies that may facilitate the development of more effective and less toxic anti-leukemic drugs (Aifantis, Raetz et al. 2008).

II. T Lymphocyte Development

T-cell acute lymphoblastic leukemia is a malignancy arising from early progenitors of T lymphocytes (also called T cells). T lymphocytes are cells of the immune system that play a significant role in the adaptive system, protecting against infection from viruses, bacteria, fungi, protozoa, and even cancer cells (Delves and Roitt 2000). Their function relies on their T-cell receptor (TCR) recognizing peptides derived from pathogens (antigens) presented on major histocompatibility complexes (MHC), which are found on the cell membrane of all nucleated cells (Delves and Roitt 2000, Parkin and Cohen 2001). The specific interaction of the TCR with the antigen-presenting MHC complex triggers a T-cell mediated immune response. There are two major types of T cells that elicit different responses in the immune system: T helper (Th) cells expressing the CD4 surface molecule, and T cytotoxic (Tc) cell expressing the CD8 surface molecule. TCR engagement to an MHC-presented antigen in Th cells (surface marker $CD4^+$ lymphocytes) triggers the production of cytokines, which activate surrounding cells such as macrophages, Tc cells, B cells, and eosinophils. On the other hand, Tc cells (surface marker $CD8^+$ lymphocytes) binding to antigen-MHC complex induces apoptosis, programmed cell

death, of infected cells (Swain, Bradley et al. 1991, Sallusto, Lenig et al. 1999, Delves and Roitt 2000, Parkin and Cohen 2001). There are two different types of MHC complexes, each with a specific function: (i) MHC class I present antigens produced within the cells, such as viruses and tumor antigens, and are recognized by TCRs on Tc lymphocytes; and (ii) MHC class II present antigens derived from extracellular pathogens including bacteria, fungi, and protozoa, and are recognized by Th cells (Parkin and Cohen 2001).

The key factor that determines the efficiency of the adaptive cellular immune response is the generation by the immune system of a large repertoire of T cells, with every T cell expressing a unique TCR that recognizes a specific antigen. The TCR repertoire can virtually recognize any antigen the organism may be exposed to during their lifetime and this diversity is achieved by extensive DNA recombination in a process called V(D)J recombination, which takes place during T cell development. The TCR is a heterodimer composed by two pairs of chains (TCR α/β chain heterodimer or TCR γ/δ chain heterodimer). The genes encoding the TCR β and δ chains are composed of three groups of gene segments: the variable (V), diversity (D), and joining (J). In turn, each of these groups contains multiple segments. In the case of the TCR α and γ chains, only V and J segments are present. T cell progenitors undergo somatic recombination of this locus to randomly combine one gene segment of each type (V, D, and J) creating a distinct TCR genetic sequence, which is translated into a unique TCR to recognize antigens. The different possible combinations of these gene segments allows for the generation of an incredibly variable TCR repertoire with the potential to recognize and eliminate any pathogen. V(D)J recombination is the most important event occurring during T cell differentiation and only cells that achieve the expression of a functional non-autoreactive TCR will proceed to complete their maturation and eventual differentiation to Th and Tc cells (Schatz, Oettinger et al. 1992, Agrawal and Schatz 1997, Arstila, Casrouge et al. 1999, Delves and Roitt 2000).

Hematopoiesis

Before discussing the abnormal developmental process that leads to T-ALL, it is important to understand the normal stepwise maturation process of T cells from haematopoietic stem cells (HSC) in the bone marrow to mature T cells in the thymus. All hematopoietic cells originate in the bone marrow from a rare population of hematopoietic stem cells (HSC), which have self-renewing capacity and the ability to differentiate into all blood cell lineages (Orkin and Zon 2008). This population of cells is called LSK because the cells present with the following phenotype: Lineage (Lin)$^-$, stem cell antigen 1 (SCA1)$^+$, and tyrosine kinase receptor C-KIT high (KIT)^{high} (Morrison and Weissman 1994, Sitnicka 2009). The LSK cells are further subdivided into long-term (LT)-HSCs, which have the potential to self-new and give rise to all cells for the life-span of an individual, and short-term (ST)-HSCs which have a limited self-renewal capacity (Kiel, Yilmaz et al. 2005). Low expression of fms-like tyrosine kinase reporter-3 (FLT3) in LSK cells gives rise to multipotential progenitors (MPPs), which lose their self-renewal capacity but

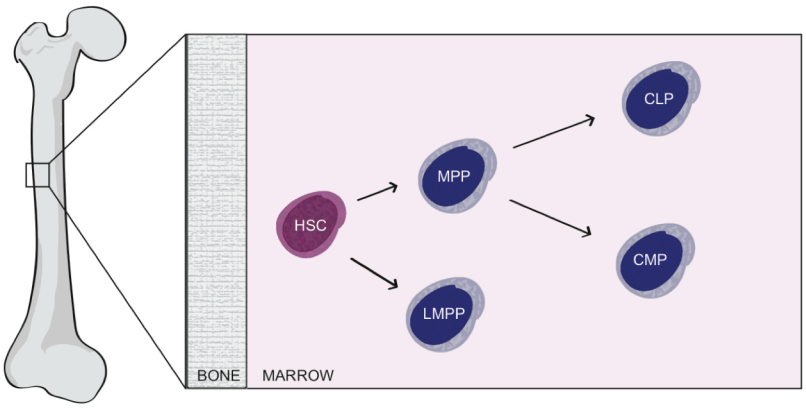

Figure 1.1. T-cell progenitors in the bone marrow. All blood cells are derived from hematopoietic stem cells (HSC) in the bone marrow. HSCs give rise to multipotent progenitors (MPP) and lymphocyte-primed multipotent progenitors (LMPP). MPPs give rise to common lymphoid progenitors (CLP) and common myeloid progenitors (CMP). Given the right microenvironment, HSC, LMPP, MPP, and CLP cells can commit to the T cell lineage.

maintain the capability to differentiate into all hematopoietic lineages (Adolfsson, Borge et al. 2001, Christensen and Weissman 2001). MPPs then bifurcate into common lymphoid and common myeloid progenitors (CLPs and CMPs) (Kondo, Weissman et al. 1997, Akashi, Traver et al. 2000). CLPs express low levels of KIT and high levels of interleukin-7 receptor α-chain (IL-7Rα) and FLT3, and have the potential to differentiate into T cells, B cells, natural killer cells, and dendritic cells (Inlay, Bhattacharya et al. 2009). CMPs, which will not be further described here, give rise to erythrocytes, megakaryocytes, monocytes, and granulocytes (Akashi, Traver et al. 2000). Additionally, there is a separate subset of cells with potential towards lymphoid, granulocyte, and macrophage development called lymphoid-primed MPPs (LMPP) that are characterized by high expression of FLT3 (**Figure 1.1**) (Adolfsson, Borge et al. 2001, Lai and Kondo 2007, Mansson, Hultquist et al. 2007, Ng, Yoshida et al. 2009).

Thymopoiesis

Thymopoiesis is the developmental process in the thymus involving the maturation of T cell progenitors (thymocytes) into mature T cells. The thymus, an organ found in the mediastinum and just above the heart, provides the microenvironment that is critical and essential for the development of T-cell lymphopoeisis (Petrie 2002). The thymus architecture is comprised of four distinct regions, each providing a specific microenvironment to assist particular stages of T cell development (Koch and Radtke 2011). The four regions include the corticomedullary junction (CMJ), the cortex, subcapsular zone, and the medulla (**Figure 1.2**). The corticomedullary junction is characterized by an abundance of blood vessels and a network of endothelial cells that facilitate the movement of cells into and out of the thymus. The cortex is composed of cortical thymic epithelial cells (cTECs), fibroblasts, macrophages and an extensive population of early T cell progenitors, whereas the subcapsular zone contains mainly cTECs and T cell precursors. Lastly, the medulla contains dentritic cells (DC), medullary thymic epithelial cells (mTECs), Hassall corpuscles, and mature T cell lymphocytes (Pearse 2006).

Although there is much ambiguity in identifying the earliest thymic seeding progenitors (TSPs), a small number of early lymphoid progenitor cells travel from the bone marrow through the blood stream and enter the thymus through blood vessels into the CMJ (Kadish and Basch 1976, Spangrude and Scollay 1990, Lind, Prockop et al. 2001, Bhandoola, von Boehmer et al. 2007). Once TSP cells enter the thymus and encounter the cTECs, they differentiate into early thymic progenitors (ETPs) characterized by $Lin^{low}CD44^{high}CD25^{-}KIT^{high}$, and undergo T-lineage specification (Bhandoola, von Boehmer et al. 2007, Yang, Jeremiah Bell et al. 2010). Early T cell progenitors undergo an extensive process of differentiation and proliferation in the thymus. However, only a few percent of cells (2-4%) survive the maturation process and are released into circulation. The majority (98%) of developing T-cells ultimately undergo apoptosis in the thymus due to the rigorous selection process required for the generation of a functional T cell receptor (TCR) repertoire and self-tolerance (Surh and Sprent 1994).

The progression of ETPs into mature T cells can be broken down into a stepwise process defined by the expression of cell-surface markers CD4 and CD8. ETPs start as $CD4^{-}$ $CD8^{-}$ double negative (DN), then progress into CD4+CD8+ double positive (DP), and finally differentiate into maturing single-positive CD4+ or CD8+ T cells (Anderson and Jenkinson 2001). The DN population of cells is further subdivided by the expression of cell-surface markers CD44 and CD25 (**Table 1.2**) (Godfrey, Kennedy et al. 1993).

The most immature thymocyte precursors are classified as DN1 ($CD44^{+}CD25^{-}KIT^{+}$) population of cells. DN1 are a heterogeneous group of cells, including the ETP subset, that maintain the potential to differentiate into αβ T cells, γδ Tcells, natural killer (NK) cells, DC, and macrophages (Shah and Zuniga-Pflucker 2014). DN1 cells proliferate extensively for approximately 10 days in the CMJ and then migrate into the cortex where they interact with cTEC, receiving stimulatory signals, interleukin-7 (IL-7) and NOTCH signaling activation, and

Table 1.1. Stages of T cell development

Developmental stage	Cell Surface phenotype	Thymus location	Notch signal	TCRB rearrangement	TCRa rearrangement
ETP/DN1	$CD44^+CD25^-CD4^-CD8^-$	CMJ	+++	Germline	Germline
DN2	$CD44^+CD25^+CD4^-CD8^-$	Cortex	+	Germline	Germline
DN3	$CD44^-CD25^+CD4^-CD8^-$	SCZ	+	DJ	Germline
DN4	$CD44^-CD25^-CD4^-CD8^-$	SCZ	+++	VDJ	Germline
DP	$CD4^+CD8^+$	Cortex	-	VDJ	Germline
SP	$CD4^+CD8^-$ or $CD4^-CD8^+$	Medulla	-	VDJ	VJ

Abbreviations: ETP (early thymic progenitor), DN (double negative), DP (double positive), SP (single positive), CMJ (corticomedullary junction), SCZ (subcapsular zone), TCR (T cell receptor), V (variable), D (diversity), J (joining). The three +++ represent the stages during T cell development requiring NOTCH1 signaling. The single + represent when NOTCH1 receptor is excpressed. Adapted from Koch et al 2011.

subsequently differentiate into DN2 thymocytes ($CD44^+CD25^+$) (Peschon, Morrissey et al. 1994, von Freeden-Jeffry, Vieira et al. 1995, Porritt, Gordon et al. 2003, Hozumi, Negishi et al. 2008, Koch, Fiorini et al. 2008). DN2 cells migrate through the cortex towards the subcapsular zone. During this process, DN2 cells initiate upregulation of T cell identity genes including *Cd3* and *Il7ra* and begin rearrangement of the D to J segments of the *TCRγ, TCRδ,* and *TCRβ* gene locus (Koch and Radtke 2011). T cell lineage commitment occurs when DN2 cells differentiate into DN3 ($CD44^-CD25^+$) cells within the subcapsular zone. DN3 cells extensively rearrange *TCRγ, TCRδ,* and *TCRβ* gene. The cells that successfully rearrange *TCRγ* and *TCRδ* progress to generate a minor population of γδ T cells, which will not be further discussed (Lauritsen, Wong et al. 2009). In contrast, cells with *TCRβ* gene rearrangement are committed to the main αβ T cell fate (Burtrum, Kim et al. 1996). Only the DN3 cells that have successful in-frame rearrangement of *TCRβ* survive this stage of differentiation. Once DN3 cells proceed through β-selection, which requires a functional pre-TCR complex consisting of a TCRβ chain, components of the CD3 chains, and a surrogate pre-TCRα chain (pTα), they mature into DN4 ($CD44^-CD25^-$) (von Boehmer 2005). DN4 cells migrate to the cortex and begin pre-TCR signaling, cell proliferation, and expression of CD4, differentiating them into immature single

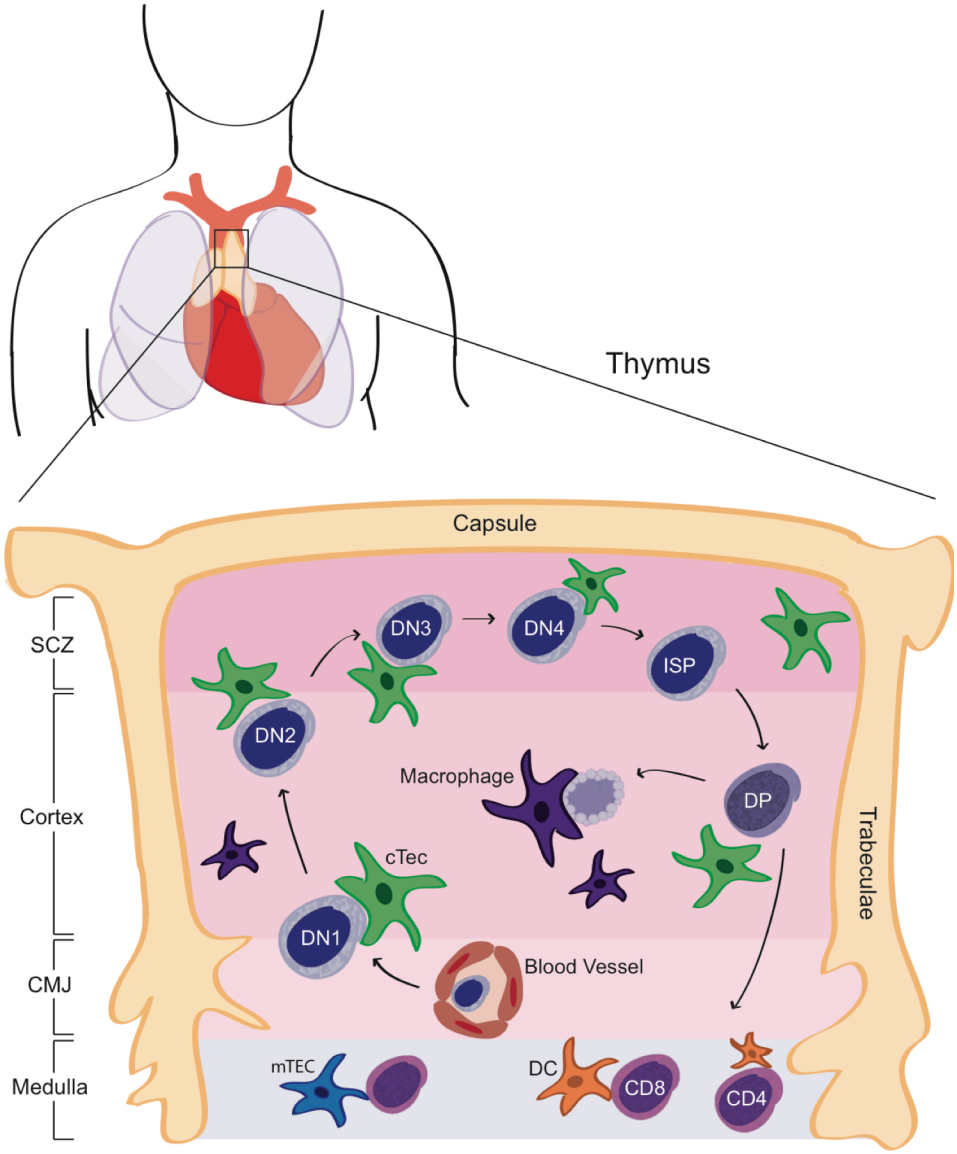

Figure 1.2. T cell development. Thymic seeding progenitors leave the bone marrow and arrive into the cotico-medullary junction (CMJ) through blood vessels. Cells interact with cortical thymic epithelial cells (cTECs) and differentiate into double negative (DN1) cells. DN1 cells migrate towards the cortex and continue to interact with cTECs to differentiate into DN2 cells. T cell lineage commitment occurs when DN2 cells differentiate into DN3 cells in the subcapsular zone (SCZ). DN3 cells rearrange *TCR*β locus and once they proceed through β-selection they differentiate into DN4 cells. DN4 cells migrate towards the cortex, begin pre-TCR signaling, and upregulate CD4 to differentiate into immature single positive (ISP). CD8 is then upregulated differentiating cells into double positive (DP) cells. DP cells rearrange *TCR*α, express αβ TCR, interact with dendritic cells (DC) and cTECs to undergo positive and negative selection. DP cells that fail to successfully undergo positive and negative selection undergo apoptosis and are engulfed by macrophages, while those that express a functional TCR complex and passed both stages of selection migrate to the medulla and differentiate into single positive CD8 or CD4 cells.

positive cells (ISP) which subsequently upregulate CD8, thus maturing them into DP (CD4+CD8+) cells (Porritt, Gordon et al. 2003). DP cells represent the majority (75-88%) of the thymus cell population (Huesmann, Scott et al. 1991, Ceredig and Rolink 2002). DP cells rearrange *TCRα* locus, thereby producing an assembled αβ TCR. The few DP cells expressing an αβ TCR capable of recognizing self-MHC presented by cTECs undergo positive selection, while the majority of cells unable to recognize self-MHC undergo apoptosis (Klein, Hinterberger et al. 2009). Positively selected cells then undergo negative selection, a process eliminating cells with high specificity towards self-peptides, in order to decrease the potential for autoreactive T cells. DP cells that have survived positive and negative selection then express high levels of TCR and commit to either CD4 SP ($CD4^+CD8^-$) or CD8 SP ($CD4^-CD8^+$) T lymphocytes and migrate to the medulla (**Figure 1.2**) (Klein, Hinterberger et al. 2009). Thus, early T cell progenitors undergo an extensive process of differentiation and proliferation in the thymus, whereby only a few percent of cells (2-4%) survive the maturation process and are released into circulation. The majority (98%) of developing T-cells ultimately undergo apoptosis in the thymus due to the rigorous selection process required for the generation of a functional T cell receptor (TCR) repertoire and self-tolerance (Surh and Sprent 1994).

III. Genetic Mechanisms Driving T-cell Transformation

T-cell transformation is a multistep process in which multiple genetic alterations cooperate to enhance self-renewal capacity, block differentiation, promote proliferation, and intensify survival signals to escape cell death. These genetic alterations are a consequence of chromosomal translocations and mutations resulting in loss of tumor suppressors and the overexpression and activation of transcription factor oncogenes in early T cell progenitors (**Table 1.2**). These transcription factors typically play key roles in embryonic development and are aberrantly expressed in malignant T-cell lymphoblasts due to chromosomal translocations, which juxtapose them to the promoters of the T- cell receptor genes. In this context, *NOTCH1* is

the most prominent T-ALL specific oncogene, to the extent that most T-ALLs can be primarily defined as tumors driven by constitutive activation of NOTCH signaling (Weng, Ferrando et al. 2004). However, the loss of the tumor suppressor genes *p16/INK4A* and *p14/ARF* in chromosome band 9p21 (*CDKN2A* locus), present in more than 70% of all T-ALL cases, is the most prevalent genetic abnormality in this disease (Hebert, Cayuela et al. 1994, Ferrando, Neuberg et al. 2002). Thus, constitutive activation of *NOTCH* signaling and loss of *p16/INK4A* and *p14/ARF* constitute the core of the oncogenic program responsible for transformation of T-cell progenitors.

T-ALLs are characterized by the translocation and aberrant expression of transcription factor oncogenes. These chromosomal alterations arise from errors in the recombination process responsible for the rearrangement of TCR genes during normal T-cell development, and typically place T-ALL transcription factor oncogenes under the control of T-cell specific enhancers in the vicinity of the *TCRB* (7q34) or *TCRA-TCRD* (14q11) loci. These translocations are present in approximately ~33% of T-ALL cases and cause deregulation of basic helix-loop-helix (bHLH) family members such as *TAL1* (Begley, Aplan et al. 1989, Bernard, Guglielmi et al. 1990, Chen, Cheng et al. 1990), *TAL2* (Xia, Brown et al. 1991), *LYL1* (Mellentin, Smith et al. 1989), *BHLHB1 (*Wang, Jani-Sait et al. 2000*)*; LIM-only domain (LMO) factors such as *LMO1*, *LMO2,* and *LMO3* (McGuire, Hockett et al. 1989, Boehm, Foroni et al. 1991, Royer-Pokora, Loos et al. 1991); *TLX1/HOX11* (Dube, Kamel-Reid et al. 1991, Hatano, Roberts et al. 1991, Kennedy, Gonzalez-Sarmiento et al. 1991), *TLX3/HOX11L2* (Bernard, Busson-LeConiat et al. 2001, Ferrando, Neuberg et al. 2002), *NKX2.5* (Nagel, Kaufmann et al. 2003) and *HOXA* homeobox genes (Soulier, Clappier et al.); *MYC* (Erikson, Finger et al. 1986, Shima, Le Beau et al. 1986); *MYB* (Clappier, Cuccuini et al. 2007) and *TAN1*, a truncated and constitutively activated form of the NOTCH1 receptor (Ellisen, Bird et al. 1991). An exception is the *TLX3/HOX11L2* locus, which is aberrantly expressed due to translocations that place it under the control of T-cell regulatory sequences in the proximity of the *BCL11B* locus

Table 1.2. GENETIC MUTATIONS IN T-ALL

Category	Gene Target	Genetic Rearrangement	Frequency
NOTCH1 pathway	*NOTCH1*	Activating muation	>50%
	TAN1	t(7;9)(q34;p13)	<1%
	FBXW7	Inactivating mutation	8-30%
Cell cycle defects	*p16/INK4A; p14/ARF*	9p21 deletion methylation	70%
	RB1	13q14 deletion	4%
	CDKN1B	12p13deletion	2%
	CCND2	t(7;12)(q34;p13)	1%
		t(12;14)(p13;q11)	
Cell growth tumor suppressors	*RUNX1*	Inactivating mutation/deletion	10-20%
	LEF1	Inactivating mutation/deletion	10-15%
	ETV6	Inactivating mutation/deletion	13%
	WT1	Inactivating mutation/deletion	10%
	BCL11B	Inactivating mutation/deletion	10%
	GATA3	Inactivating mutation/deletion	5%
	MYC	t(8;14)(q24;q11)	1%
Signal transduction	*JAK1*	Activating mutation	4-18%
	PTEN	Inactivating mutation	10%
		10q23 deletion	
	IL7R	Activating mutation	10%
	NRAS	Activating mutation	5-10%
	JAK3	Activating mutation	5%
	NUP214-ABL1	Episomal 9q34 amplification	4%
	FLT3	Activating mutation	2-4%
	NF1	Inactivating mutation/deletion	3%
	EML1-ABL1	t(9;14)(q34;q32)	<1%
	ETV6-ABL1	t(9;14)(q34;q32)	<1%
	BCR-ABL1	t(9;22)(q34;q11)	<1%
	ETV6-JAK2	t(9;12)(p24;p13)	<1%
Chromatin remodeling	*EZH2*	Inactivating mutation/deletion	10-15%
	SUZ12	Inactivating mutation/deletion	10%
	EED	Inactivating mutation/deletion	10%
	PHF6	Inactivating mutation/deletion	20-40%
bHLH family members	*TAL1*	t(1;14)(p32;q11);	3-30%
		t(1;7)(p32;q34);	
		1p32 deletion	
	TAL2	t(7;9)(q34;q32)	1%
	LYL1	t(7;19)(q42;p13)	1%
	BHLHB1	t(14;21)(q11.2;q22)	1%
LMO family members	*LMO1*	t(11;14)(p15;q11)	1%
		t(7;11)(q34;p15)	
	LMO2	t(11;14)(p13;q11)	6%
		t(7;11)(q34;p13)	
	LMO3	t(7;12)9q34;p12)	<1%
Homeobox family members	*TLX1*	t(11;14)(p15;q11)	5-30%
	TLX3	t(11;14)(p15;q11)	5-20%
	HOXA	Inv(7)(p15q34)	3%
		t(7;7)(p15;q34)	
	CALM-AF10	t(10;11)(p13;q14)	5-10%
	MLL-ENL	t(11;19)(q23;p13)	1%
	SET-NUP214	9q34 deletion	3%
		inv(14)(q11.2q13)	
	NKX2.1	inv(14)(q13q32.22)	5%
		t(7;14)(q34;q13)	
	NKX2.2	t(14;20)(q11;p11)	1%
Proto-oncogene	*c-MYB*	t(6;7)(q23;q34)	3%

Adapted from Van Vlierberghe et al 2012

(Bernard, Busson-LeConiat et al. 2001). In addition, some T-ALLs activate these T-cell transcription factor oncogenes as a result of alternative genetic rearrangements. For example, small intrachromosomal deletions in chromosome 1p32 result in *TAL1* regulation by the *SIL* promoter (Aplan, Lombardi et al. 1990) and cryptic deletions in chromosome 11p13 can lead to aberrant expression of the *LMO2* oncogene (Van Vlierberghe, van Grotel et al. 2006).

The set of known genetic alterations associated with T-cell transformation is completed with a number of rare but recurrent cytogenetic and molecular alterations resulting in: (i) expression of fusion transcription factor oncogenes such as *PICALM/MLLT10/CALM-AF10* (Asnafi, Radford-Weiss et al. 2003), *MLL-MLLT1/MLL-ENL* (Chervinsky, Sait et al. 1995, Rubnitz, Behm et al. 1996), *SET-NUP214* (Van Vlierberghe, van Grotel et al. 2008) and *NUP98-RAP1GDS1* (Hussey, Nicola et al. 1999), (ii) activation of multiple genetic factors that drive proliferation, including *LCK* (Tycko, Smith et al. 1991), *CCND2* (Clappier, Cuccuini et al. 2006), *JAK1* (Flex, Petrangeli et al. 2008), *ETV6-JAK2* (Lacronique, Boureux et al. 1997), *ETV6-ABL1* (Van Limbergen, Beverloo et al. 2001), *ETV6-ARNT* (Otsubo, Kanegane et al.), *NUP214-ABL1* (Graux, Cools et al. 2004), *EML1-ABL1* (De Keersmaecker, Graux et al. 2005), *FLT3* (Paietta, Ferrando et al. 2004, Van Vlierberghe, Meijerink et al. 2005) and *NRAS* (Bar-Eli, Ahuja et al. 1989), and (iii) loss or inactivation of tumor suppressor genes such as *PTPN2* (Kleppe, Lahortiga et al.), *NF1* (Balgobind, Van Vlierberghe et al. 2008), *PTEN* (Palomero, Sulis et al. 2007), *WT1* (Tosello, Mansour et al. 2009), *LEF1* (Gutierrez, Sanda et al. 2010), *BCL11B* (De Keersmaecker, Real et al. 2010), *PHF6* (Van Vlierberghe, Palomero et al. 2010), and *RUNX1* (Della Gatta, Palomero et al. 2012)

IV. NOTCH1 Signaling Pathway in T-ALL

Aberrant NOTCH1 signaling was first implicated in the pathogenesis of T-ALL upon characterization of the t(7;9)(q34;q34.3) chromosomal translocation, present in 1% of T-ALL

cases (Paganin and Ferrando 2011). This translocation leads to the expression of TAN1, a truncated and constitutively active form of NOTCH1 (Ellisen, Bird et al. 1991). However, the role of NOTCH1 in T-ALL was not fully appraised until activating mutations in the *NOTCH1* gene were found in more than 50% of patients diagnosed with T-ALL (Weng, Ferrando et al. 2004).

NOTCH1 Signaling Pathway

The NOTCH1 receptor, a class I transmembrane protein, functions as a ligand-activated transcription factor that directly controls gene expression in response to extracellular signals (Aster, Pear et al. 2008). The NOTCH1 receptor can be broken down into the N-terminal extracellular domain and the C-terminal transmembrane and intracellular domain. The extracellular domain consists of 36 epidermal growth factor (EGF)-like repeats responsible for the interaction with the NOTCH1 activating ligands (Delta-like ligand 1,2, and 3 or Jagged 1 and 2). Following the EGF repeats are the three LIN-12/Notch Repeat (LNR) modules responsible for preventing activation of the receptor in the absence of ligand by folding over and stabilizing the heterodimerization domain (HD). The HD domain links the extracellular domain with the intracellular domain of NOTCH1 (ICN1), the domain responsible for the transcriptional activation of NOTCH1 target genes. ICN1 consists of a RAM domain, a series of ankarin repeats, a transactivator domain, nuclear localization signals and a C-terminus PEST domain (proline (P), glutamic acid (E), serine (S), threonine (T) rich) responsible for the proteasomal degradation of ICN1 (Aster, Pear et al. 2008).

Activation of NOTCH1 is triggered by binding to the Jagged and Delta-like family of ligands expressed on the surface of nearby cells. This ligand-receptor interaction causes a conformation change exposing the extracellular heterodimerization domain (HD) and allowing for proteolytic cleavage by an ADAM metalloprotease. Cleavage of the HD domain allows for the immediate subsequent cleavage by the γ-secretase complex in the transmembrane region

of the NOTCH1 receptor, resulting in the release of the intracellular domain of NOTCH1 receptor (ICN1) from the cell membrane into the cytosol (Radtke, Wilson et al. 2004). Following cleavage, ICN1 rapidly translocates into the nucleus where it associates with RBPJ/CSL DNA-binding protein and recruits members of the mastermind (MAML) family of coactivators and CBP/p300 to activate the expression of target genes such as *HES1*, *HEY1*, *MYC*, *PTCRA*, *DTX1,* and *CCR7* (**Figure 1.3**) (Grabher, von Boehmer et al. 2006, Palomero, Lim et al. 2006).

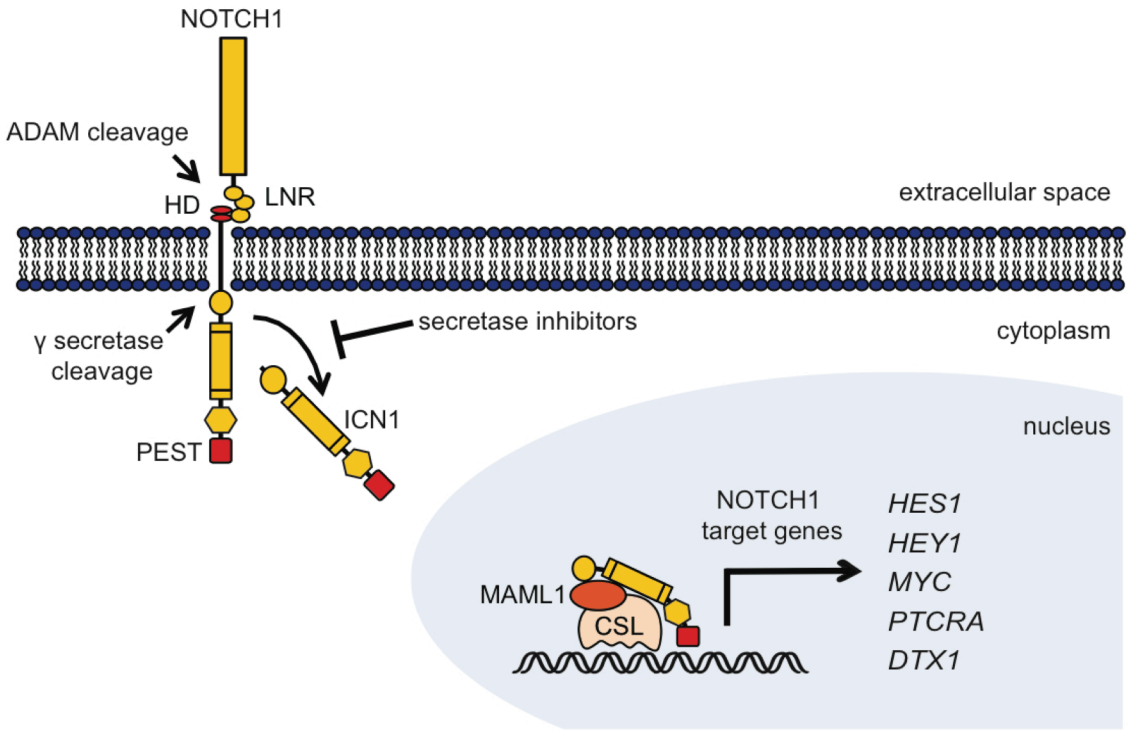

Figure 1.3. NOTCH1 signaling. Schematic representation of the NOTCH1 signaling pathway. Briefly, the NOTCH1 transmembrane receptor protein undergoes a series of two consecutive proteolytic cleavages upon ligand activation; the first cleavage by the ADAM family metalloproteases and the second by the γ-secretase complex releasing the intracellular portion of NOTCH1 (ICN1). ICN1 translocates into the nucleus, associates with the RBPJ/CSL protein, recruits MAML coactivators and active expression of target genes. Adapted from Ferrando 2009.

Finally, termination of NOTCH1 signaling occurs after recruitment of the RNA polymerase II holoenzyme to the ICN1-RBPJ/CSL/MAML transcriptional complex, which triggers phosphorylation of the C-terminal PEST domain of the receptor. Phosphorylation of the PEST domain recruits the FBXW7/SCF ubiquitin ligase to the transcriptional complex and triggers the polyubiquitination and proteasomal degradation of ICN1 (Aster, Pear et al. 2008).

NOTCH1 Signaling in T-cell Development

NOTCH signaling plays a critical role in establishing cell lineage commitment decisions in multi-potent precursor cells (Greenwald 1998). In the hematopoietic system, NOTCH1 signaling drives the initial commitment of progenitor lymphocytes to the T-cell lineage (Tanigaki and Honjo 2007) and subsequent intrathymic T-cell maturation (**Table 1.A**) (Schmitt, Ciofani et al. 2004). The exact progenitor cells and location of NOTCH1 signaling prior to thymus entry remain unknown; however, loss of NOTCH1 in bone marrow progenitors drives cells towards B-cell lineage commitment in the thymus (Wilson, MacDonald et al. 2001). Once ETPs enter the thymus, NOTCH1, activated by Delta-like ligand 4 (DL4), provides the signaling pathway for cells to inhibit commitment towards B-cell and myeloid lineages and favor T-cell development (Pui, Allman et al. 1999, Heinzel, Benz et al. 2007, Bell and Bhandoola 2008, Wada, Masuda et al. 2008, Feyerabend, Terszowski et al. 2009). In addition, DN cells require continuous NOTCH1 signaling to support cells into T-cell lineage commitment at the DN3 stage of development (Ciofani and Zuniga-Pflucker 2006, Ikawa, Kawamoto et al. 2006). NOTCH1 signaling in combination with weak pre-TCR signals is then required to drive DN3 cells towards αβ lineage (Ciofani, Schmitt et al. 2004, Lauritsen, Wong et al. 2009). Finally, NOTCH1 is critical during the β-selection checkpoint in order to sustain T-cell development and cellular metabolism. Cellular metabolism is sustained by the activation of the PI3K-AKT pathway downstream of NOTCH1 (Ciofani and Zuniga-Pflucker 2005). Specifically, NOTCH1 upregulates

important transcription factors involved in survival, proliferation, and differentiation, including pre-T cell receptor alpha (*PTCRA*), Interleukin 7 receptor alpha (*IL7RA*), and *MYC* (Reizis and Leder 2002, Ciofani and Zuniga-Pflucker 2006, Palomero, Lim et al. 2006, Gonzalez-Garcia, Garcia-Peydro et al. 2009).

NOTCH1 Signaling Pathway Mutations and Prognosis in T-ALL

NOTCH1 mutations typically involve specific domains responsible for controlling the initiation and termination of NOTCH signaling (**Figure 1.4**). HD domain (exon 26 and 27) mutations, found in 40% of human T-ALLs, destabilize the HD subunits resulting in ligand-independent activation or ligand hypersensitivity (Weng, Ferrando et al. 2004, Malecki, Sanchez-Irizarry et al. 2006, Sulis, Williams et al. 2008). Other rare mutations involving the distal part of the HD domain and the juxtamembrane region result in the displacement of the HD domain away from the membrane and constitutive cleavage by the ADAM metalloprotease (Sulis, Williams et al. 2008). The second category of mutations involves extending the NOTCH1 signal or half-life rather than inducing constitutive activation of the signaling pathway. For example, truncating and nonsense mutations in the C-terminal region of the protein delete the PEST domain in 15% of T-ALL patients, extending NOTCH1 signaling by impairing ICN1 degradation in the nucleus (Weng, Ferrando et al. 2004). Additionally, mutations in *FBXW7* are present in 15% of T-ALL cases, and similar to NOTCH1 PEST domain mutations, impair the proteasomal degradation of ICN1 (O'Neil, Grim et al. 2007, Thompson, Buonamici et al. 2007). Furthermore, because FBXW7 also mediates the degradation of MYC, JUN, mTOR, cyclin E, preseniline, NF1, c-Myb, Aurora A, and SREBP, increased levels of these genes may also participate in the transformation of T-ALL harboring *FBXW7* mutations (Li, Pauley et al. 2002, Nateri, Riera-Sans et al. 2004, Sundqvist, Bengoechea-Alonso et al. 2005, Finkin, Aylon et al. 2008, Welcker and Clurman 2008, Kitagawa, Hiramatsu et al. 2009, Tan, Zhao et al. 2011).

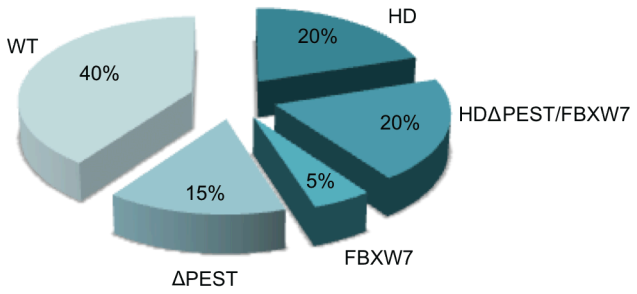

Figure 1.4. NOTCH1 mutations in T-ALL. The majority of NOTCH1 activating mutations involve the HD and PEST domain of the transmembrane receptor in patients diagnosed with T-ALL. In addition, *FBXW7* mutations, found in 15% of T-ALL cases, contribute to NOTCH1 activation by impairing the proteasomal degradation of ICN1. Adapted from Ferrando 2009.

Given the high frequency of aberrant NOTCH1 activation in T-ALL patients, various clinical studies analyzed the prognostic significance in T-ALL patients harboring mutations in *NOTCH1* and *FBXW7.* A retrospective trial of children with T-ALL treated on DCOG or COALL protocols identified the presence of NOTCH1 pathway mutations were associated with an improved early therapeutic response. However, this response did not translate into a change in overall outcome (Zuurbier, Homminga et al. 2010). The increased sensitivity to glucocorticoid treatment with no improved outcome in patients with T-ALL was independently recapitulated in a separate study of children with T-ALL treated on EORTC trials 58881 and 58951 (Clappier, Collette et al. 2010). In addition, mutations in *NOTCH1* in T-ALL patients treated according to the NOPHO protocols showed no differences in overall or event-free survival. However, increased NOTCH1 activity measured by *HES1* expression was associated with improved outcome in pediatric T-ALL (Fogelstrand, Staffas et al. 2014). In contrast to the DCOG/COALL and EORTC clinical reports, a third trial analyzing patients treated on ALL-BFM protocols

identified an association of activating NOTCH1 receptor mutations with improved prognosis. This study documented an improved outcome to treatment and a decrease in disease relapse in T-ALL patients with aberrant NOTCH1 activation (Kox, Zimmermann et al. 2010). Similarly, analysis of children diagnosed with T-ALL and treated under the BCH-2003 and CCLG-2008 protocols showed a better prognosis and overall outcome in patients harboring *NOTCH1* mutations (Gao, Liu et al. 2014). Taken together, these results demonstrate NOTCH1 mutations in T-ALL patients are more sensitive to the initial treatment with glucocorticoids. However, the presence of NOTCH1 mutations does not necessarily improve the prognosis of patients with T-ALL.

Downstream Effects of Aberrant NOTCH1 Activation in Metabolism

Much research has focused on identifying the downstream targets of NOTCH1 driving T cell transformation. Analysis of the NOTCH1 binding sites in target gene promoters by chromatin immunoprecipitation (ChIP) in T-ALL cells revealed enrichment of genes regulating cellular growth, proliferation, and metabolism. Specifically, NOTCH1 was shown to bind the promoter and activate transcription of the *MYC* oncogene (Palomero, Lim et al. 2006, Margolin, Palomero et al. 2009). Closer analysis of the NOTCH1 target genes regulating cellular proliferation, growth and metabolism revealed a significant intersection of those genes with MYC target genes (Palomero, Lim et al. 2006). Thus, suggesting a feed-forward loop in which NOTCH1 and MYC reinforce the expression of genes promoting cell growth and metabolism. In addition, NOTCH1 was recently identified to bind a long-range acting enhancer in the *MYC* promoter that is targeted for chromosomal duplications in 5% of patients, highlighting the importance of the NOTCH1-MYC axis in T-ALL (Herranz, Ambesi-Impiombato et al. 2014). A second pathway downstream of NOTCH1 involved in the activation of anabolic cellular metabolism is the PI3K-AKT-mTOR signaling pathway. The initial identification of NOTCH1 regulation in metabolism was established by Ciofani et. al. who described a key role for this

interaction in the regulation of cell size, glycolysis and glucose uptake (Ciofani and Zuniga-Pflucker 2005). Later, HES1, a major downstream target of NOTCH1, was shown to transcriptionally inhibit the expression of the known tumor suppressor and inhibitor of PI3K, *PTEN* (Palomero, Sulis et al. 2007). Also, NOTCH1 has been identified to target this signaling pathway at multiple levels through the activation of the *IGF1R, IL7RA,* and *PTCRA* promoters, all leading to AKT activation in T-cell development and in T-ALL (Reizis and Leder 2002, Sade, Krishna et al. 2004, Gonzalez-Garcia, Garcia-Peydro et al. 2009).

Effects of Aberrant NOTCH1 Activation in Cell Cycle Progression

Cell cycle progression is a highly regulated process involving three main checkpoints during the transitions into the different phases of the cell cycle: the G1/S, S phase, and G2/M checkpoints. The different checkpoints are regulated by specific cyclins and cyclin-dependent kinases (CDK) that can either halt cell cycle progression in the case of unfavorable environmental conditions, such as DNA damage and chromosomal abnormalities, or conversely, allow cells to transition into the next phase of the cell cycle (Kastan and Bartek 2004). NOTCH1 directly targets genes involved in the regulation of cell cycle progression and survival. NOTCH1 transcriptional activation of cyclin D3 *(CCND3),* cyclin-dependent kinase 4 (*CDK4),* and cyclin-dependent kinase 6 (*CDK6)* allows cells to progress through the checkpoints involved in the G1/S transition (Sicinska, Aifantis et al. 2003, Joshi, Minter et al. 2009). NOTCH1 also promotes the transcription of E3 ubiquitin ligase protein SKP2 that targets p27 (CDKN1B) and p21 (CDKN1A) for proteasomal degradation. Given the p27 and p21 are inhibitors of G1 and S phase cell cycle progression respectively, NOTCH1-induced transcription of *SKP2* thus allows malignant cells to progress through the cell cycle (Dohda, Maljukova et al. 2007). Finally, NOTCH1 promotes the survival of T cell lymphoblasts and T-ALL through the activation of the NF-κB signaling pathway. NOTCH1 directly upregulates the expression of NF-

κB factors *Relb* and *Nfkb2*, promotes IKK complex activation, and induces the nuclear localization of NF-κB in T-ALL (Shin, Minter et al. 2006, Thompson, Buonamici et al. 2007).

Therapeutic Targeting of NOTCH1

The high frequency of *NOTCH1* mutations in T-ALL has sparked interest in the development of anti-NOTCH1 targeted therapies for the treatment of T-ALL. Thus, γ-secretase inhibitors (GSI), which block the proteolytic cleavage of the NOTCH receptors and preclude the release of ICN1 from the membrane, have been proposed as potential targeted therapy in T-ALL. Early studies revealed that inhibition of NOTCH by GSI treatment results in G1 cell cycle arrest and decreased cell size in T-ALL cell lines harboring activating mutations in NOTCH1 (Weng, Ferrando et al. 2004, Lewis, Leveridge et al. 2007, Paganin and Ferrando 2011). However, systemic inhibition of Notch signaling with GSIs blocks the function of all four NOTCH family members (NOTCH1-4) and results in gastrointestinal toxicity resulting from accumulation of secretory goblet cells in the intestine (Milano, McKay et al. 2004, van Es, van Gijn et al. 2005). Notably, glucocorticoids may abrogate the gastrointestinal toxicity induced by GSIs, while suppression of NOTCH signaling enhances the antileukemic effects of glucocorticoids (Real, Tosello et al. 2009), suggesting that the combination of GSIs and glucocorticoids may have increased efficacy and decreased toxicity in the treatment of T-ALL. In addition, synthetic peptides targeting the NOTCH transcriptional complex, and inhibitory antibodies specific for NOTCH1 have been proposed as alternative approaches to inhibit aberrant NOTCH1 signaling in T-ALL (Moellering, Cornejo et al. 2009, Wendorff, Koch et al. 2010).

V. NOTCH1-HES1 Axis

Hairy and Enhancer of Split 1

Hairy and enhancer of Split 1 (HES1) is one of the seven members of the Hes gene family of bHLH transcriptional repressors (Kageyama, Ohtsuka et al. 2007). The *HES* family of genes encode a nuclear protein which functions by forming homodimers or heterodimers with other Hes-related proteins and binds promoter sequences in the DNA to inhibit transcription. All seven *Hes* members share three conserved domains: bHLH domain, orange domain and WRPW domain. The bHLH contains two regions important for HES function: the basic region for binding promoter sequences in the DNA and the helix-loop-helix region for dimerization. Most bHLH proteins bind conserved E-box (CANNTG) sequences in the promoter region of their target genes, however, the HES factors bind with a higher affinity to a different consensus sequence called an N-box (CACNAG) sequence because of a proline residue present in the middle of the basic region (Sasai, Kageyama et al. 1992, Ohsako, Hyer et al. 1994). The orange domain assists in the selection and binding of bHLH heterodimer partners (Taelman, Van Wayenbergh et al. 2004). The C-terminus WRPW domain, consisting of tryptophan-arginine-proline-tryptophan amino acids, is necessary for binding to the transcriptional corepressor Groucho and its mammalian homologues, the transducin-like enhancer of split (TLE) family of proteins, leading to the recruitment of histone deacetylases (HDACs) and subsequent transcriptional repression. Finally, the WRPW domain also acts as a polyubiquitination signal to target HES for proteasomal degradation (Grbavec and Stifani 1996, Kang, Seol et al. 2005). Proteasomal degradation of HES proteins results in a short half-life of about 20 minutes (Hirata, Yoshiura et al. 2002). The HES family of proteins negatively regulates transcription through both active and passive repression. Active transcriptional repression results from the formation of HES homodimers or heterodimers between different members of the HES family. The HES dimers bind to the N-box sequences in promoter regions leading to the formation of a complex with Groucho/TLE corepressor and recruitment of histone deacetylases (HDACs).

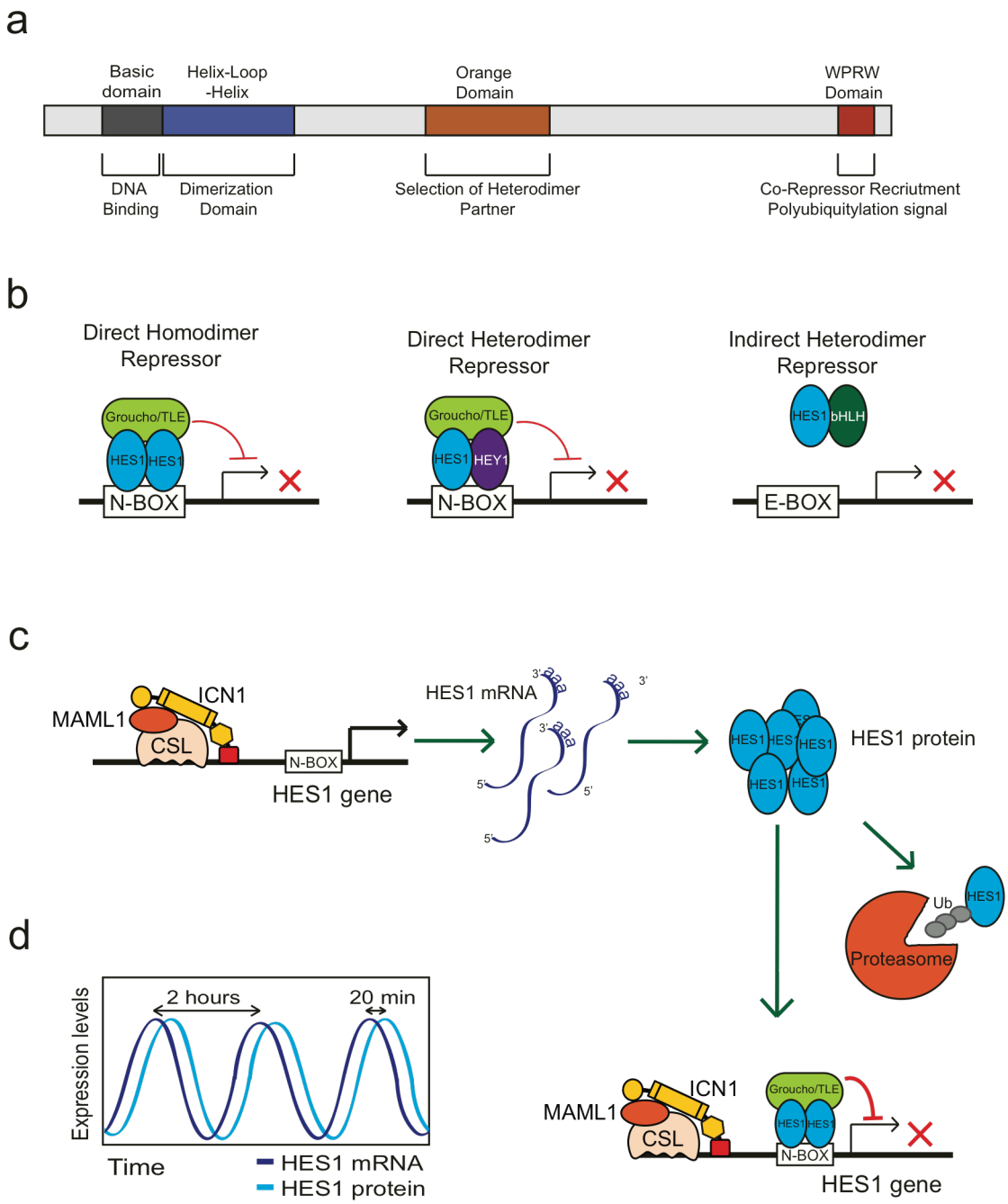

Figure 1.5. HES1 bHLH repressor protein. (**a**) HES1 protein domains and corresponding function. (**b**) Mechanisms of HES1 mediated gene repression, (**c**) Schematic representation of the HES1 auto-regulatory loop. Briefly, ICN1 translocates into the nucleus, associates with the RBPJ/CSL protein, recruits MAML co-activators and activate expression of HES1 which then is transcribed and translated leading to either proteasomal degradation of the HES1 protein of translocation of the HES1 protein to the nucleus and repressing *HES1* expression by binding to the TSS proximal N-box. (**d**) Oscillatory pattern of HES1 expression due to short half-life and HES1 auto-regulation.

Passive repression is a consequence of HES proteins binding to bHLH transcriptional activators and disrupting their ability to bind E-box sequences in the DNA, therefore inhibiting transcriptional activation of target genes (**Figure 1.5**) (Johnson, Birren et al. 1992, Dawson, Turner et al. 1995).

HES1 Function in Normal and Malignant Non-lymphoid Cells

The HES proteins are critical regulators during embryogenesis, with a central role in the timing of cell differentiation and cell fate. The hypothesis of HES1 functioning as a biological clock is in part due to a negative auto-regulatory loop in which HES1 homodimers bind to an N-box situated in the *HES1* promoter and repress its own transcription, creating an oscillatory pattern of expression with a periodicity of 2 hours (**Figure 1.5. c and d**) (Hirata, Yoshiura et al. 2002). HES1 is involved in the development of the nervous system, immune system, digestive system, and sensory organs (Sade, Krishna et al. 2004, Sang, Roberts et al. 2010). The function of HES1 is context dependent; in some cases it inhibits cells from differentiation and in other cases it promotes the differentiation towards a specific lineage. During early embryogenesis, HES1 is an essential transcription factor for the maintenance of stem cell populations in the nervous and digestive system. Specifically, NOTCH1-induced expression of HES1 inhibits the premature differentiation of neuroepithelial and radial glial cells into neurons (Ohtsuka, Ishibashi et al. 1999, Gaiano, Nye et al. 2000, Ohtsuka, Sakamoto et al. 2001, Takatsuka, Hatakeyama et al. 2004). HES1 inhibition of neurogenesis is especially important for the formation of the boundaries between the compartments of the nervous system (Baek, Hatakeyama et al. 2006). Similarly, HES1 maintains the stem cell population of pancreatic cells by downregulating the critical transcription factors involved in the differentiation of progenitors cells into the exocrine or endocrine cells of the pancreas. Furthermore, HES1 inhibits stem cells in the intestine from differentiating into goblet, enteroendocrine, and Paneth cells (van Es, van Gijn et al. 2005). On the other hand, HES1 regulates binary cell fate decision in the nervous,

digestive, and immune systems. For example, HES1 signaling in the nervous systems promotes astrocyte formation by upregulating pathways involved in the differentiation of astrocytes and downregulating pro-neural bHLH activators (Nakashima, Yanagisawa et al. 1999, Tomita, Moriyoshi et al. 2000, Kamakura, Oishi et al. 2004). Additionally, HES1 promotes the cell lineage gene expression signals required for the differentiation of biliary epithelial cells in the liver and enterocytes in the intestine (Kodama, Hijikata et al. 2004, Crosnier, Vargesson et al. 2005). Lastly, during embryonic development, HES1 was recently shown to promote human pluripotent stem cells to commit to the hematopoietic lineage rather than the endothelial lineage (Lee, Werbowetski-Ogilvie et al. 2013). HES1 was also implicated in promoting the expansion of HSC cells without exhausting stem cell activity (Kunisato, Chiba et al. 2003).

HES1 promotes the proliferation potential of cells by regulating factors involved in cell cycle progression. For example, HES1 promotes the proliferation of fibroblasts by repressing transcription of p27 and p21, CDK inhibitors of the G1 to S progression, and therefore allowing cells to progress through the cell cycle (Murata, Hattori et al. 2005). Additionally, HES1 maintains the reversibility of quiescence, a state in which cells do not divide, by inhibiting the p21 driven irreversible senescent-like state (Sang, Coller et al. 2008). Similarly, HES1 directly represses p57, a CDK inhibitor involved in G1 cell cycle arrest, thus allowing cells to escape cellular senescence (Giovannini, Gramantieri et al. 2012). Given the context dependent function of HES1 in cellular differentiation, HES1 is also involved in the interaction of components involved in cell cycle arrest. High levels of HES1 expression results in cell cycle arrest of mammary cells due to the direct inhibition of E2F1, a cell cycle regulator involved in S phase progression (Hartman, Muller et al. 2004). Furthermore, HES1 was shown to be involved in DNA damage pathways important to the regulation of the cell cycle progression. Specifically, TP53 is indirectly activated by HES1 due to the transcriptional repression of MDM2, a negative regulator of TP53 (Huang, Raya et al. 2004). HES1 was also shown to directly interact with the

Fanconi anemia core complex, a complex that responds to DNA cross-link damage during normal S phase (Tremblay, Huang et al. 2008).

The significant role of HES1 plays in the maintenance of stem cells and regulation of the differentiation of cells allows for the opportunity for cancer cells to target HES1 in tumorigenesis. HES1 is found upregulated in various cancers including breast ductal carcinoma in situ, ovarian carcinoma, non-small cell lung cancers, meningiomas, medulloblastoma, oral squamous cell carcinoma, colon cancer, pancreatic cancer, and cutaneous T cell lymphoma (Hallahan, Pritchard et al. 2004, Cuevas, Slocum et al. 2005, Hopfer, Zwahlen et al. 2005, Fan, Matsui et al. 2006, Farnie, Clarke et al. 2007, Konishi, Kawaguchi et al. 2007, Kamstrup, Gjerdrum et al. 2010, Maniati, Bossard et al. 2011, Lee, Hong et al. 2012, Gao, Zhang et al. 2014). Additionally, elevated levels of HES1 were documented in rhabdomyosarcoma and skeletal muscle tumor patient samples (Sang, Coller et al. 2008). The significant quantity of tumors with elevated levels of HES1 suggests that HES1 provides a selective advantage for the malignant transformation or maintenance of these tumors.

The Role of HES1 in T-cell development

HES1 is a major negative regulator activated by NOTCH1 signaling during early T cell development. An important role for Hes1 in T-cell development was first discovered in *Hes1* knockout mice where 90% of *Hes1*-null embryos completely lack a thymus and <10% develop a rudimentary thymic structure with T development blocked at the double negative stage ($TCR\beta^-$ and $TCR\gamma\delta^-$) (Tomita, Hattori et al. 1999). Targeted deletion of Hes1 in bone marrow progenitors results in an 80% decrease in thymic cellularity (Wendorff, Koch et al. 2010). In addition, Hes1 deficient progenitor cells fail to generate normal numbers of T cells, specifically in the DN and DP populations in competitive fetal liver or bone marrow chimeras. This suggests Hes1 promotes the expansion of lymphoid progenitor cells, an essential process for clonal diversification and selection resulting in mature T cells (Tomita, Hattori et al. 1999). The

importance of Hes1 in adopting T-cell lineage fate is further supported by intrathymic transfer of HSC cells with *Hes1* knockout, showing a decrease in cells adopting the T cell lineage within the DN1 population (Wendorff, Koch et al. 2010). Hes1 is highly expressed in ETP and DN cells, and is critical for assisting immature cells in adopting T-cell lineage and supporting cells through β–selection. Specifically, Hes1 inhibits myeloid lineage differentiation by directly binding to and inhibiting the *Cebpα* promoter (De Obaldia, Bell et al. 2013). Also, Hes1 promotes cell survival, differentiation and metabolism through β–selection by inhibiting PTEN and therefore increasing activation of the PI3K-AKT signaling pathway (Wong, Knowles et al. 2012). Furthermore, HES1 facilitates the commitment of DP cells to the CD8+ lineage by repressing the expression of CD4 corepressor (Kim and Siu 1998, Kathrein, Chari et al. 2008).

The Role of Hes1 in T-ALL

HES1 is a target of the NOTCH pathway and a key negative regulator of transcriptional pathways involved in T-cell transformation. HES1 was discovered to contribute significantly to the development of NOTCH1 induced T-ALL. More specifically, loss of *Hes1* in Lin^- hematopoietic cells with aberrant NOTCH1 signaling inhibits the malignant transformation of cells into T-ALL (Wendorff, Koch et al. 2010). However, the specific HES1 transcriptional network facilitating NOTCH1 driven transformation has yet to be identified. In regards to tumor maintenance, the NOTCH1-HES1 regulatory axis is implicated in the upregulation of PI3K signaling via direct transcriptional downregulation of the *PTEN* tumor suppressor gene (Palomero, Dominguez et al. 2008). In addition, HES1 can promote NF-κB signaling by directly binding to and inactivating CYLD, a negative regulator of NF-κB signaling (**Figure 1.6**) (Espinosa, Cathelin et al. 2010). Still, the genes and pathways controlled by HES1 in T-cell transformation and tumor maintenance remain largely unknown. The requirement of *Hes1* for the establishment of NOTCH1 induced tumors highlights the significant role HES1 plays in T-

cell transformation and the potential to target HES1 and its downstream targets in the treatment of T-ALL.

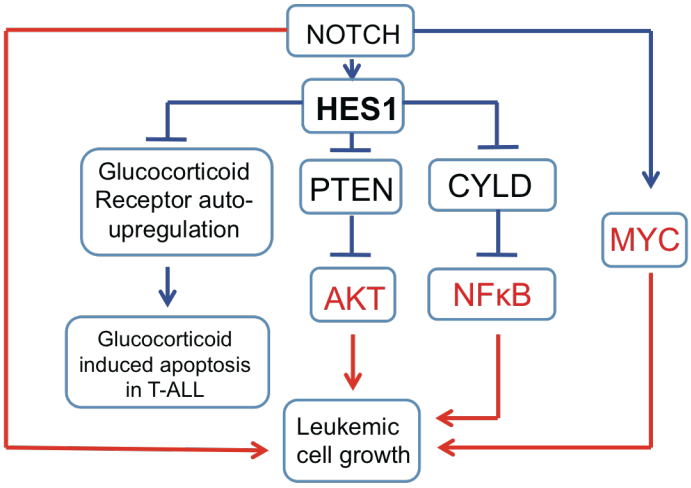

Figure 1.6. NOTCH1-HES1 axis in T-cells. NOTCH1 activation of HES1 leads to the repression of tumor suppressors *PTEN* and *CYLD* resulting in increased cellular proliferation. In addition, HES1 represses the auto-upregulation of the glucocorticoid receptor therefore decreased glucocorticoid induced apoptosis.

VI. Specific Aims

T-cell acute lymphoblastic leukemia (T-ALL) is an aggressive hematological malignancy resulting from the oncogenic transformation of immature T-cell progenitor. Aberrant activation of the NOTCH signaling pathway plays a critical role in the pathogenesis of more that 50% of human T-ALLs, in which activating mutations in *NOTCH1* result in aberrant signaling. Over the last decade, our laboratory and others have published insightful information on the mechanisms that mediate the effects downstream of activated NOTCH receptors during development and leukemia. However, the mechanisms of transformation induced by aberrant NOTCH signaling are yet to be fully understood. Here we aim to establish the mechanisms of action of *HES1* a transcriptional repressor controlled by NOTCH1, as a key regulator of transcriptional pathways in T-ALL. The fundamental role of *HES1* as a NOTCH1 target gene in

T-ALL is shown by results from our lab demonstrating a critical role of *HES1* in the control of glucocorticoid resistance, *PTEN* regulation downstream of NOTCH1, and by animal model studies showing that *Hes1* expression is required for NOTCH1 induced transformation in mice. Our central hypothesis was that aberrant expression of *HES1*, driven by aberrant activation of NOTCH1, contributes to the pathogenesis of T-ALL by disrupting specific transcriptional regulatory networks that control cell proliferation, differentiation, and survival in T-cell progenitor cells. Thus, the central goal of my thesis was to define the transcriptional programs and regulatory networks controlled by *HES1* in the context of T-cell acute lymphoblastic leukemia and to elucidate potential pathways for targeted therapy**.**

To achieve this objective we proposed the following specific aims:

Aim 1: To investigate and characterize the role of HES1 in the pathogenesis of T-ALL.

Aim 2: To identify the transcriptional network regulated by HES1 that facilitates the cellular growth and survival of malignant T lymphoblasts.

Aim 3: To identify novel antileukemic drugs targeting the HES1 transcriptional network for the treatment of T-ALL.

Chapter 2
Materials and Methods

I. Cell Culture

Cell Lines

HEK-293T, CUTLL1, CCRF-CEM, JURKAT, RPMI 8402, DND41 and HPB-ALL cells were cultured in standard conditions in RPMI 1640 media supplemented with 10% FBS and 1% Penicillin/Streptomycin. HEK-239T cells, CCRF-CEM, JURKAT, RPMI 8402 were from ATCC, DND41 and HPB-ALL were from DSMZ, and the CUTLL1 cell line generated in our lab has been previously described (Palomero, Lim et al. 2006).

Patient Samples

Primary T-ALL cells were cultured *in vitro* with MS5-DL1 stromal cells in MEM-alpha and in the presence of glutamax, insulin, human serum, IL7, SCF, FLT3 (Armstrong, Brunet de la Grange et al. 2009). More specifically, 300,000 primary T-ALL cells were seeded over 15,000 MS5-DL1 stromal cells for at least 24 hours before starting treatment. All cells were cultured at 37°C in a humidified atmosphere under 5% CO_2.

Cell Proliferation and Viability Assays

Relative cell growth was determined in triplicates by measurement of metabolic reduction of the tetrazolium salt MTT using Cell Proliferation Kit I (Roche) according to the manufacturer's instructions. Apoptosis was analyzed by flow cytometry with APC AnnexinV Apoptosis Kit I (BD Biosciences). For *in vitro* analysis of primograft T-ALL samples, we assessed cell viability using the BD Cell Viability kit (BD Biosciences) and fluorescent counting

beads. In these experiments $3x10^5$ leukemic cells were plated with $1.5x10^4$ MS5-DL1 stroma cells into 24-well plates and treated after 24 hours with vehicle only (DMSO) or Perhexiline for 3 days.

Lentivirus Production and Infections

CUTLL1 cells were infected with lentiviruses expressing control *Renilla* luciferase shRNA (plko.1shLUC) or shRNA targeting HES1 (shHES1) and NOTCH1-*Hes1*$^{flox/flox}$TmxCre T-ALL cells were infected with lentiviruses expressing control *Renilla* luciferase shRNA (plko.1shLUC) or two independent shRNA targeting Bbc3 (shBbc3) with gag-pol and V-SVG-expressing vectors into HEK293T cells using JetPEI transfection reagent (Polyplus). We collected viral supernatants after 48 hours and used them for infection of CUTLL1 cells and NOTCH1-*Hes1*$^{flox/flox}$TmxCre tumor 1 cells by spinoculation. After infection, we selected cells for 5 days in media containing 1 µg/ml puromycin and separated live from dead cells by Ficoll separation.

Microarray Expression Analysis

CUTLL1 cells infected with shRNA LUC and shHES1 were collected 72 hours post puromycin selection. RNA was isolated, labeled, and hybridized to the HumanT-12v4 Expression BeadChip (Illumina) using standard procedures. Cells from ΔE-NOTCH1 *Hes1*$^{flox/flox}$ TmxCre tumor 1 T-ALL were cultured *in vitro* and treated for 36 hours with ethanol (ETOH) or 4-hydroxy-tamoxifen (4-OH TMX). RNA was isolated labeled and hybridized to the MouseRef-8 v2.0 Expression BeadChip (Illumina) using standard procedures. Raw gene expression data were log2 transformed and quantile-normalized using MATLAB. Differentially expressed transcripts were analyzed by t-test and fold change. Gene Set Enrichment Analysis (GSEA) was carried out to test for enrichment of up-regulated genes by *Hes1* knockout against HES1

knockdown in the CUTLL1 cell line. Similarly GSEA was carried out to test for enrichment of up-regulated genes by GSI treatment of T-ALL against the *Hes1* knockout genetic signature in NOTCH1 induced T-ALL. The procedure was implemented in MATLAB as described in (Subramanian, Tamayo et al. 2005) using the *t*-test metric and 1,000 permutation of the gene list. Similarly, GSEA was used to test for enrichment of gene sets from C2 Molecular Signature Database against the ranked list of genes sorted by *t*-score comparing HES1 knock-down *vs*. control.

Luciferase reporter assays

We performed reporter assays in HEK293T cells using a pGL3-Luc *BBC3* promoter (-544 to -121), pGL3-Luc BBC3 with a scramble sequence in place of the N-box (-415 to -410), and pGL3-Luc BBC3 with a (-415 to -410) N-box deletion. In these assays we transfected *BBC3* reporter constructs together with a plasmid driving the expression of the Renilla luciferase gene (pCMV-Renilla) used as transfection control and either empty vector (pcDNA3) or a construct expressing HES1 (pcDNA3 HES1). We measured luciferase activity 48 hours after transfection with the Dual-Luciferase Reporter Assay kit (Promega).

Development of Mouse Primary T-ALL Cell Line

Mouse primary tumors were cultured *in vitro* with OP9 stromal cells in OPTIMEM-Glutamax medium supplemented with mouse IL-7 (10ng/mL), β-mercaptoethanol (55 μM), 10% FBS, and 1% Penicillin/Streptomycin. More specifically, 150,00 OP9 cells were plated onto 10cm plates over night, 12-16 hours later murine T-ALL cells were plated at a concentration of 1-2 million cells/ml in media supplemented with IL-7, IL-2, and β-mercaptoethanol. Cells were split every 48-72 hours for two weeks by gently resuspending the murine T-ALL cells without resuspending the stromal cells, filtering T-ALL cells through a 70 μm cell strainer, washed once with PBS, and re-plated onto fresh OP9 cells supplemented with IL-7 and β-mercaptoethanol.

After two weeks, cells were removed from stromal cells and were seeded at 1 million cells/mL supplemented with IL-7 and β-mercaptoethanol. After 4 weeks, IL7 was removed and cells were allowed to expand. These cells underwent three rounds of freezing in liquid nitrogen in 90% FBS 10% DMSO medium and thawing. Only then were experiments conducted in the established cell lines.

Drugs

4-hydroxytamoxifen (CAS#68047-06-3) and perhexiline (CAS#6724-53-4) were purchased from Sigma-Aldrich. 4-hydroxytamoxifen was resuspended in 100% ethanol and a working stock of 5mg/ml of perhexiline was resuspended in DMSO.

II. Mouse Experiments

Generation of Hes1 Conditional Knockout Mice

All animals were maintained in specific pathogen-free facilities at the Irving Cancer Research Center at Columbia University Medical Campus. Animal procedures were approved by the Columbia University Institutional Animal Care and Use Committee. To generate conditional inducible *Hes1* knockout mice we bred *Hes1* conditional knockout mice ($Hes1^{flox/flox}$) (Imayoshi, Shimogori et al.) with $ROSA26^{Cre\text{-}ERT2/+}$ mice, which express a tamoxifen-inducible form of the Cre recombinase from the ubiquitous *Rosa26* locus (Chen, Chang et al. 2007).

Generation of Hes1 Conditional Knockout in NOTCH Induced T-ALL

To generate *NOTCH1*-induced T-ALL tumors in mice, we performed retroviral transduction of bone marrow cells enriched in lineage negative cells (Lin^-) using magnetic beads

(Lineage cell depletion kit by Miltenyi kit #130-090-858 following manufacturer's guidelines) with an activated form of the NOTCH1 oncogene (ΔE-NOTCH1) and transplanted them via intravenous injection into lethally irradiated NOD rag gamma (NRG) immunodeficient mice (JAX: 007799) as previously described (Kopan, Schroeter et al. 1996, Tarantola, Quatresous et al. 2009). We treated secondary recipients with vehicle only or with tamoxifen (5 mg/mouse) by intra-peritoneal injection to induce deletion of the *Hes1* locus.

Treatment of Mice with Perhexiline

We infected NOTCH1 (NOTCH1 L1601P ΔPEST) induced T-ALL cells with lentiviral particles expressing the mGFP fluorescent protein and luciferase (Migr-mGFP-LUC) and injected them intravenously into C57BL/6. We treated groups of 6 animals with vehicle (water with 5% DMSO) or Perhexiline (53.68 mg kg^{-1}). We evaluated disease progression and therapy response by *in vivo* bioimaging with the In Vivo Imaging System (IVIS, Xenogen).

Primary Xenografts Treatment

Primary human sample PDTALL 9 was injected intravenously into 8 NRG immunodeficient mice. Nine days post transplant, mice were treated with vehicle (water with 5% DMSO) or perhexiline (53.68 mg kg^{-1}) for three consecutive days. Mice were sacrificed after the 72 hours of treatment and bone marrow and spleen tissues were collected and analyzed. Primary human sample PDTALL 10 was injected intravenously into 12 NRG immunodeficient mice. Nine days post transplant, mice were treated with vehicle (water with 5% DMSO) or perhexiline (40 mg kg^{-1}) for 5 consecutive days of treatment. Mice were sacrificed after treatment, bone marrow and spleen were analyzed for tumor load.

Flow Cytometry Analysis

For the analysis of T cell populations in spleen and bone marrow, tissues from mice transplanted with T-ALL and treated with vehicle, tamoxifen, or perhexiline were collected and processed through an 80 μm mesh to obtain single cell suspensions. Red cells in spleen samples were removed by 5 minute incubation at room temperature with red blood cell lysis buffer (155 mM NH_4Cl; 12 mM $KHCO_3$; 0.1 mM EDTA). Cells were stained with a APC-conjugated antibody against mouse CD4 (BD Pharmingen-553051) and a PE-conjugated antibody against mouse CD8a (BD Pharmingen-553032). Flow cytometry analyses were performed in a FACS Canto flow cytometer (BD Biosciences).

Histology

Mouse spleen, liver, and kidney were isolated using standard procedures and then processed for histologic analysis following 48 hours of fixation in 10% neutral buffered formalin and stored in 75% ethanol before processing for histological studies. Hematoxylin and eosin staining was performed by the Columbia Histology Core Facility according to standard procedures and slides were analyzed on a Nikon Eclipse E600e microscope with NIS Elements F 3.20 Software.

Drugs and Administration

Tamoxifen (CAS#T5648-1G) and Perhexiline (CAS#6724-53-4) were purchased from Sigma-Aldrich. Tamoxifen was resuspended in 100 uL of ethanol per 100 mg then 2mL of corn oil was added. Suspended tamoxifen was rotated for 1 hour at 55°C and frozen in aliquots at -20°C. Mice were injected with 5mg of tamoxifen. Perhexiline was resuspended in 5% DMSO and pH was adjusted to 7.2.

Statistical Analysis

We performed statistical analysis by Student's *t*-test. Survival in mouse experiments was represented with Kaplan-Meier curves and significance was estimated with the log-rank test (Prism GraphPad).

III. Biochemical Assays

Western Blot

Western blot was performed using standard procedures. In brief, cells were lysed in RIPA lysis buffer (50mM Tris-HCL, 150mM NaCL, 1% NP40, 0.5% sodium deoxycholate, 0.1% SDS) supplemented with Phosphatase Inhibitor Cocktails 2 and 3 (Sigma Aldrich 231-791-2 and 200-664-3) and Complete Protease Inhibitor (Roche 11873589001) for 30 minutes on ice and then centrifuged at max speed for 30 minutes. Protein concentrations in cell lysates were quantified using the BCA Protein Assay Kit (Pierce Biotochnology). All proteins were detected by resolving proteins in 10% Bis-Tris SDS-PAGE (Ivitrogen) and blotted onto nitrocellulose membranes. Membranes were blocked by 5% non-fat dry milk and blotted with antibodies against: HES1 (Aviva Systems Biology Corp: ARP32372_T100), Puma (SC-28226), Bcl2 (DB biosciences: 554218), and GAPDH (SC-20357) (Santa Cruz Biotechnologies) and mouse Gapdh (Cell Signaling Technology: 5174S). Detection of protein bands was performed using Super Signal Chemiluminescent Substrate (Pierce Biotechnology) after incubation with the horseradish peroxidase-conjugated secondary antibody.

Chromatin Immunoprecipitation

We performed chromatin immunoprecipitation using the Agilent Mammalian ChIP-on-chip chromatin immunoprecipitation protocol as described before (Palomero 2007). Briefly, 10^8 CUTLL1 cells were fixed with formaldehyde in a final concentration of 1% for 10 minutes at room temperature. We quenched the crosslinking reaction with a 2.5 M glycine solution and the cells were then centrifuged, washed twice with ice-cold phosphate saline buffer and lysed. Cell nuclei were resuspended in lysis-buffer (10 mM Tris-HCl, pH 8.0; 100 mM NaCl; 1 mM EDTA; 0.5 mM EGTA; 0.1% sodium deoxycholate; 0.5% N-lauroylsarcosine) and fragmented to a 150-300 bp size using a Bioruptor sonicator (Diagenode). We incubated fragmented chromatin overnight at 4°C with magnetic beads (Dynal) loaded with 10 µg of the following specific antibodies against HES1 (sc-166410; Santa Cruz Biotechnology) or rabbit IgG (sc-2027; Santa Cruz Biotechnology). We washed chromatin-antibody-bead complexes six times with RIPA buffer (50 mM Hepes-KOH, pH 7.6; 0.5 M LiCl; 1 mM EDTA; 1% Igepal and 0.7% sodium deoxycholate), and once with TE-buffer containing 50 mM NaCl. Then we eluted the chromatin from the beads with elution buffer (50 mM Tris-HCl, pH 8.0 10 mM EDTA and 1%SDS) and reversed the cross-link by incubation at 65°C overnight. We purified DNA fragments with phenol-chloroform and ethanol precipitation. We tested enrichment of specific immunoprecipitated DNA fragments by quantitative PCR (using *ACTB* genomic sequence levels as a loading control) to analyze ChIP enrichment of *BBC3* promoter sequences in total genomic DNA, and in chromatin immunoprecipitates preformed with antibodies against HES1 and IgG used as a negative control.

Southern Blot

Southern blot was used to detect TCRβ rearrangements of $Hes1^{flox/flox}$Cre-ERT2 NOTCH1-induced T-ALL tumors. Genomic DNA was isolated from tumors or normal tissues

from control mice, digested with 10 μg of EcoRI and analyzed by Southern blot analysis using standard procedures. The probe used detects DJβ2 gene cluster rearrangements. Presence of two hybridizing EcoRI bands in addition to the WT band represents a clonal population, whereas more than two additional bands would represent a non-clonal population (Khor and Sleckman 2005).

RT-PCR

We performed reverse transcription reactions with the ThermoScript RT-PCR system (Invitrogen) and analyzed resulting complementary DNA products by quantitative real-time PCR (FastStart Universal SYBR Green Master Mix (Roche) using a 7300 Real-Time PCR System (Applied Biosystems). Relative expression levels were normalized using *Gapdh* as a reference control.

IV. T-ALL Primary Samples

Patient Samples

T-ALL samples were provided by Columbia Presbyterian Hospital, the Eastern Cooperative Oncology Group (ECOG), University of Padova, and Hospital Central de Asturias with informed consent and analyzed under the supervision of the Columbia University Medical Center Institutional Review Board committee.

Chapter 3
The role of *HES1* in NOTCH1-induced T-ALL

Introduction

T-ALL results from a multistep process involving the activation of oncogenes and loss of tumor suppressor genes, which disrupt specific mechanisms regulating proliferation, differentiation and survival during T-cell development (Van Vlierberghe and Ferrando 2012). In this setting, the identification of activating mutations in the *NOTCH1* gene in over 60% of T-ALLs highlights the central role of aberrant NOTCH signaling in the pathogenesis of this disease (Weng, Ferrando et al. 2004). Constitutive activation of mutant NOTCH1 in T-ALL drives a transcriptional program promoting leukemia cell growth and proliferation via multiple direct and indirect mechanisms including, most prominently, transcriptional activation of the *MYC* oncogene and upregulation of the PI3K-AKT-mTOR signaling pathway (Paganin and Ferrando 2011). In this circuitry, Hairy and Enhancer of Split 1 (HES1), a basic helix-loop-helix (bHLH) transcriptional regulator directly controlled by NOTCH1, functions as a critical factor mediating transcriptional repression downstream of NOTCH signaling (Jarriault, Le Bail et al. 1998).

An important role for Hes1 in T-cell development was first realized in *Hes1* knockout mice, which show rudimentary or complete absence of thymic development (Tomita, Hattori et al. 1999). Consistently, conditional deletion of *Hes1* in hematopoietic progenitors impaired T-cell development by compromising the capacity of early lymphoid progenitors to seed and populate the thymus (Wendorff, Koch et al. 2010). In T-ALL, the NOTCH1-HES1 regulatory axis is implicated in upregulation of PI3K (Palomero, Dominguez et al. 2008) and NF-κB signaling (Espinosa, Cathelin et al. 2010). And in the absence of *Hes1,* aberrant NOTCH1 signaling fails to transform hematopoietic cells into T-ALL (Wendorff, Koch et al. 2010). However, the specific roles and mechanisms of HES1 in NOTCH1 induced leukemia remain incompletely understood.

In this chapter we describe the transcriptional network repressed by HES1 and the contribution of HES1 to the maintenance of NOTCH1-induced T-ALL.

Results

HES1 promotes survival of NOTCH1-driven human T-ALL

Given the well-established role of HES1 as an evolutionarily conserved downstream effector of NOTCH1 required for thymocyte development and NOTCH1-induced transformation, we hypothesized that HES1 is also required for tumor maintenance in T-ALL. In order to test our hypothesis, we analyzed the effects of *HES1* knockdown in two human T-ALL cell lines driven by aberrant NOTCH1 activation: CUTLL1 cells expressing a truncated and constitutively-active form of NOTCH1 as a result of the t(7;9)(q34;q34) chromosomal translocation (Palomero, Lim et al. 2006), and DND41 cells containing two mutations in the HD domain of NOTCH1 (Weng, Ferrando et al. 2004). In these experiments, CUTTL1 and DND41 cells were infected with lentivirus expressing two independent short hairpins targeting *HES1* (shHES1#1 and shHES1#2) or a control short hairpin targeting the *Renilla* luciferase gene (shLUC). Knockdown of *HES1* was evaluated by western blot analysis in both CUTLL1 and DND41 cells infected with lentivirus expressing shLUC, shHES1 #1, and shHES1 #2 (**Figure 3.1.a**). Analysis of cell viability by MTT proliferation assays over the course of five consecutive days displayed a marked decrease in cell growth in both CUTLL1 and DND41 cells silenced for *HES1* compared to shLUC controls (**Figure 3.1.b**). Flow cytometry analysis after propidium iodine (PI) staining showed minor defects in the cell cycle progression of HES1-depleted cells. However, the cell cycle changes were not consistent between the two different human cell lines. CUTLL1 cells showed a modest accumulation of G1 and G2-M cells compared with controls. Whereas DND41 cells showed a decrease in cells arrested in G1 with no statistically significant increase in the other phases of the cell cycle compared to controls (**Figure 3.1.c**).

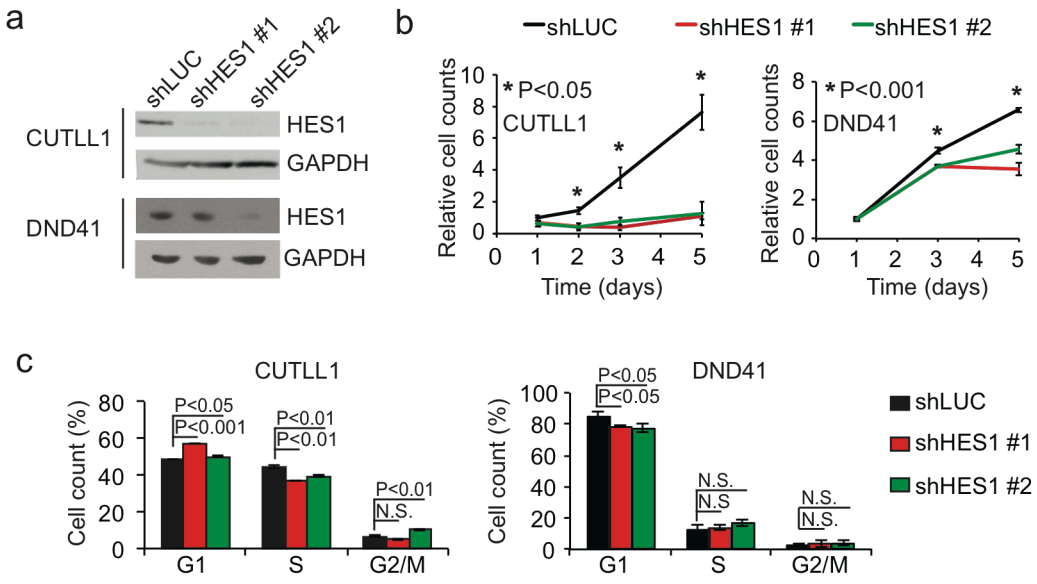

Figure 3.1. Cellular effects of *HES1* knockdown in human T-ALL. (**a**) Western blot analysis of HES1 expression in CUTLL1 and DND41 human T-ALL cells transduced with shRNAs targeting the *Renilla* luciferase gene (shLUC) or *HES1* (shHES1 #1, shHES1 #2). (**b**) Quantification of cell growth in CUTLL1 and DND41 cells expressing shLUC, shHES1 #1, shHES1 #2 measured by MTT analysis at 24, 48, 72, and 120 hours after 5 days of selection with puromycin. (**c**) Cell cycle analysis of CUTLL1 and DND41 cells infected with lentiviruses expressing shLUC or two independent shHES1 at **24** hours after selection. Graphs in **b** and **c** indicate mean values and error bars represent s.d. *P* values in **b** and **c** were calculated using the two-tailed Student's *t*-test.

The minimall effects of *HES1* loss in cell cycle progression suggest the previous results from the MTT proliferation assay may be due to an increase in cell death rather than cell cycle arrest. To determine whether the cells undergo apoptosis upon loss of HES1, we analyzed CUTLL1 and DND41 cells expressing either our control hairpin (shLUC) or two hairpins targeting *HES1* (shHES1 #1 and shHES1 #2) 72 hours after puromycin selection by flow cytometry assays utilizing fluorochrome-labelled annexin V. Annexin V is a calcium-dependent phospholipid-binding protein that preferentially binds to phosphatidylserine (PS). PS, a phopholipid of the plasma membrane, normally located in the cytoplasmic surface, is translocated to the outer leaflet of the membrane during the early stages of apoptosis (Vermes,

Haanen et al. , Zhang, Gurtu et al.). The plasma membrane is still intact during the early stages of apoptosis, therefore adding a viability stain suchs as 7-AAD or Dapi distinguishes between the early apoptotic cells which would exclude the viability stain (annexinV-positive, viability dye-negative) and late-stage apoptotic/necrotic cells whose cell membrane lose integrity (annexinV-positive, viability dye-positive). Annexin V staining of both CUTLL1 and DND41 cells revealed a marked increase in both apoptotic and necrotic cells upon HES1 inactivation (**Figure 3.2**). *HES1* knockdown in CUTLL1 cells resulted in a 3 fold increase in early and late apoptotic cells (**Figure 3.2.a**). Similarly, DND41 cells lacking *HES1* had a 3.2 fold increase in apoptotic cells (**Figure 3.2.b**).

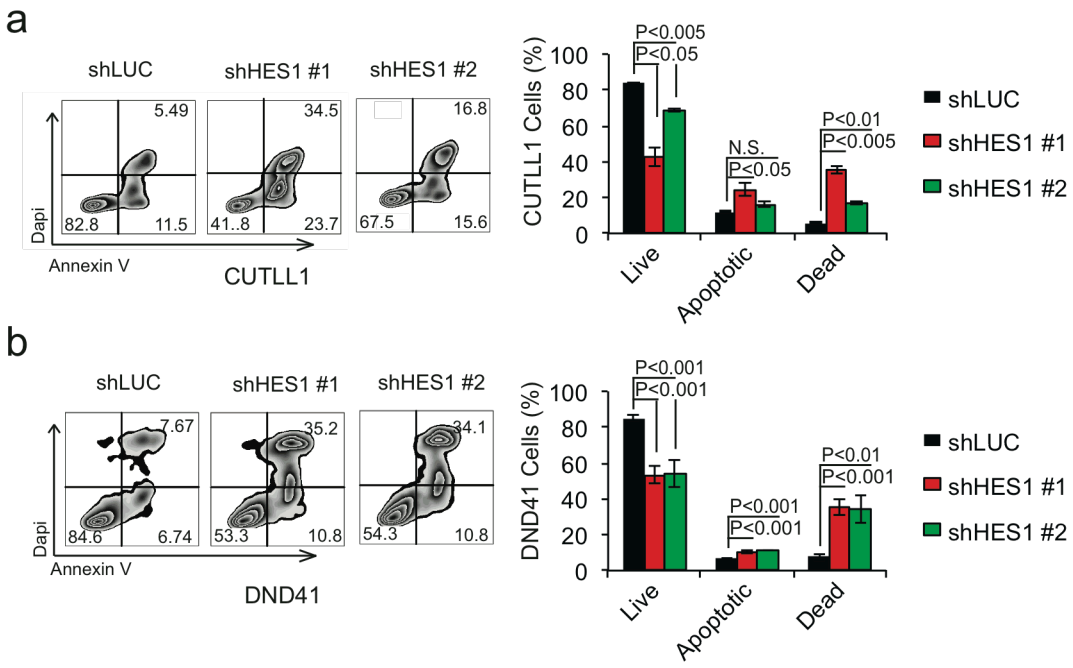

Figure 3.2. *HES1* knockdown in human T-ALL induces apoptosis. (**a**) Representative flow cytometry plots after AnnexinV-APC and Dapi staining and quantification of apoptosis 72 hours post selection in CUTLL1 infected with lentivirus expressing shLUC, shHES1 #1 or shHES1 #2. (**b**) Representative flow cytometry plots after AnnexinV-APC and Dapi staining and quantification of apoptosis 72 hours post selection in DND41 cells infected with lentivirus expressing shLUC, shHES1 #1 or shHES1 #2. Percentage populations are indicated in each quadrant of **a** and **b**. Bar graphs in **a** and **b** indicate mean values and error bars represent s.d. *P* values in **a** and **b** were calculated using the two-tailed Student's *t*-test.

These results demonstrate a key role for HES1 in the maintenance of NOTCH1-induced T-ALL and functionally implicate HES1 in leukemia cell survival.

To assess the mechanisms governing the induction of apoptosis upon *HES1* loss in T-ALL cells, we analyzed the transcriptional programs associated with HES1 knockdown. Microarray gene expression profiling of shHES1 CUTLL1 cells and shLUC CUTLL1 controls identified 32 upregulated and 18 downregulated transcripts (fold change > 1.57; P <0.01) upon HES1 inactivation (**Figure 3.3**). These results are displayed using a volcano plot in order to visualize the distribution of differentially expressed genes by fold change (x-axis) and significance (p-value) (**Figure 3.3.a**). Heatmap representation displays the top 50 differentially expressed genes in descending order of fold change. Among these, and in agreement with the established role of HES1 as a transcriptional repressor and potential leukemia oncogene, HES1 knockdown resulted in the upregulation of multiple known T-ALL tumor supressors including *CDKN1A* (Davies, Hogarth et al. 2011), *FBXW7* (Malyukova, Dohda et al. 2007, O'Neil, Grim et al. 2007, Thompson, Buonamici et al. 2007) and *EZH2* (Ntziachristos, Tsirigos et al. 2012, Simon, Chagraoui et al. 2012, Zhang, Ding et al. 2012) (**Figure 3.3.b**).

In an effort to explore the potential pathways represented by the differentially expressed genes induced by *HES1* inactivation, we crossed our data set with the C2 molecular signature database, a collection of 4,722 curated gene sets collected from various sources such as online pathway databases, publications in PubMed, and knowledge of domain experts. Remarkably, gene set enrichment analysis (GSEA) of the genes upregulated by HES1 knockdown against the C2 molecular signature database, were significantly enriched in DNA damage response genes, TP53 targets, and cell cycle genes (**Figure 3.4.a**). Furthermore, analysis of the genes downregulated upon HES1 inactivation were significantly enriched in MYC targets, the NF-κB pathway, and metabolic pathways including gluconeogenesis, amino acid synthesis, and glucose metabolism. The representation of these data sets highlights HES1 as a significant contributor to the pathways governed by NOTCH1 (**Figure 3.4.b**). Overall these results support

a major role for HES1 downstream of NOTCH1 in T-ALL as a negative regulator of tumor suppressor pathways, and link the transcriptional programs repressed by HES1 with leukemia cell survival.

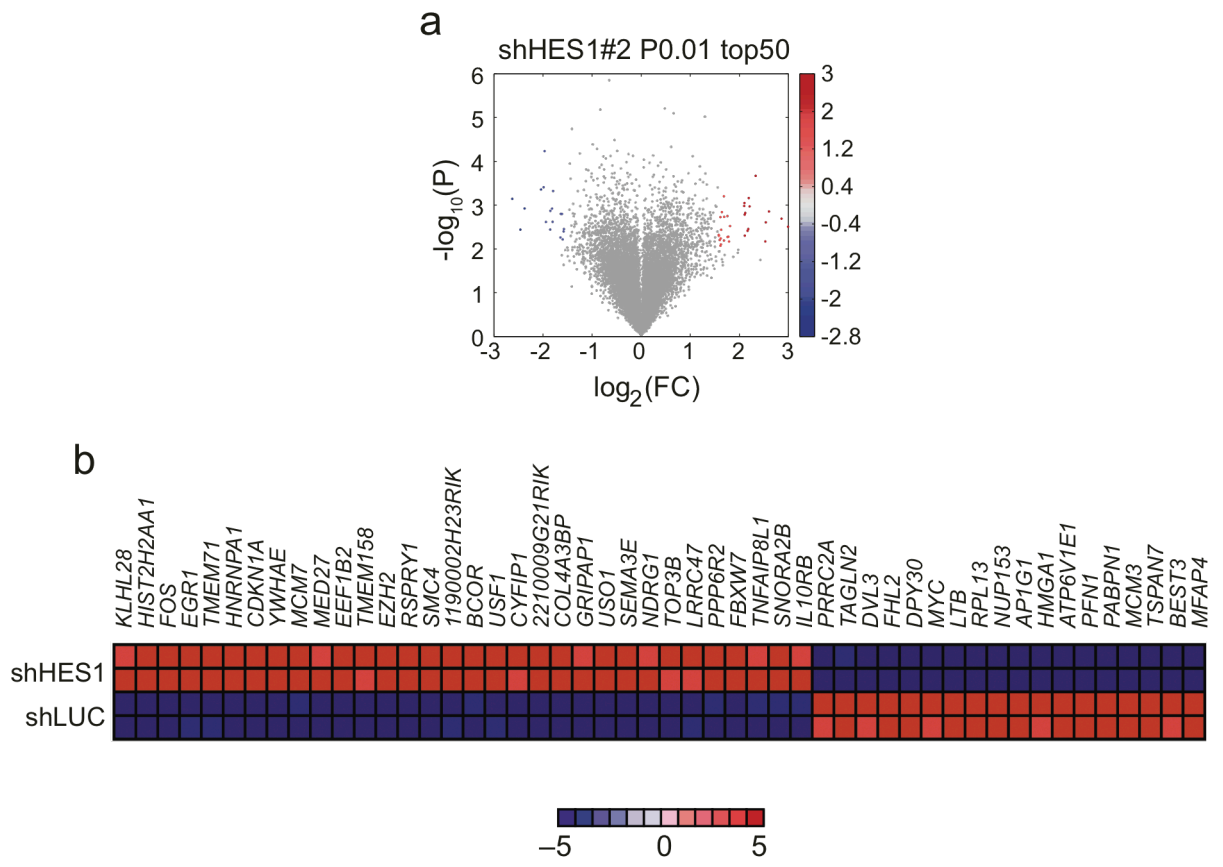

Figure 3.4. Gene expression changes associated with *HES1* inactivation. (**a**) Volcano plot representation of the differentially expressed genes upon loss of *HES1* P<0.01 and -1.57>F.C.<1.5 (**b**) Heat map representation of the top 50 differentially expressed genes (*P* < 0.01) between shLUC and shHES1 CUTLL1 cells. The scale bar shows color-coded differential expression with red indicating higher levels of expression and blue indicating lower levels of expression.

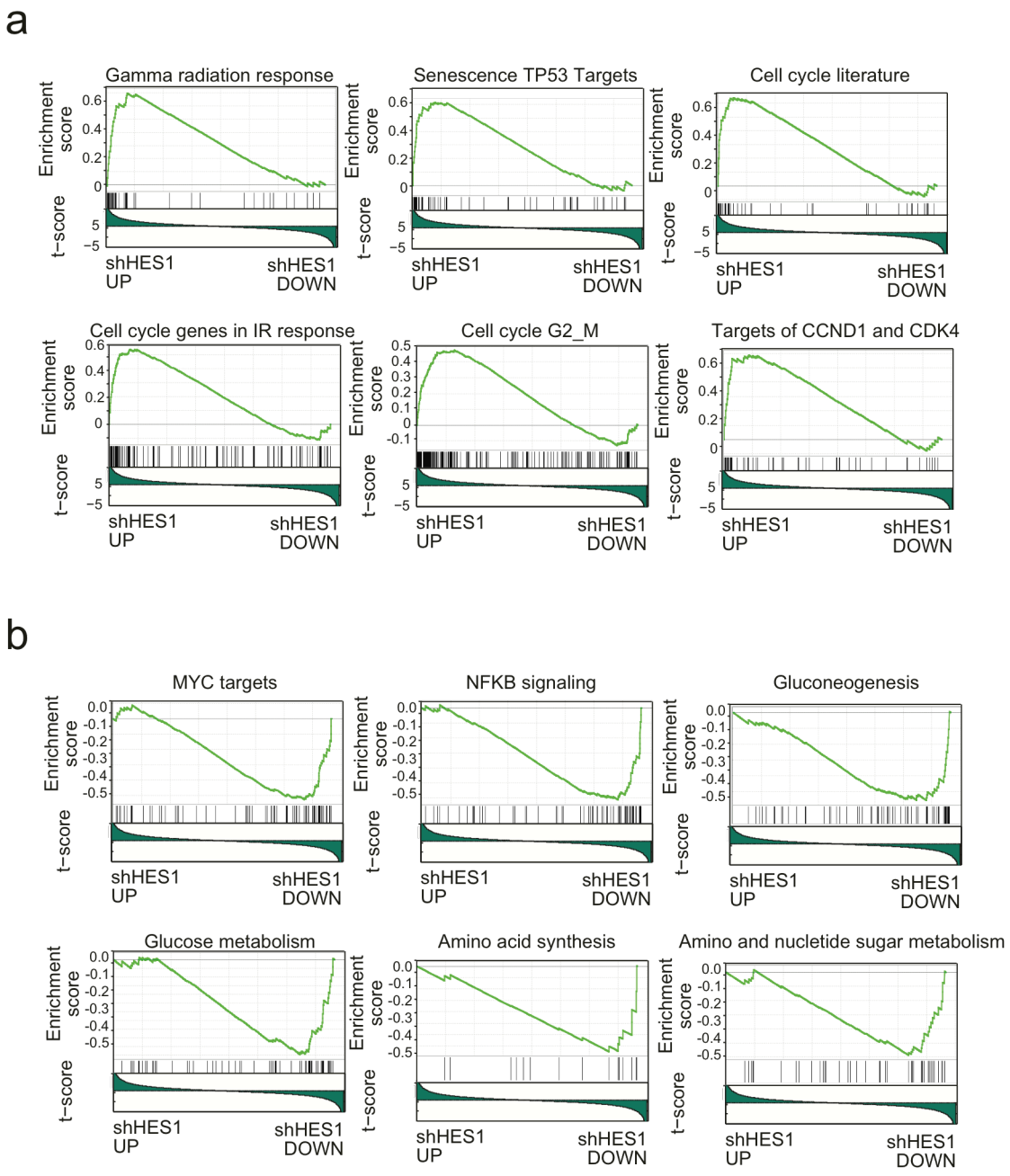

Figure 3.4. GSEA of genes differentially expressed upon *HES1* inactivation (**a**) Representative examples of gene set enrichment plots corresponding to GSEA analysis of MSigDB C2 data sets enriched in the upregulated expression signature associated with shHES1 CUTLL1 cells compared with shLUC controls. (**b**) Representative examples of gene set enrichment plots corresponding to GSEA analysis of MSigDB C2 data sets enriched in the downregulated expression signature associated with shHES1 CUTLL1 cells.

The Role of Hes1 in T-ALL progression

Having established the importance of *HES1* in the survival of human T-ALL cell lines *in vitro,* we next set to examine whether *HES1* deletion *in vivo* would produce a similar phenotype. To test the *in vivo* requirement for *Hes1* in NOTCH1 driven T-ALL we first established a *HES1* conditional knockout model. *HES1*^{flox} conditional knockout mice, generously provided by Dr. Kageyama from Kyoto University, contain two LoxP sites flanking exons 2 and 4, which upon expression of Cre-recombinase show complete ablation of *Hes1* expression (Imayoshi, Shimogori et al. 2008). These mice were bred with the Rosa26 Cre-ERT2 mouse line provided by Dr. Ludwig at Ohio State University, which expresses a tamoxifen-inducible Cre from the ubiquitous *Rosa26* locus (Chen, Chang et al. 2007). To generate tamoxifen inducible *Hes1* knockout mice we first crossed *HES1*$^{flox/wt}$ and Cre-ERT2 mice and then backcrossed the resulting *HES1*$^{flox/wt}$ Cre-ERT2 with *HES1*$^{flox/wt}$ animals to generate *HES1*^{floxwt} Cre-ERT2 and *HES1*$^{flox/flox}$ Cre-ERT2.

Next, we sought to generate NOTCH1 induced T-ALL with the capability of conditionally deleting either one allele or both alleles of *Hes1*. *We* infected hematopoietic (Lin^{-}) progenitors from tamoxifen-inducible Rosa26 Cre-ERT2 *Hes1* heterozygous (*Hes1*$^{flox/wt}$) and homozygous (*Hes1*$^{flox/flox}$) knockout mice (Imayoshi, Shimogori et al. 2008) with retroviruses driving the expression of a mutant oncogenic form of NOTCH1 (ΔE-NOTCH1) (Jarriault, Brou et al. 1995, Kopan, Schroeter et al. 1996). The ΔE-NOTCH1 construct encodes a truncated form of the NOTCH1 transmembrane receptor lacking the entire extracellular domain with exception to the 61 amino acids immediately external to the transmembrane region (Aster, Robertson et al. 1997). The ΔE-NOTCH1 receptor is readily and constitutively processed by the γ-secretase complex due to the lack of the HD-LNR repeats, resulting in oncogenic activity. This truncated form of the NOTCH1 transmembrane receptor resembles rare mutant forms of NOTCH1 found in patients with T-ALL, and when expressed in hematopoietic cells transplanted into immunocompromised mice rapidly induces T cell lymphoblastic tumors (**Figure 3.5)**. Consistent

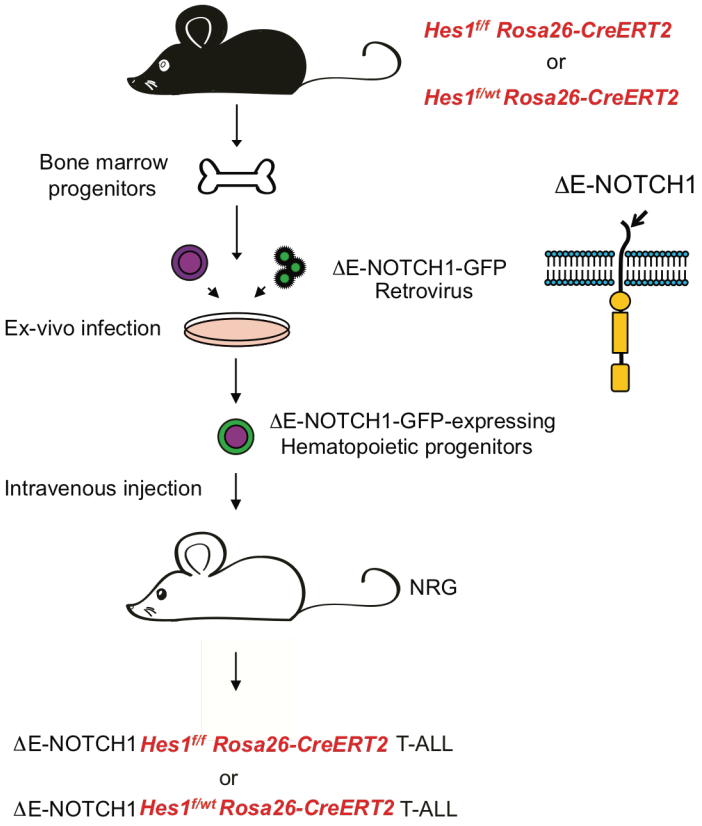

Figure 3.5. Generation of conditional *Hes1* knockout model in T-ALL. Strategy for the development of NOTCH1 driven T-ALL with conditional knockout of one or two alleles of *HES1*

with previous reports, transplantation of activated NOTCH1-expressing *HES1*$^{flox/wt\text{-}Cre\text{-}ERT2}$ and *HES1*$^{foxl/flox\text{-}Cre\text{-}ERT2}$ hematopoietic progenitor cells into lethally irradiated recipients resulted in the development of NOTCH1-driven T-ALL within 6-8 weeks (Pear, Aster et al. 1996, Chiang, Xu et al. 2008) (**Figure 3.6**). Two mice transplanted with ΔE-NOTCH1-*Hes1*$^{flox/flox\ Cre\text{-}ERT2}$ hematopoietic progenitors developed T-ALL. The first mouse exhibited the characteristic CD4+ and CD8+ double positive (DP) immunophenotype (**Figure 3.6.a**), whereas the second mouse developed a heterogeneous immunophenotype T-ALL with the highest percentage of cells in the double positive and CD4+ populations (**Figure 3.6.b**). One mouse transplanted with ΔE-

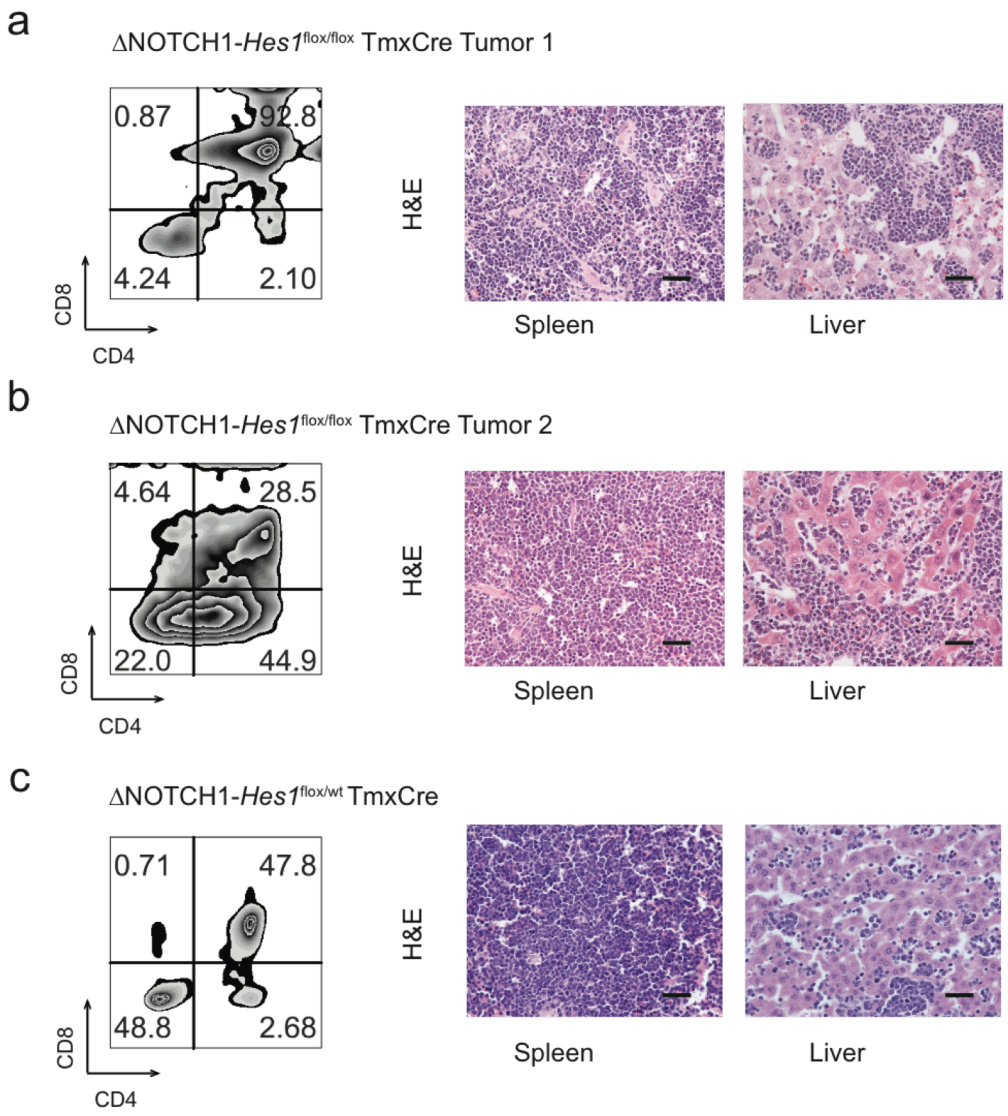

Figure 3.6. Characterization of conditional *Hes1* knockout NOTCH1 induced T-ALLs. Flow cytometry analysis of CD4 and CD8 expression in (**a** and **b**) two *Hes1* homozygous (ΔE-NOTCH1 Rosa26 Cre-ERT2 *Hes1*$^{flox/flox}$) and (**c**) one heterozygous (ΔE-NOTCH1 Rosa26 Cre-ERT2 *Hes1*$^{flox/wt}$) conditional knockout NOTCH1 induced T-ALLs. Percentages of populations are indicated in each quadrant. Representative images of hematoxylin and eosin staining tissue micrographs of spleen and liver sections from ΔE-NOTCH1 Rosa26 Cre-ERT2 *Hes1*$^{flox/flox}$ and ΔE-NOTCH1 Rosa26 Cre-ERT2 *Hes1*$^{flox/wt}$. Scale bar represent 50 μm.

NOTCH1-*Hes1*$^{flox/wt\ \ Cre\text{-}ERT2}$ hematopoietic progenitors developed the characteristic double positive T-ALL (**Figure 3.6.c**). All three *Hes1* conditional knockout T-ALL bearing mice showed enlarged spleens populated by immature lymphoblasts and infiltration of peripheral organs including the liver and kidney.

To assess the long-term effects of *Hes1* inactivation in T-ALL, we transplanted T-ALL cells from a tamoxifen-inducible *Hes1* knockout mouse (ΔE-NOTCH1 Rosa26 Cre-ERT2 *Hes1*$^{flox/flox}$ tumor 1) into a broad cohort of sub-lethally irradiated recipient mice. Following intravenous injection of leukemic lymphoblasts (and allowing 48 hours for tumor engraftment), leukemia-transplanted mice were randomized to receive tamoxifen to induce Cre-mediated deletion of the *Hes1* gene or vehicle (sunflower oil) as control. Following treatment, mice were monitored for disease progression and survival. In this experiment, tamoxifen-induced *Hes1* deletion resulted in a significant decrease in circulating leukemia lymphoblasts two weeks after transplant (**Figure 3.7.a**) and a markedly prolonged survival (P < 0.005) (**Figure 3.7.b**).

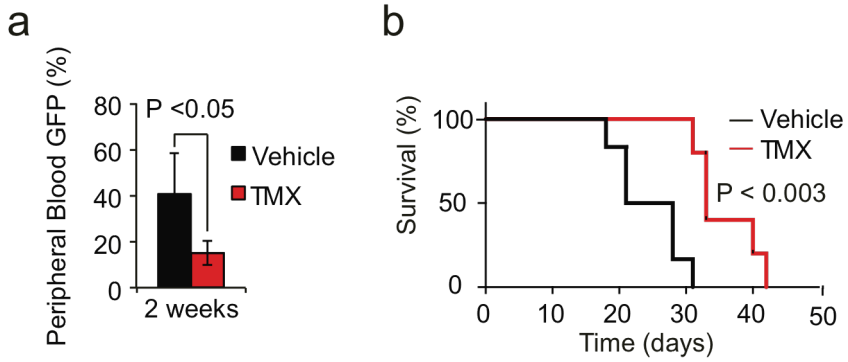

Figure 3.7. Loss of *Hes1* delays NOTCH1 induced T-ALL. (**a**) Quantification of leukemia lymphoblasts as percentage of GFP positive cells in *Hes1* conditional knockout NOTCH1-induced leukemia bearing mice treated with vehicle only (n=6) or tamoxifen (n=5) *in vivo*. (**b**) Kaplan-Meier survival curves of *Hes1* conditional knockout NOTCH1-induced leukemia bearing mice treated with vehicle only (n=6) or tamoxifen (n=5) *in vivo*. Bar graph in **a** indicate mean values and error bars represent s.d. P value in **b** was calculated using the log-rank test. P values in **a** was calculated using the two-tailed Student's t-test.

The median survival of the tamoxifen treated group was 33 days compared to 24 days in the vehicle treated. Cre-mediated excision of *Hes1* was evaluated from splenic DNA and RNA collected at time of death from both treatment groups. PCR revealed tamoxifen treatment induced effective deletion of *Hes1* by DNA (**Figure 3.8.a**) and RNA **(Figure 3.8.b**).

To validate the long-term anti-leukemic effects induced by *Hes1* deletion, we repeated the experiment with the second *Hes1* conditional knockout T-ALL (ΔE-NOTCH1 Rosa26 Cre-ERT2 *Hes1*$^{flox/flox}$ tumor 2). Consistent with the previous experiment, mice treated with tamoxifen showed a significant decrease in tumor burden two weeks after treatment (**Figure 3.9.a**). Overall survival was not significantly increased in those mice with *Hes1* inactivation compared to control, but the trend for delayed tumor progression remained (**Figure 3.9.b**). Mice treated with tamoxifen showed efficient deletion of the *Hes1* allele by PCR (**Figure 3.9.c**) and RT-PCR (**Figure 3.9.d**).

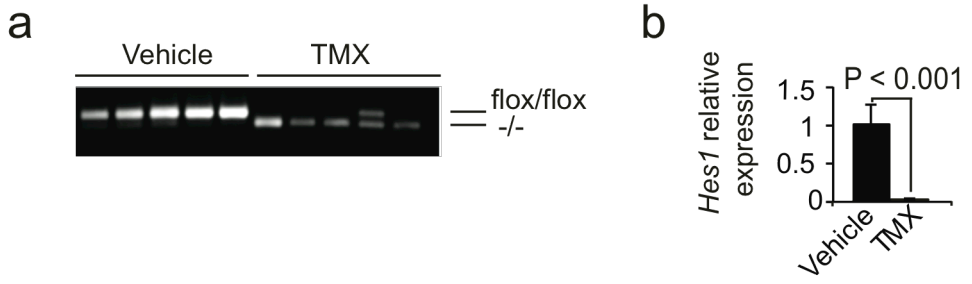

Figure 3.8. Cre-mediated deletion of *Hes1*. (**a**) PCR analysis of genomic DNA prepared from spleen cells treated 48 hours post transplant and collected at time of death. (**b**) Quantitative RT-PCR of *Hes1* expression in spleen cells treated 48 hours post transplant with tamoxifen or vehicle. Bar graph in **b** indicates mean values and error bars represent s.d. *P* values in **b** was calculated using the two-tailed Student's *t*-test.

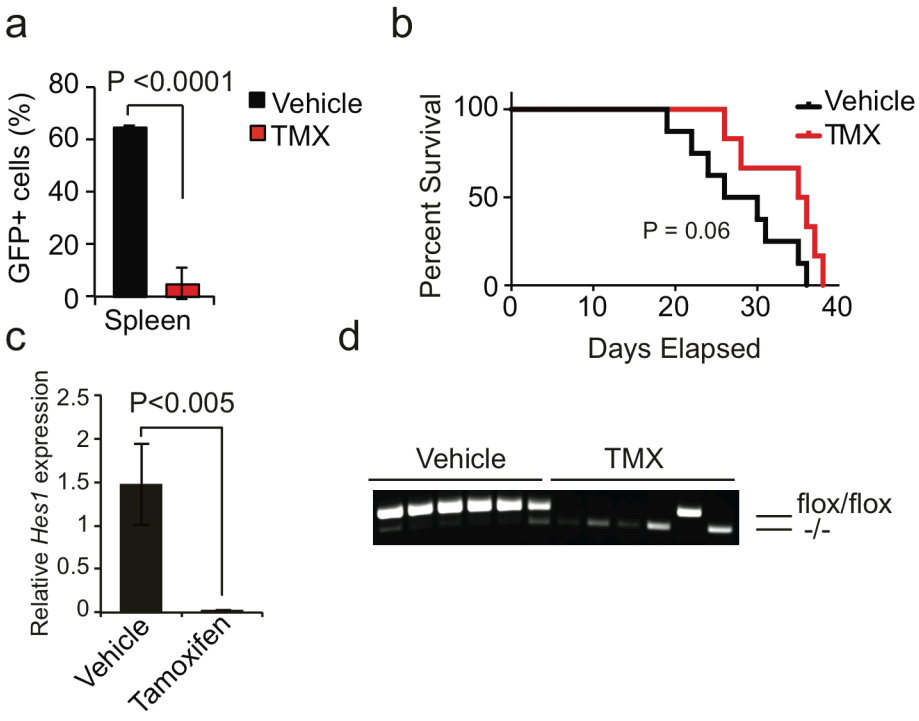

Figure 3.9. *Hes1* inactivation in NOTCH1-induced T-ALL (tumor 2). (**a**) Quantification of leukemia lymphoblasts as percentage of GFP positive cells in *Hes1* conditional knockout NOTCH1-induced leukemia (tumor 2) bearing mice treated with vehicle only (*n*=8) or tamoxifen (*n*=8) *in vivo*. (**b**) Kaplan-Meier survival curves of *Hes1* conditional knockout NOTCH1-induced leukemia bearing mice treated with vehicle only (*n*=8) or tamoxifen (*n*=8) *in vivo*. (**c**) Quantitative RT-PCR of *Hes1* expression in spleen cells treated 48 hours post transplant with tamoxifen or vehicle. (**d**) PCR analysis of genomic DNA prepared from spleen cells treated 48 hours post transplant and collected at time of death. Bar graph in **a** and **b** indicates mean values and error bars represent s.d. *P* values in **a** and **c** was calculated using the two-tailed Student's *t*-test. *P* value in **b** was calculated using the log-rank test.

Given that ΔE-NOTCH1 driven T-ALLs are highly aggressive tumors, we sought to evaluate if the tumor cells "evolved" to compensate for the loss of Hes1 by upregulating other pathways that would promote their proliferation and survival. Interestingly, flow cytometry quantitative analysis of the T-cell lymphoblast populations at time of death revealed that ΔE-NOTCH1 *Hes1*$^{\text{flox/flox Cre-ERT2}}$ (tumor 1) treated with tamoxifen had evolved from a characteristic

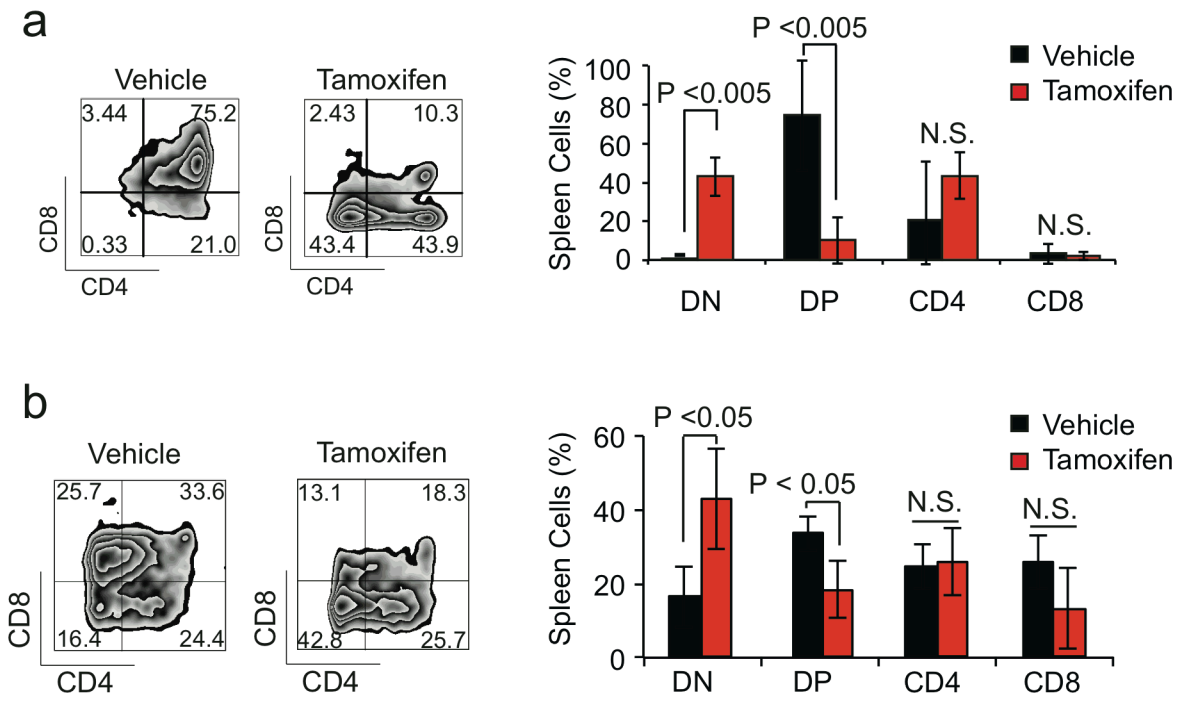

Figure 3.10. *Hes1* deletion drives T-ALL into an immature immunophenotype. (**a**) Flow cytometry analysis and quantification of CD4 and CD8 expression in ΔE-NOTCH1 Rosa26 Cre-ERT2 *Hes1*$^{flox/flox}$ tumor 1 treated with vehicle or tamoxifen and collected at time of death. (**b**) Flow cytometry analysis and quantification of CD4 and CD8 expression in ΔE-NOTCH1 Rosa26 Cre-ERT2 *Hes1*$^{flox/flox}$ tumor 1 treated with vehicle or tamoxifen and collected at time of death. Bar graph in **a** and **b** indicates mean values and error bars represent s.d. *P* values in **a** and **b** was calculated using the two-tailed Student's *t*-test.

double positive T-ALL into a more immature $CD4^{-}CD8^{-}$ double negative immunophenotype (DN) compared to vehicle treated controls (**Figure 3.10.a**). Similarly, *Hes1* inactivation in ΔE-NOTCH1 *Hes1*$^{flox/flox\ Cre\text{-}ERT2}$ tumor 2 resulted in a significant increase in double negative lymphoblasts (**Figure 3.10.b**). We hypothesized that the change in immunophenotype may be due to poly-clonality of the leukemia. However, southern blot analysis of Vβ rearrangement of the TCR revealed all mice transplanted with NOTCH1-*Hes1*$^{flox/flox}$ TmxCre tumor 1 T-ALL

contained the same Vβ rearrangement and were therefore derived from the same clone (**Figure 3.11**). In order to further explore the pathways facilitating for the progression of T-ALL in the absence of *Hes1,* as well as the shift of DP positive cells towards DN cells, we performed microarray gene expression profiling using splenic cells collected at death from ΔE-NOTCH1 *Hes1*$^{flox/flox\ Cre\text{-}ERT2}$ (tumor 1) bearing mice treated with vehicle only or tamoxifen. Microarray analysis identified 47 upregulated and 52 downregulated transcripts (fold change>2.5; *P* <0.01)

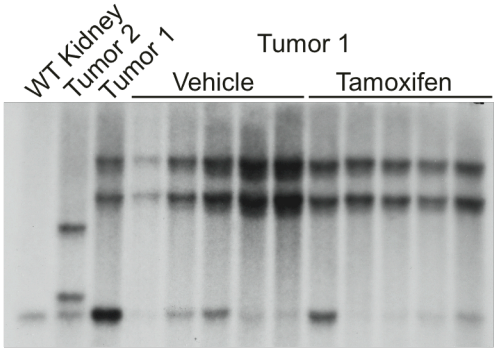

Figure 3.11. Clonality of *Hes1* conditional knockout T-ALL. Southern blot analysis of TCR rearrangement in *Hes1* conditional knockout NOTCH1-induced T-ALL primary tumors (tumor 1 and 2) and secondary transplant of tumor 1 treated with vehicle only or tamoxifen.

(**Figure 3.12**). Interestingly, the gene with the second highest fold change is a member of the *Hes/Hey* family, *Hey1.* The upregulation of *Hey1* may be acting in a compensatory mechanism, in which the Hey1 may drive the regulation of pathways normally controlled by *Hes1.* To idenfiy pathways contributing to the pathogensis of T-ALL in the absense of Hes1, we performed GSEA anaylsis across the C2 database. Genes upregulated in mice infiltrated with *Hes1* inactivated NOTCH1-induced T-ALL showed enrichment in pathways involved in T cell signaling, differentiation and proliferation including MAPK, GATA3, IL4, RUNX1, and WNT signaling

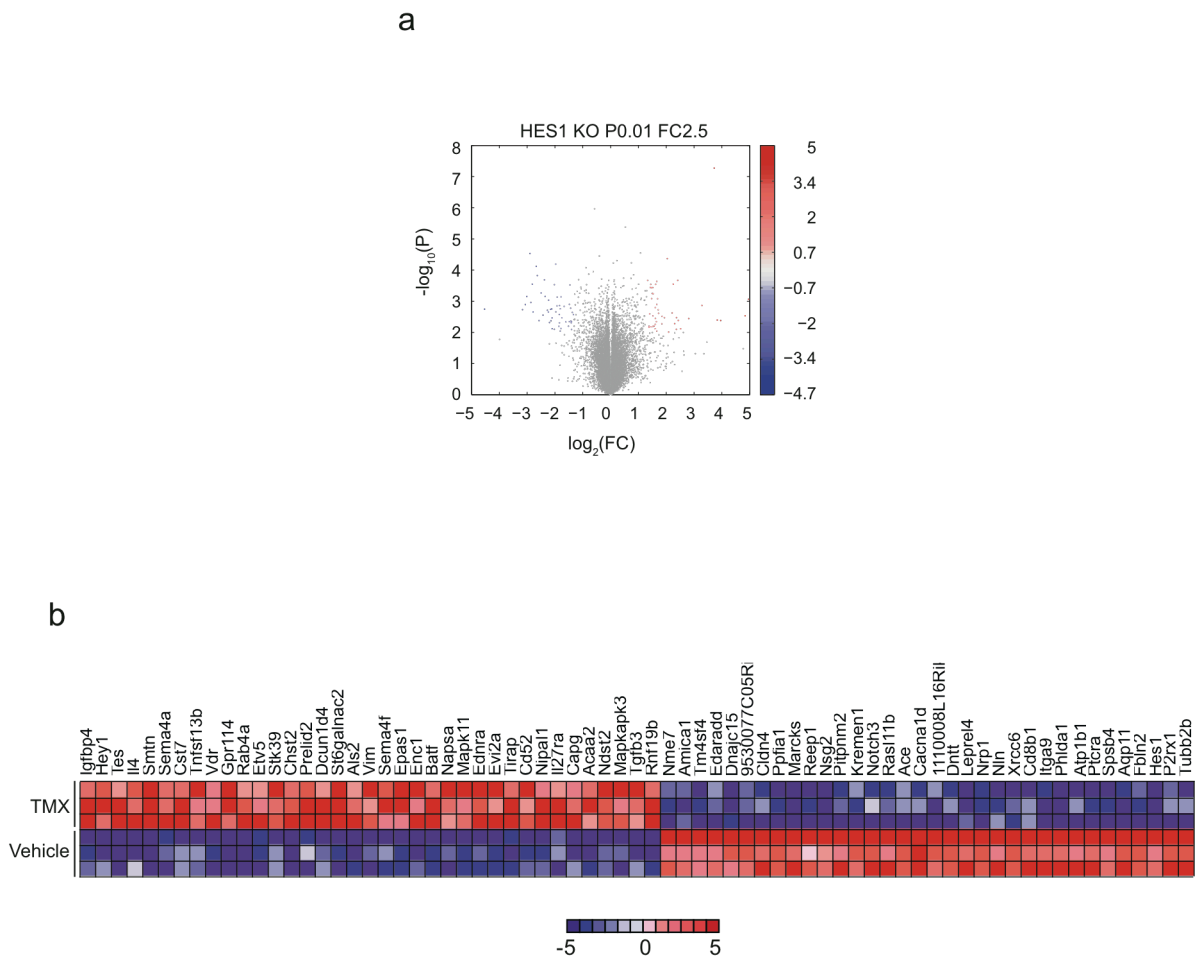

Figure 3.12. Gene expression changes after *Hes1* deletion in T-ALL. (**a**) Volcano plot representation of the differentially expressed genes upon loss of *HES1* P<0.01 and -1.4>F.C.<1.4 (**b**) Heat map representation of the top differentially expressed genes (*P* < 0.01) between mice transplanted with *Hes1* conditional knockout NOTCH1-induced T-ALL cells (Tumor 1), treated with vehicle vs. tamoxifen, and collected at time of death. The scale bar shows color-coded differential expression with red indicating higher levels of expression and blue indicating lower levels of expression.

pathways (**Figure 3.13.a**). Furthermore, GSEA of genes downregulated after *Hes1* deletion in mice infiltrated with T-ALL had a significant enrichment in genes involved in telomere maintenance, NOTCH1 signaling pathway, RNA polymerase promoter opening, fanconi pathway, early T lymphocyte differentiaiton, and double positive thymocytes (**Figure 3.13.b**).

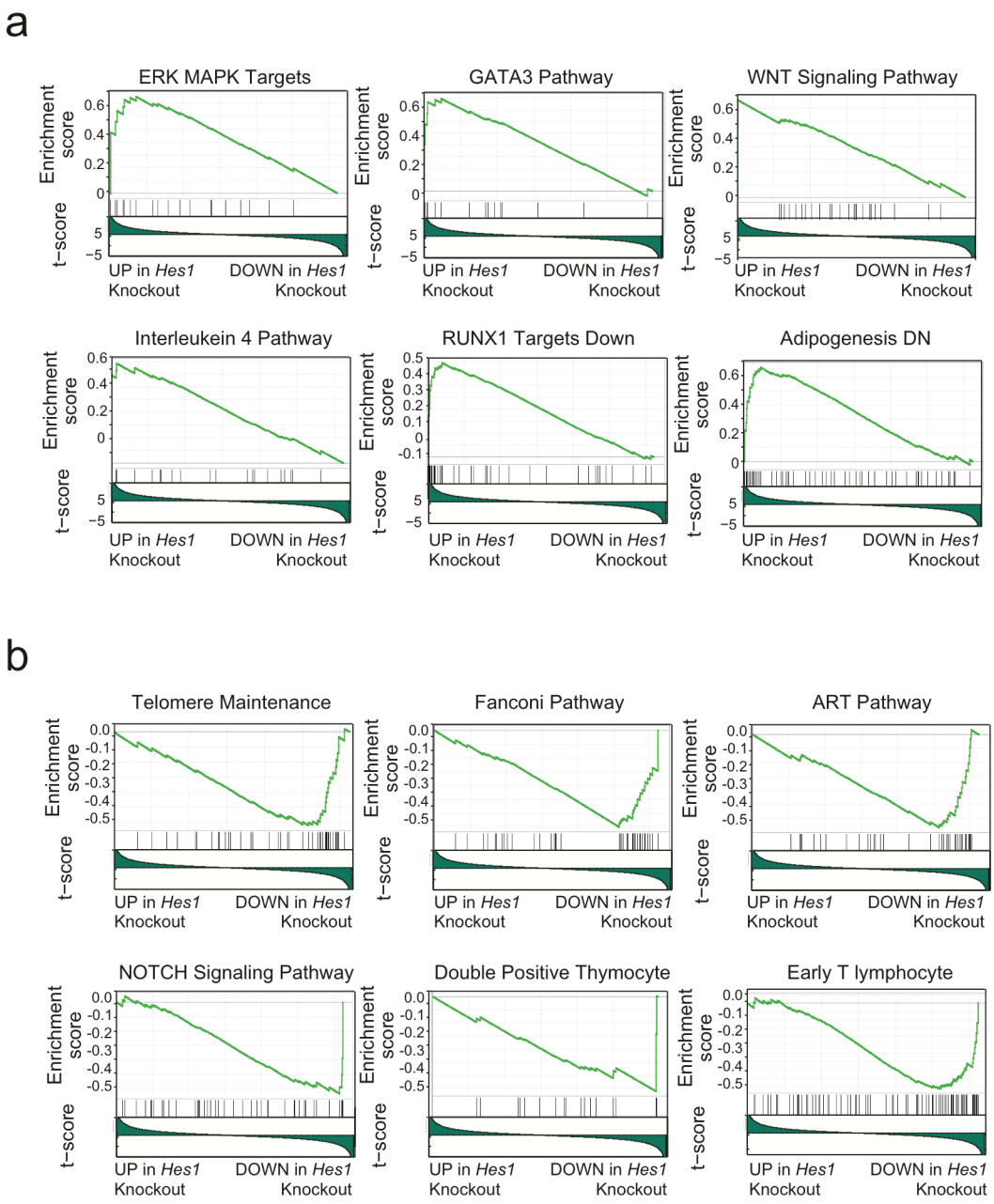

Figure 3.13. GSEA of genes differentially expressed after *Hes1* knockout (**a**) Representative examples of gene set enrichment plots corresponding to GSEA analysis of MSigDB C2 data sets enriched in the upregulated expression signature associated with *Hes1* knockout in NOTCH1-induced T-ALL. (**b**) Representative examples of gene set enrichment plots corresponding to GSEA analysis of MSigDB C2 data sets enriched in the downregulated expression signature associated with *Hes1* knockout in NOTCH1-induced T-ALL.

Hes1 requirement for the maintenance of T-ALL

We established that loss of *Hes1* during the early phases of infiltration delays the progression of T-ALL, but within that experiment we were not able to capture the early effects of *Hes1* inactivation in T-ALL. We set to answer the question: What are the immediate consequences induced by *Hes1* loss in mice infiltrated with NOTCH1-induced T-ALL? Towards this goal, we transplanted ΔE-NOTCH1 Rosa26 Cre-ERT2 *Hes1*$^{flox/flox}$ tumor 1 into 6 lethally irradiated mice and waited for the leukemia to infiltrate the mice. We monitored mice for disease progression by FACS analysis of NOTCH1-GFP lymphoblasts in the peripheral blood. Once 40-70% GFP+ blasts were detected we treated leukemia-bearing recipients with tamoxifen to induce Cre-mediated deletion of the *Hes1* gene or with vehicle only (sunflower oil) as control. In these experiments, tamoxifen-induced activation of Cre-recombinase rapidly and effectively abrogated *Hes1* expression which was validated by DNA and RNA (**Figure 3.14.a** and **b**). Remarkably, and consistent with the cellular effects induced by HES1 depletion in human cells, genetic ablation of *Hes1* in mouse NOTCH1-induced leukemia resulted in marked antileukemic effects *in vivo*. Analysis of leukemia tumor burden 24 hours after *Hes1* deletion revealed a marked decrease of spleen size in tamoxifen-treated animals compared with controls (**Figure 3.14.c** and **d**). Moreover, histological analysis of spleen revealed a “starry sky” morphology indicative of extensive apoptosis in tamoxifen-treated mice compared to vehicle-treated controls. Peripheral organ histology including the liver and kidneys in tamoxifen treated mice showed a profound decrease in leukemia compared to vehicle treated controls (**Figure 3.14.e**).

The antileukemic effects of *Hes1* inactivation were validated in a similar experiment performed with T-ALL cells from an independent ΔE-NOTCH1 tamoxifen-inducible Hes1 knockout mouse (**Figure 3.15**). In this experiment we treated a cohort of mice transplanted with ΔE-NOTCH1 Rosa26 Cre-ERT2 *Hes1*$^{flox/flox}$ tumor 2 with vehicle only (n=4) or tamoxifen (n=4) after they displayed over 50% peripheral lymphoblast infiltration (**Figure 3.15**). Tamoxifen treated mice had over a two-fold decrease in spleen size compared to

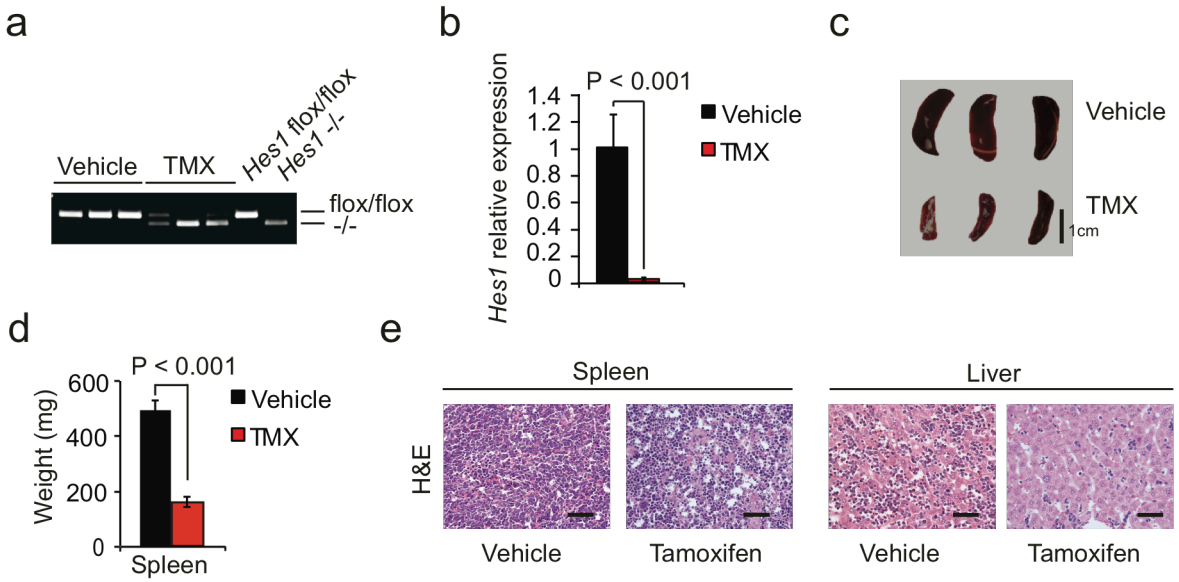

Figure 3.14. Acute antileukemic effects of *Hes1* inactivation in NOTCH1-induced T-ALL tumor 1. (**a**) PCR analysis of genomic DNA from *Hes1* conditional knockout T-ALL tumor 1 (ΔE-NOTCH1 Rosa26 Cre-ERT2 *Hes1*$^{flox/flox}$ tumor 1) bearing mice after 24 hour treatment with vehicle only (*n*=3) or tamoxifen (*n*=3) *in vivo*. (**b**) Quantitative RTPCR analysis of *Hes1* expression in cells isolated from *Hes1* conditional knockout T-ALL (ΔE-NOTCH1 Rosa26 Cre-ERT2 *Hes1*$^{flox/flox}$ tumor 1) bearing mice treated with vehicle only (*n*=3) or tamoxifen (*n*=3) *in vivo*. (**c**) Spleen size *Hes1* conditional knockout leukemia (ΔE-NOTCH1 Rosa26 Cre-ERT2 *Hes1*$^{flox/flox}$ tumor 1) bearing mice treated with vehicle only (*n*=3) or tamoxifen (*n*=3) *in vivo* (**d**) Quantification of spleen weight in *Hes1* conditional knockout leukemia bearing mice treated with vehicle only (*n*=3) or tamoxifen (*n*=3) *in vivo.* (**e**) Representative images of hematoxylin and eosin staining tissue micrographs of liver and spleen sections from *Hes1* conditional knockout leukemia bearing mice treated with vehicle only or tamoxifen. Scale bars represent 50 μm. **a-e** represents 3 individual mice per group from 1 representative experiment. Bar graphs in **b** and **d** indicate mean values and error bars represent s.d. *P* values in **b** and **d** were calculated using the two-tailed Student's *t*-test.

vehicle controls (**Figure 3.15.c)**. Analysis of tumor burden by FACS analysis of NOTCH1-GFP+ in spleen cells showed a ten-fold decrease in transformed lymphoblasts in those mice treated with tamoxifen compared to their vehicle paired controls (**Figure 3.15.d**). The acute deletion of *Hes1* in two independent NOTCH1-driven T-ALL tumors display the major role Hes1 plays in the maintenance of T-ALL. To rule out off-target effects possibly induced by the treatment of

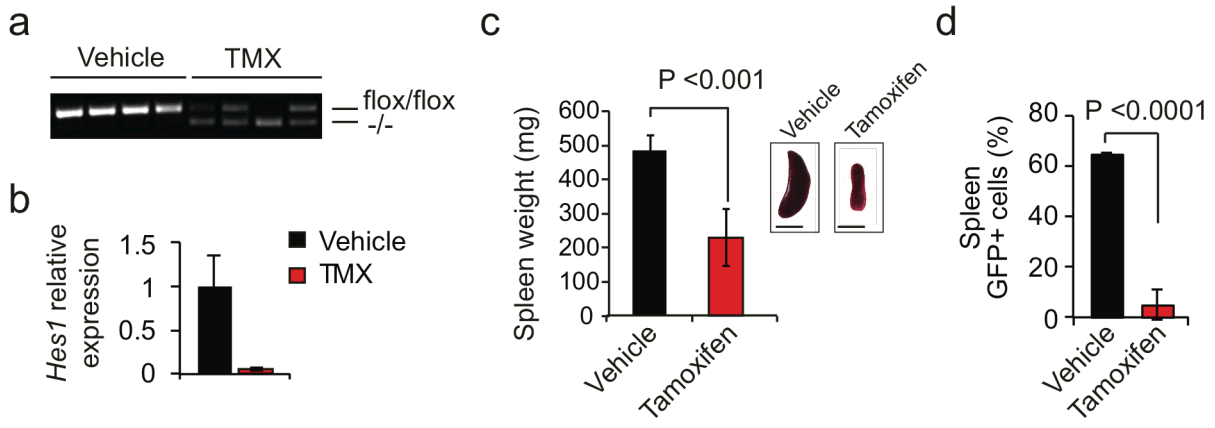

Figure 3.15. Acute antileukemic effects of *Hes1* inactivation in NOTCH1-induced T-ALL tumor 2. (**a**) PCR analysis of genomic DNA from *Hes1* conditional knockout T-ALL tumor 2 (ΔE-NOTCH1 Rosa26 Cre-ERT2 *Hes1*$^{flox/flox}$ tumor2) bearing mice after 24 hour treatment with vehicle only (*n*=4) or tamoxifen (*n*=4) *in vivo*. (**b**) Quantitative RT-PCR analysis of *Hes1* expression in cells isolated from *Hes1* conditional knockout T-ALL (ΔE-NOTCH1 Rosa26 Cre-ERT2 *Hes1*$^{flox/flox}$ tumor2) bearing mice treated with vehicle only (*n*=4) or tamoxifen (*n*=4) *in vivo*. (**c**) Quantification of spleen weight in *Hes1* conditional knockout tumor 2 T-ALL bearing mice treated with vehicle only (*n*=4) or tamoxifen (*n*=4) and representative image of spleen of *Hes1* conditional knockout leukemia (ΔE-NOTCH1 Rosa26 Cre-ERT2 *Hes1*$^{flox/flox}$) bearing mice treated with vehicle or tamoxifen *in vivo* (**d**) Quantification of tumor burden by flow cytometry analysis of NOTCH1-GFP in *Hes1* conditional knockout T-ALL tumor 2 after 24 hour treatment with vehicle or tamoxifen. **a-d** represents 4 individual mice per group from 1 representative experiment. Bar graphs in **c** and **d** indicate mean values and error bars represent s.d. *P* values in **c** and **d** were calculated using the two-tailed Student's *t*-test.

tamoxifen or Cre activity, we repeated the experiment by treating mice bearing heterozygous conditional tamoxifen-inducible *Hes1* knockout T-ALL tumor (ΔE-NOTCH1 Rosa26 Cre-ERT2 *Hes1*$^{flox/wt}$) with tamoxifen (n=3) or vehicle (n=3) for 24 hours (**Figure 3.16**). Cre-mediated deletion of one allele of *Hes1* by tamoxifen treatment showed no change in tumor burden measured by spleen size (**Figure 3.16.a**) and weight (**Figure 3.16.b**). In addition, histological analysis of spleen and liver by hematoxylin and eosin staining showed no change in lymphoblast infiltration in peripheral organs (**Figure 3.16.c**). Analysis of the spleens in this cohort of mice made us aware that there were no changes in tumor burden, but we still needed to rule out any slight cellular effects induced by Cre-mediated activity upon tamoxifen treatment.

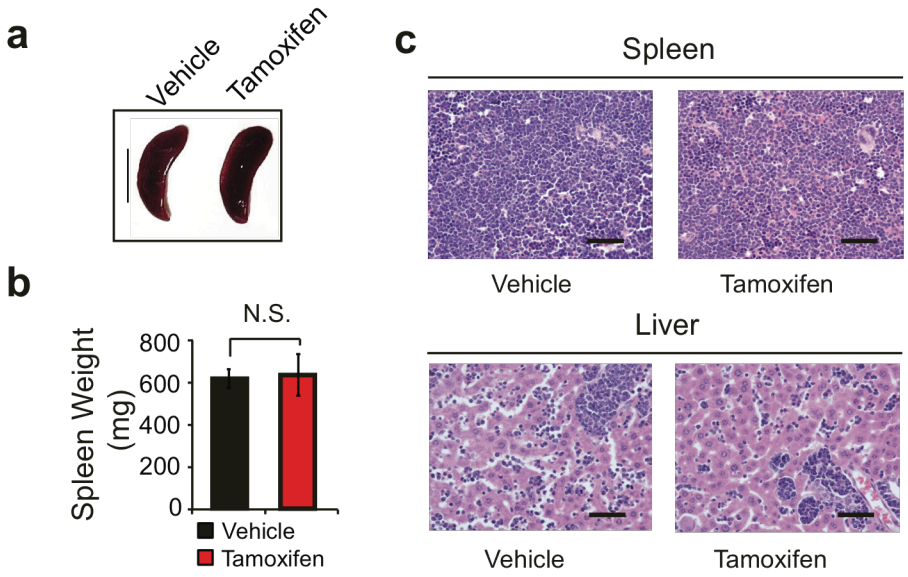

Figure 3.16. Tamoxifen induced activation of Cre-recombinase in T-ALL. (**a**) Representative image of spleens in ΔE-NOTCH1 *Hes1*$^{flox/wt}$ TmxCre leukemia bearing mice treated with vehicle only (n=3) or tamoxifen (n=3). (**b**) Quantification analysis of spleen weight in ΔE-NOTCH1 *Hes1*$^{flox/wt}$ TmxCre leukemia bearing mice treated with vehicle only (n=3) or tamoxifen (n=3). (**c**) Representative images of hematoxylin and eosin staining tissue micrographs of liver and spleen tissue sections from *Hes1* conditional knockout leukemia bearing mice treated with vehicle only or tamoxifen. Experiment conducted once across 3 individual mice per group Scale bars represent 50 μm.

We collected spleen and bone marrow cells from each of the mice treated with vehicle or tamoxifen and looked for differences in the cell cycle and cellular viability between the two treatment groups (**Figure 3.17**). Cell cycle analysis by propidium iodide staining showed no difference between the treatment groups in the populations of cells at G1, S, or G2-M (**Figure 3.17.a**). Likewise, cellular viability measured by AnnexinV/7-AAD had no significant change between vehicle control or tamoxifen treated mice bearing heterozygous conditional tamoxifen-inducible *Hes1* knockout T-ALL (**Figure 3.17.b**).

These results demonstrate that genetic ablation of *Hes1 in vivo and* inactivation of HES1 *in vitro* is detrimental to the survival of NOTCH1 induced T-ALL. Thus, confirming a major role

for Hes1 in maintenance of primary NOTCH1-induced T-ALL and supporting a potential role for Hes1 as a therapeutic target in this disease.

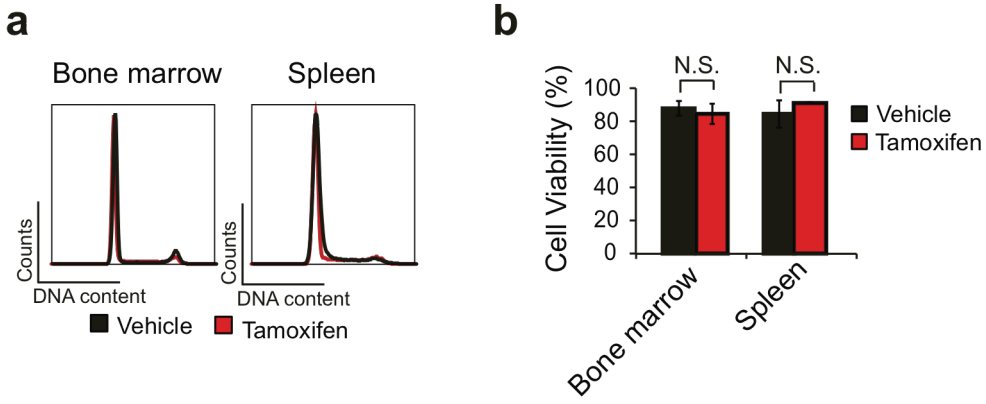

Figure 3.17. Cellular Effects after tamoxifen induced deletion of one *Hes1* allele. (**a**) Cell cycle analysis of spleen cells derived from ΔE-NOTCH1 Rosa26 Cre-ERT2 *Hes1*$^{flox/flox}$ leukemia bearing mice treated with vehicle only or tamoxifen. (**b**) Cell viability analysis of leukemia cells from bone marrow and spleen in ΔE-NOTCH1 Rosa26 Cre-ERT2 *Hes1*$^{flox/flox}$ bearing mice treated with vehicle only or tamoxifen. Experiment conducted once across 3 individual mice per group. Bar graph indicates mean values and error bars represent s.d. *P* values were calculated using the two-tailed Student's *t*-test.

Discussion

Malignant transformation in T-ALL is driven by genetic alterations that target key aspects of early progenitor T cell proliferation, metabolism, differentiation, and survival. In this context, oncogenic NOTCH1 acts as a master and pleiotropic oncogenic factor with multiple effector mechanisms. Among NOTCH1 targets, *HES1* plays an important role downstream of oncogenic NOTCH1 as a regulator of key oncogenic pathways including PI3K and NF-κB signaling (Palomero, Dominguez et al. 2008, Espinosa, Cathelin et al. 2010). The studies outlined here represent the first comprehensive analysis of the phenotypic and transcriptional effects of HES1

loss in NOTCH1-induced T-ALL. Together with previous studies implicating *Hes1* in thymocyte development and NOTCH1-induced transformation (Tomita, Ishibashi et al. 1996, Wendorff, Koch et al. 2010), our integrative analysis of human and murine NOTCH1-driven T-ALLs define a strict requirement for HES1 in tumor maintenance. Specifically, we show that *HES1* inactivation in two different NOTCH1 driven T-ALL human cell lines results in the induction of apoptosis. The induction of apoptosis after HES1 loss was recapitulated in our *Hes1* conditional knockout NOTCH1-driven T-ALL experiments. Cre-mediated deletion of *Hes1* resulted in an increase in overall survival in mice infiltrated with T-ALL. Furthermore, acute deletion of *Hes1* in T-ALL revealed a significant decrease of tumor burden due to the induction of apoptosis of T-ALL cells.

HES1 repression of cell cycle tumor suppressor pathways

Prior to conducting the experiments described above, we hypothesized that given the importance of HES1 in the expansion of early T cell progenitors, HES1 plays a significant role in supporting the proliferation of transformed T cells. Our hypothesis was supported by our results *in vivo* and *in vitro*, however the mechanisms regulating the proliferation were unexpected. Previous advancements in understanding the pathways regulated by HES1 had unveiled the regulation of HES1 in the progression of cell cycle. Specifically, HES1 was shown to suppress *p27 (CDKN1B)* expression in normal fetal thymus, liver, and brain as well as in a cervical cancer cell line (HeLA) (Murata, Hattori et al. 2005). In this same study, HES1 inactivation resulted in the increase of p21 (CDKN1A) in HeLA cells. HES1 was also shown to antagonize p21 induced cellular senescence in fibroblasts (Sang, Coller et al. 2008). Lastly, HES1 was shown to suppress p57 in pancreatic progenitors to promote self-renewal. Because of the involvement of HES1 in the suppression of these cell cycle regulators, I hypothesized that HES1 in T-ALL was promoting cell cycle progression and therefore the proliferation of T-ALL. Our CUTLL1 human cell line knockout cells show a small increase in cells arrested at the G1 phase, and expression

arrays also confirms the upregulation of the known HES1 target p21 supporting our initial hypothesis. However, the arrest was minor compared to the significant decrease in cellular proliferation documented by MTT analysis. In addition, once we repeated the experiment using DND41 cells, cell cycle changes were not consistent. A limitation within our experimental procedures involves the plko.1 vectors used for the expression of the control and HES1 hairpins. The cells analyzed for the cellular effects after HES1 knockout had been expressing the shRNAs for over 1 week because of the 5-day puromycin selection. There is a possibility that HES1 had a more significant effect in cell cycle progression during the initial phases of HES1 inactivation and our experimental set up missed the critical time when the gene expression network upregulated by loss of HES1 exerted its effects. To explore this hypothesis and to capture the early cellular effects of HES1 inactivation, the next step would involve the use of the pINDUCER, a lentiviral vector encoding an shRNA, rtTA3, and a selection marker (Meerbrey, Hu et al. 2011). Briefly, CUTLL1 and DND41 cells would be infected with the pINDUCER lentiviral system expressing shHES1 hairpins or shLUC control. Cells infected would be selected with puromycin and after selection the addition of doxycycline would result in the expression of the rtTA3 with subsequent expression of the shRNAs and therefore inactivation of HES1. Alternatively, HES1 could be targeted for conditional knockout in the human T-ALL lines through the use of the clustered regulatory interspaced short palindromic repeats/Cas9 (CRISPR/Cas9) system (Sander and Joung 2014).

Gene set enrichment analysis of the upregulated genes in CUTLL1 cells with HES1 inactivation crossed over to the C2 database showed a significant enrichment for pathways involved in DNA damage repair, TP53 activation and cell cycle progression. The NOTCH1 pathway is implicated in the suppression of TP53 through the repression of ARF, which normally stabilizes TP53 (Beverly, Felsher et al. 2005). However, this study did not analyze the role of HES1 within the suppression of TP53. The presence of the DNA damage response pathways suggests that HES1 may promote cellular proliferation by inhibiting pro-apoptotic signaling even

under the presence of DNA damage or oncogenic signaling. This hypothesis is supported by the experimental results showing that deletion of HES1 in hematopoietic progenitors results in complete inhibition of NOTCH1 induced T cell transformation (Wendorff, Koch et al. 2010). In addition, oncogenic Kras expressing cells have a proliferative and survival advantage when HES1 is upregulated (Feng, Bommer et al. 2011, Maniati, Bossard et al. 2011). HES1 is critical for the proliferation capacity of DN3 cells differentiating through β-selection (Wong, Knowles et al. 2012). Perhaps, HES1 acts as a protective mechanism of cellular maintenance during the phase of T cell differentiation in which genomic DNA is unstable due to the V(D)J recombination occurring at the *TCR* locus. Therefore, in this scenario HES1 represses DNA damage response pathways to promote cell survival in T cells undergoing DNA recombination in early T cell progenitors of the thymus.

HES1 transcriptional regulation of proliferation and metabolism

The role of HES1 in the maintenance of T-ALL includes the upregulation of pathways involved in cellular proliferation such as PI3K and NF-κB in T-ALL. More specifically, HES1 was demonstrated to directly repress tumor suppressor genes *PTEN* and *CYLD*, proteins involved in the negative regulation of the PI3K and NF-κB pathways respectively (Palomero, Dominguez et al. 2008, Espinosa, Cathelin et al. 2010). Gene set enrichment analysis of the downregulated genes in CUTLL1 cells with HES1 inactivation crossed over to the C2 database showed a significant enrichment for pathways involved in NF-κB, MYC signaling, and cellular metabolism involved in gluconeogenesis and nucleic and amino acid synthesis. The presence of these pathways supports the established role of HES1 in repressing negative regulators of these pathways to promote T-ALL proliferation. HES1 is a known direct repressor of *PTEN*, and PTEN was shown to inhibit AKT signaling and decrease glucose metabolisms in T-ALL cells (Palomero, Dominguez et al. 2008). The significant decrease in metabolism may in part be due release of the HES1 repression at the *PTEN* promoter, therefore resulting in the upregulation of

PTEN and increase inhibition of the AKT pathway. Although there is a high frequency of PTEN mutations in patients (10%), which indicates a worse prognosis, CUTLL1 and DND41 cells express wild type PTEN, and could therefore support the hypothesis that HES1 upregulates cellular metabolism of T-ALL cells through the direct transcriptional repression of *PTEN* tumor suppressor (Palomero, Barnes et al. 2006, Jotta, Ganazza et al. 2010). In addition, the identification of MYC as one of the top downregulated genes upon HES1 inactivation and the GSEA enriched for the MYC transcriptional pathway, brings to question whether there is a NOTCH1-HES1-MYC regulatory loop. NOTCH1 directly binds to the *MYC* proximal and enhancer promoter to activate transcription (Palomero, Lim et al. 2006, Palomero and Ferrando 2009, Herranz, Ambesi-Impiombato et al. 2014). Additionally, there is much crossover between the downstream genes activated by NOTCH1 and MYC, thus reinforcing the genes promoting tumor maintenance (Palomero, Lim et al. 2006). The significant gene expression changes involved in both the NOTCH1 and MYC pathways may suggest that HES1 may directly or indirectly regulate similar gene expression changes and promote cellular survival, proliferation and metabolism.

HES1 is a context-dependent regulator of apoptosis

Our results suggest that although HES1 may regulate the cell cycle progression through various mechanisms in T-ALL, the more significant role of HES1 in the maintenance of T-ALL involves the suppression of apoptotic signaling. Previous studies implicated the NOTCH1-HES1 axis in regulating and promoting apoptosis in B cell acute lymphoblastic leukemia (B-ALL) through the interaction with PARP1, a molecular censor of DNA damage that regulates chromatin structure, DNA metabolism and induction of apoptosis (Kannan, Fang et al. 2011). This study also reported that the pro-apoptotic effects of HES1 expression were specific to B-ALL and not to T-ALL. The difference in the regulation of apoptotic signaling between B and T cells supports the established importance of the NOTCH1-HES1 axis in the bifurcation between

T and B cell lineage commitment in early lymphocyte development and suggests a context dependent function of HES1; HES1 expression in T-ALL inhibits apoptotic signaling whereas pro-apoptotic signals are upregulated by HES1 in B-ALL.

The loss of Hes1 in T-ALL pathogenesis

Given the significant acute antileukemic effects of HES1 inactivation in T-ALL, I hypothesized the deletion of Hes1 would significant increase the survival of mice harboring *Hes1 null* T-ALL. This hypothesis is supported by the significantly increase in survival of mice infiltrated with *Hes1 null* NOTCH1 driven T-ALL (Wendorff, Koch et al. 2010). In this experiment, the mice with *Hes1* inactivation ultimately died from T-ALL, however this was due to a small population of cells that escaped *Hes1* deletion and then progressed to infiltrate the mice. Our experiments similarly show an increase in overall survival upon *Hes1* inactivation supporting the importance of the NOTCH1-HES1 axis in the maintenance of T-ALL. However, in our experiments the mice treated with tamoxifen to induce the deletion of *Hes1* died an average of 10 days after the vehicle-paired controls and did not escape *Hes1* inactivation as PCR analysis of the DNA of these mice showed that the T lymphoblasts had complete deletion of the *Hes1* alleles. Therefore *Hes1* null cells continued the malignant progression of T-ALL in a Hes1 independent pathway. In addition, the transformed T lymphoblast immunophenotype had shifted from mainly DP cells to DN cells. This raises two different questions: (i) what are the pathways involved in adjusting and compensating for the lack of *Hes1* expression in T-ALL? and (ii) why does *Hes1* deletion shift the immunophenotype of T lymphoblasts to a more immature (DN) T cell.

To explore the pathways involved in allowing NOTCH1-induced T-ALL to progress in the absence of Hes1 we explored the differentially expressed genes identified in the mice from our survival experiment (**Figure 3.12**). Gene expression analysis of the top differently expressed genes in *Hes1* knockout T-ALL cells from samples collected in the survival study revealed *Hey1*

as the second most significantly upregulated gene. *Hey1* is a bHLH repressor protein that is often associated with *Hes1*. From this data we could hypothesize that Hey1 represses the HES1 transcriptional network as a compensatory mechanism. However, there is little evidence that Hey1 has a significant role in T cell development and transformation. Also, GSEA shows enrichment in NOTCH signaling pathways among the genes downregulated by *Hes1* inactivation, suggesting that the progression of T-ALL proceeded through a NOTCH1 independent pathway. Our hypothesis is supported by GSEA analysis of the upregulated genes after *Hes1* inactivation across the C2 database, which shows enrichment for pathways involved in WNT signaling pathway, ERK-MAPK, and GATA3. All three pathways are important in the development and maintenance of T cells and have been implicated in assisting the malignant transformation of T cells. For example, the WNT signaling pathways promotes the proliferation of DN1, DN2 and DN3 cells during T cell development, and inhibits DP cells from undergoing apoptosis (Gounari, Aifantis et al. , Weerkamp, Baert et al.). Upregulation of the WNT pathway may provide an alternate to the NOTCH1-HES1 signals to promote proliferation and sustain cellular maintenance in T-ALL in the absence of HES1. In addition, the ERK-MAPK signaling pathway is known to promote cellular proliferation, hematopoietic cell differentiation, cell metabolism (Geest and Coffer 2009, Carr, Kelman et al. 2010). Furthermore the MAPK regulates the stability of GATA3, also found enriched by GSEA, in T cells (Yamashita, Shinnakasu et al. 2005). GATA3 is a zinc-finger master regulator transcription factor essential for T cell development, especially during early T cell commitment, β-selection, and $CD4^+$ T cell development (Ho, Tai et al. 2009). A method in which to further support our hypothesis that these cells are promoting their own survival and proliferation through NOTCH1 independent pathways, would involve the treatment of GSI to the T-ALL cells with *Hes1* inactivation collected from the survival mice treated with tamoxifen. Lack of antileukemic effects of GSI would provide evidence of the activation of NOTCH1 independent pathways involved in tumor maintenance. Taken together, the gene expression analysis suggests transformed lymphoblasts that survived

after *Hes1* inactivation, upregulated T cell transcriptional regulators and signaling pathways to promote cellular proliferation and survival.

HES1 inactivation in the hematopoietic stem cell compartment results in a significant decrease in all T cell populations of the thymus (Tomita, Hattori et al. 1999, Wendorff, Koch et al. 2010). However, on closer inspection, the percentage of DP cells significantly decreases, while the percentage of DN cells increases (Wendorff, Koch et al. 2010). Our tumor immunophenotype data collected in our survival experiment shows a similar trend, cells lacking HES1 decreased the population of DP cells and increased the population of DN in two independent $Hes1^{flox/flox}$ NOTCH1-induced T-ALL (**Figure 3.10**). An interesting aspect about the decrease in the DP population is that during normal T cell development, HES1 is expressed at high levels during the early phases T cell development especially within the DN population of cells, however after β-selection and differentiation towards DP cells, *HES1* is downregulated. Thus, it is surprising that the percentage of DP cells would decrease in the absence of HES1. A possible mechanism regulating the decrease of the DP population in T-ALL arises in the gene expression changes documented. GSEA of the genes downregulated across the C2 database reveal enrichment in the double positive thymocyte gene signature, suggesting a possible mechanism in which the decrease of double positive cells could relate to the inhibition of the signature that drives differentiation towards DP cells. Looking more closely at the specific genes, *Ptcra* is significantly downregulated in the population of cells with *Hes1* inactivation. The pre-T-cell receptor, composed of the TCR and CD3 molecules is critical for the development of αβ T cells. *Ptcra* homozygous knockout mice have normal populations of hematopoietic cells, however, thymocytes are reduced to less than 10% of the normal amount of cells, with an increase in the percentage of DN and a decrease in the percentage of DP cells (Fehling, Krotkova et al. 1995). The comparable phenotypes between cells lacking *Ptcra* or *Hes1* suggest a possible regulatory loop in which HES1 promotes the upregulation of the *Ptcra* gene through either direct or indirect regulation. In addition to the decrease in *Ptcra*, there is a

downregulation of pathways involved in DNA maintenance and repair including telomere maintenance, fanconi anemia pathway, ATR pathway and E2F targets. The downregulation of these pathways is indicative of *Hes1* knockout T-ALL cells promoting their survival by downregulating the checkpoint mechanisms involved in the progression in G1 and S phase of cell cycle. This may be of particular importance in T-cell immunophenotype and development due to the DNA replication and recombination occurring in both double negative and double positive cells.

Chapter 4
HES1 inhibits *BBC3* in NOTCH1 induced T-ALL

Introduction

The NOTCH1-HES1 axis is implicated in sustaining cellular growth signaling in T-cell leukemogenesis. HES1 is known to promote the PI3K pathway by downregulating the tumor suppressor PTEN, and the NF-κB signaling pathway by inhibiting CYLD (Palomero, Sulis et al. 2007, Espinosa, Cathelin et al. 2010). Until now, there was no specific link suggesting that HES1 inhibits apoptotic pathways to promote and sustain T cell transformation. Our findings discussed in chapter three show that inhibition of the NOTCH1-HES1 axis is detrimental to the survival of T lymphoblasts. Thus, interrogation of the gene expression changes after *HES1* inactivation by GSEA showed enrichments in DNA damage pathways and the TP53 pathway. Furthermore, deletion of *Hes1* delayed disease progression of NOTCH1-induced T-ALL by activating apoptosis in cells lacking the expression of Hes1.

The acute deletion of *Hes1* in mice bearing NOTCH1-induced T-ALL displayed a significant decrease in tumor load quantified by total number and histological analysis (**Figure 3.14** and **Figure 3.15**). In addition, mice treated with tamoxifen to induced *Hes1* deletion showed more signs of physical illness than those treated with vehicle control, including lack of movement, decreased weight and body temperature, and hunched backs. Given the massive induction of cellular death, we hypothesized that they were undergoing what is known as tumor lysis syndrome. Tumor lysis syndrome is an oncological emergency that occurs when tumor cells release their contents into the bloodstream; in our case this was induced by *Hes1* loss. The large quantity of tumor cells releasing their intracellular contents creates more potassium, phosphorus, nucleic acids, and cytokines than the body can dispose of, and ultimately leads to hyperuricemia, hyperkalemia, hyperphosphatemia, and hypocalcemia (Howard, Jones et al. 2011). In our experiment, 24 hours post treatment was actually too late to actively capture the

cell undergoing apoptosis. The "starry" sky appearance in the spleenic histology is in fact the macrophages engulfing the dead apoptotic tumor cells (Ogden, Pound et al. 2005). In this chapter, we unveil the specific mechanisms driving these cells into programmed cell death.

Results

Knockout of *Hes1* in NOTCH1 driven T-ALL *in vitro*

In an effort to establish a system in which we could monitor the induction of apoptosis after *Hes1* inactivation in a fully controlled setting, we developed a cell line that could be maintained in cell culture from our *Hes1* conditional knockout NOTCH1 induced T-ALL tumor 1 (**Figure 3.6**). Under normal serum conditions without any cytokine support, T-ALL cells can grow in cell culture for only a few days. To enable the changes needed in order for these cells to proliferate continuously as a cell line *in vitro* we tested different growing conditions: (1) serum (+β-mercaptoethanol), (2) serum (+β-mercaptoethanol) plus IL2, IL7 (3) serum (+β-mercaptoethanol) plus OP9 stromal cells (4) serum (+β-mercaptoethanol) plus OP9 stromal cells, IL2, and IL7. We found that primary murine T-ALL cells grow most optimally if plated in co-culture with OP9 cells for two weeks and supplemented with IL7 and β-mercaptoethanol. After the two weeks, T cells can be removed from the stromal cells and grown in suspension culture with IL7 and β-mercaptoethanol supplementation. After 4 weeks, cells were weaned off of the cytokines and underwent three consecutive rounds of freezing in 90% FBS and 10% DMSO and thawing before subsequent experiments were performed. Having established a *Hes1* conditional knockout NOTCH1-induced cell line we set to determine whether *in vitro* deletion would produce the similar cellular changes we established in prior experiments. We analyzed the changes in cell cycle, proliferation and cellular viability in a time course experiment of 3 consecutive days. Supporting previous findings (**Figure 3.1**), loss of Hes1 did not induce significant changes in cell cycle at any of the three times points (**Figure 4.1**). AnnexinV staining revealed a gradual increase in apoptotic and dead cells, with the most significant decrease in viability at 72 hours

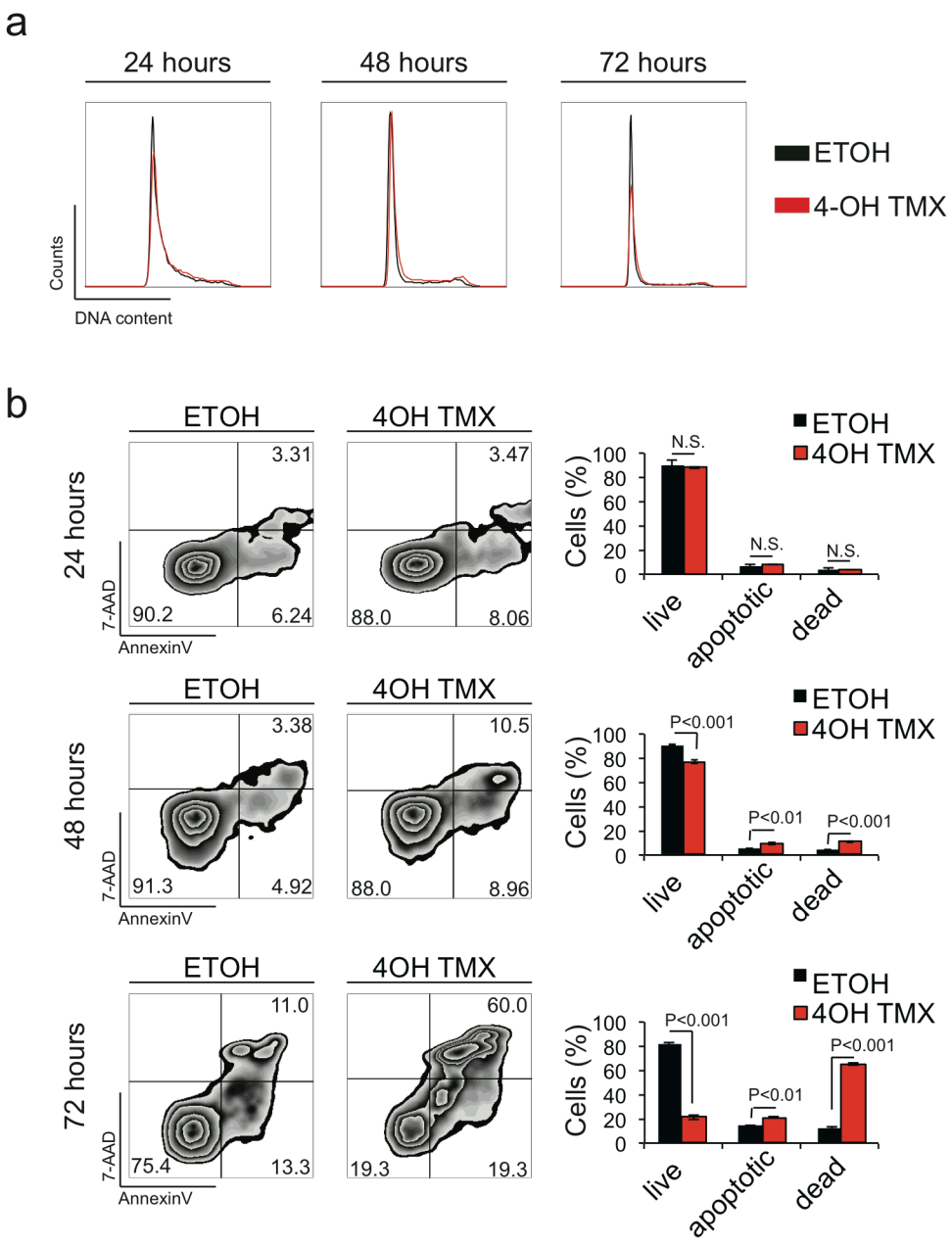

Figure 4.1. *In vitro* knockout of *Hes1* in NOTCH1-induced T-ALL cell line. (**a**) Cell cycle analysis by propidium iodide staining of *Hes1* conditional knockout NOTCH1 induced T-ALL cells 24, 48, and 72 hours after treatment with 4-hydroxy tamoxifen (4-OH TMX) or vehicle only (ethanol) control (**b**). Cell viability analysis by AnnexinV and 7-AAD staining of *Hes1* conditional knockout NOTCH1 induced T-ALL cells 24, 48, and 72 hours after treatment with 4-hydroxy tamoxifen (4-OH TMX) or vehicle only (ethanol) control *in vitro.* Bar graphs indicate mean values and error bars represent s.d. of biological triplicates. *P* values were calculated using the two-tailed Student's *t*-test.

post treatment with 4-hydroxy tamoxifen (4-OH TMX) (**Figure 4.1.b**).

It did not escape our attention that the induction of apoptosis was significantly delayed *in vitro* compared to our *in vivo* experiments. There are various hypotheses to why the cells are more resistant in a cell culture setting. For one, the cells acquired genetic changes during the establishment of these cells as a cell line. These changes allowed the cells to survive in a setting where they would normally induce programmed cell death, and may therefore be less sensitive to the loss of *Hes1.* However, ultimately the cells died after 72 hours, indicating that *Hes1* is critical for the maintenance of NOTCH1-induced T-ALL. Secondly, cells in culture are maintained in an artificial environment, with fresh media, serum, and cytokines provided every third day. This provides a relatively stress-free microenvironment that may not be representative of T lymphoblasts actively infiltrating peripheral organs. The loss of *Hes1* may be more detrimental to cells under cellular stress, because Hes1 may be downregulating tumor suppressers and pro-apoptotic signals. To test this hypothesis, we seeded cells in decreasing concentrations of serum to induce stress on the NOTCH1-induced T-ALL murine cell line. At the same time we treated cells with tamoxifen or vehicle only (ethanol) and analyzed the cellular viability by AnnexinV over the course of three days. In these experiments, cells under lower serum conditions had a significant decrease in viability within 48 hours compared to those cells in normal serum conditions (**Figure 4.2**). Cells under normal serum conditions were at 70% viability after loss of *Hes1* compared to less than 30% viability in the low serum cultures (**Figure 4.2.a**). By 72 hours, there was less of a difference in apoptotic and dead cells between the tamoxifen treated cells in different concentration of serum (**Figure 4.2.b**). Therefore, cellular stress increases the early apoptotic effects of *Hes1* inactivation in T-ALL. We further tested our hypothesis by inducing DNA damage with etoposide, a topoisomerase inhibitor. *Hes1* conditional knockout NOTCH1-induced cells were treated with either tamoxifen or vehicle and with increasing doses of etoposide. Cellular viability was measured 72 hours after treatment by

MTT analysis (**Figure 4.3**). Dose response viability cell curves shows that cells lacking Hes1 expression are more sensitive to DNA damaging environments.

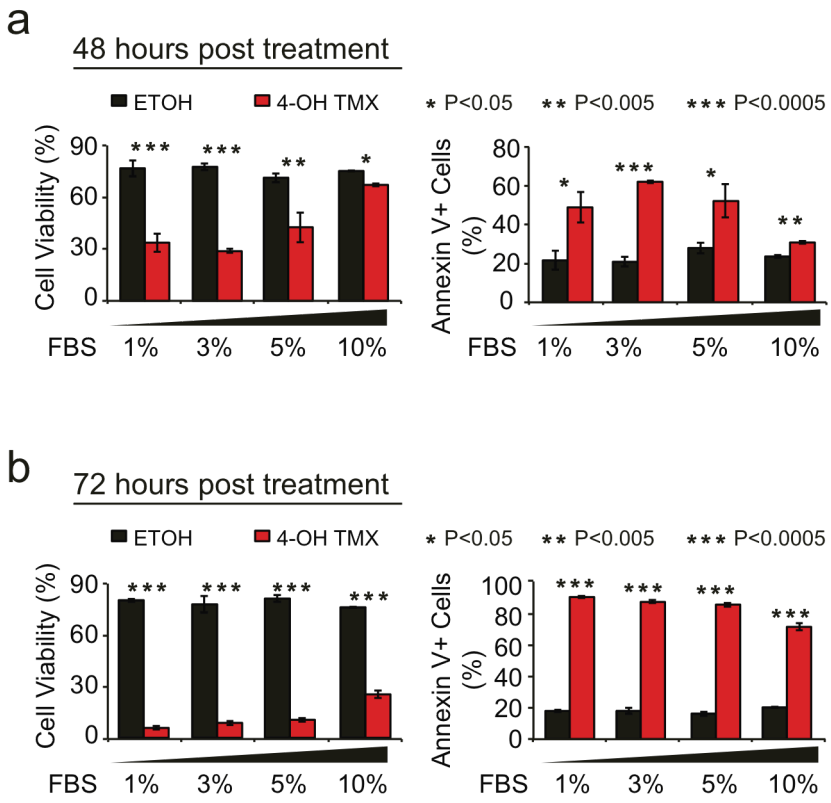

Figure 4.2. *Hes1* inactivation in NOTCH1 induced T-ALL under cellular stress. (**a**) Cell viability analysis by AnnexinV and 7-AAD staining of *Hes1* conditional knockout NOTCH1 induced T-ALL cells in decreasing amounts of serum 48 hours after treatment with 4-hydroxy tamoxifen (4-OH TMX) or vehicle only (ethanol) control. (**b**) Cell viability analysis by AnnexinV and 7-AAD staining of *Hes1* conditional knockout NOTCH1 induced T-ALL cells in decreasing amounts of serum 72 hours after treatment with 4-hydroxy tamoxifen (4-OH TMX) or vehicle only (ethanol) control *in vitro.* Bar graphs indicate mean values and error bars represent s.d. of biological triplicates. *P* values were calculated using the two-tailed Student's *t*-test.

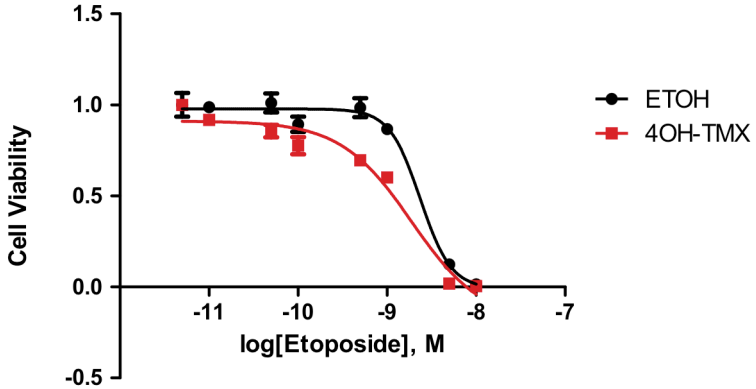

Figure 4.3. *Hes1* inactivation in T-ALL under DNA damaging conditions. Dose response cell viability curves of *Hes1* conditional knockout NOTCH1 induced T-ALL cells after 72-hour treatment with increasing concentrations of etoposide in combination with vehicle (ethanol) control or 4-hydroxy tamoxifen *in* vitro. Data points on the curve indicate mean values and error bars represent s.d. of biological triplicates. *P* values were calculated using the two-tailed Student's *t*-test.

HES1 transcriptional targets regulate apoptotic signaling

We established that the *Hes1* conditional knockout cells undergo apoptosis within the first 72 hours after tamoxifen treatment with no significant changes in the cell cycle. Next, we analyzed the transcriptional programs triggered upon Hes1 knockout in primary NOTCH1-induced T-ALL lymphoblasts *in vitro*. Given that after 48 hours of tamoxifen treatment under normal serum conditions, cells are beginning to undergo apoptosis, we collected cells at 36 hours post treatment with tamoxifen or vehicle to capture to initiating gene expression changes that drive cells towards programmed cell death. Volcano plot shows the distribution of differentially expressed genes by significance on the y-axis (P-value) and fold change (log FC) on the x-axis (**Figure 4.4.a**). Microarray analysis of *Hes1* knockout T-ALL cells collected 36 hours after tamoxifen treatment identified 34 upregulated and 17 downregulated genes (fold change >1.3, $P < 0.005$). Most notably, the transcriptional programs upregulated by *Hes1* inactivation included important mediators of cell signaling such as *Wnt6*, *Cxcr5, Smad3* and

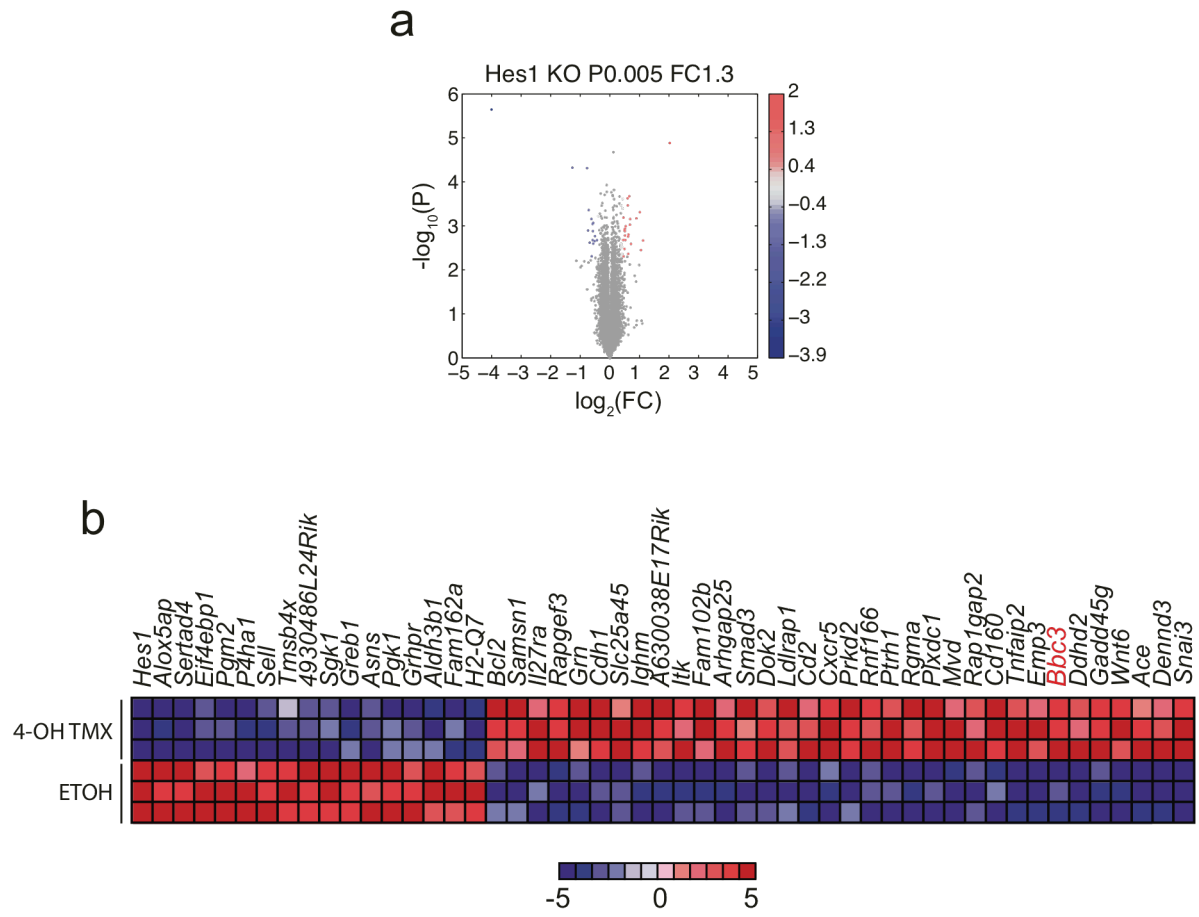

Figure 4.4. Acute gene expression changes upon *Hes1* inactivation in NOTCH1 induced T-ALL. (**a**) Volcano plot representation of the differentially expressed genes upon loss of *Hes1* P < 0.005 and -1.3> F.C. <1.3 (**b**) Heat map representation of the top 50 differentially expressed genes (*P* < 0.005) between *Hes1* conditional knockout NOTCH1-induced T-ALL treated for 36 hours with 4-hydroxy tamoxifen (4-OH TMX) or ethanol control (ETOH). The scale bar shows color-coded differential expression with red indicating higher levels of gene expression and blue indicating the lower levels of gene expression.

Il27ra; the *Gadd45g* cell cycle regulator and *Bbc3*, the gene encoding Puma, a major BH3-only Bcl2-member pro-apoptotic factor (**Figure 4.4.b**). These genes are of particular interest given that they are the early genes upregulated after *Hes1* loss. Therefore, they are potential direct targets repressed by Hes1.

We previously analyzed the gene expression changes induced by *HES1* inactivation in CUTLL1 cells (**Figure 3.3**). To see whether the upregulated gene set after *Hes1* knockout aligned in the same direction as the differentially expressed genes in the human cell line, we preformed GSEA. The genes upregulated upon genetic deletion of *Hes1* were significantly enriched for genes that comprise the transcriptional signature associated with *HES1* shRNA-mediated depletion in CUTLL1 T-ALL cells (**Figure 4.5.a**). In addition, consistent with a major role of Hes1 as a transcriptional repressor downstream of NOTCH1, we observed a significant positive enrichment for murine genes upregulated upon *Hes1* deletion in the upregulated gene expression signature triggered by NOTCH1 inactivation via γ-secretase inhibitor treatment of mice infiltrated with NOTCH1 driven T-ALL (**Figure 4.5.b**). Furthermore, C2-analysis showed enrichment of datasets involved in the apoptotic cascade, including caspase activation and IFN-α and IFN-β (**Figure 4.6.**). Genes downregulated by *Hes1* deletion were also enriched for cellular metabolism, cell cycle progression, Myc transcription and pediatric cancer markers, again supporting the significant role *Hes1* has in the regulation of the NOTCH1 signature.

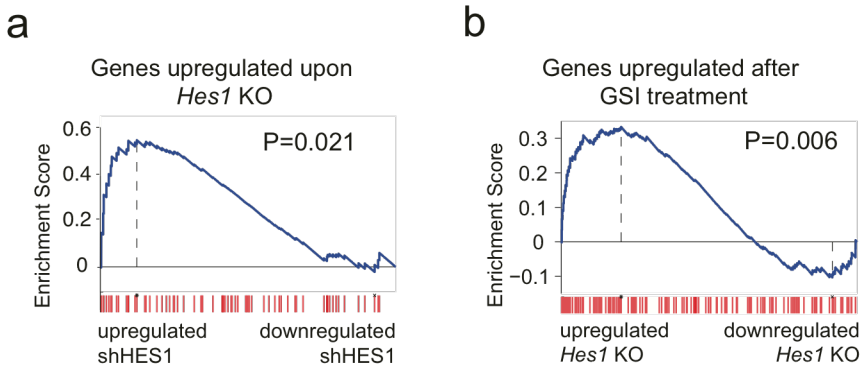

Figure 4.5. GSEA of *Hes1* inactivation in NOTCH1 induced T-ALL. (**a**) GSEA of genes upregulated 36 hours after *Hes1* knockout in NOTCH1-induced T-ALL *in vitro* compared to the transcriptional signature associated with HES1 knockdown in CUTLL1 cells. (**b**) GSEA of genes upregulated after DBZ gamma-secretase inhibitor (GSI) treatment of NOTCH1-induced murine T-ALL cells compared to the transcriptional signature induced by 4-hydroxy tamoxifen treatment in *Hes1* conditional knockout T cell leukemia cells (*Hes1* KO).

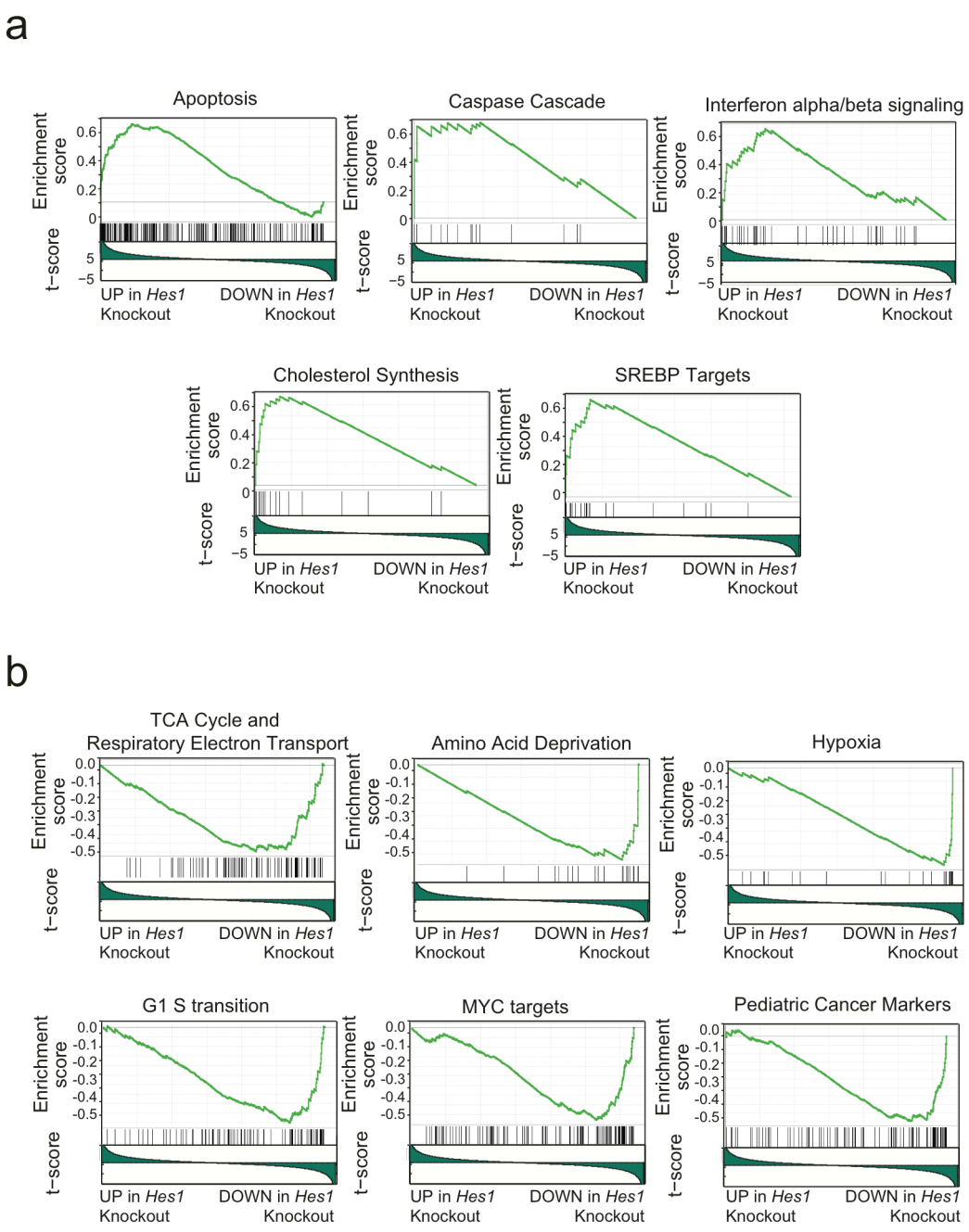

Figure 4.6. GSEA of acute *Hes1* deletion in NOTCH1 induced T-ALL. (**a**) GSEA of genes upregulated 36 hours after *Hes1* knockout in NOTCH1-induced T-ALL *in vitro* compared to the C2 database show enrichment for pathways involved in apoptosis. (**b**) GSEA of genes downregulated after 36 hours after *Hes1* knockout in NOTCH1-induced T-ALL *in vitro* compared to the C2 database show enrichment in pathways involved in cellular metabolism, Myc pathway, cell cycle progression, and cancer markers upregulated in pediatric cancers.

BBC3 is a direct transcriptional target of HES1

Based on these results, we carefully analyzed the differentially expressed genes to determine which might be activating the apoptotic pathway. *Bbc3,* also known as Puma, is a major activator of P53 dependent and P53 independent apoptosis. Puma is upregulated during times of stress including DNA damage, cytokine withdrawal, and serum starvation (Jeffers, Parganas et al. 2003). Puma functions by directly activating Bax to induce cytochrome C release from the mitochondria into the cytoplasm, resulting in the activation of the caspase pathway. In addition, Bbc3 can directly bind anti-apoptotic Bcl2 factors to inhibit their functions. Given the well-established role of Puma as mediator of programmed cell death downstream of multiple apoptotic stimuli including p53 activation (Hikisz and Kilianska 2012), we hypothesized that HES1 could promote leukemia cell survival via direct transcriptional repression of the *BBC3* gene. We first validated the upregulation of *Bbc3* in our murine NOTCH1-induced T-ALL cell line treated with 4-OH Tamoxifen when compared to vehicle (ethanol) control. RT-PCR shows a 50% increase in Bbc3 expression upon treatment with tamoxifen (**Figure 4.7.a**). Western blot analysis of *Hes1* conditional knockout T-ALL cells treated with tamoxifen for 48 hours in different serum conditions shows Puma protein upregulation (**Figure 4.7.b**) upon *Hes1* inactivation. Here we see an incremental increase in protein expression especially as the cells are put under stress, recapitulating the phenotype we see by AnnexinV staining. Bcl2, a anti-apoptotic factor, was also upregulated among the top 50 differentially expressed genes identified by the microarray analysis. However, western blot analysis shows a slight decrease in Bcl2 protein expression when Bbc3 is upregulated. Furthermore, we analyzed the protein expression level of BBC3 in cells infected with lentivirus expressing shLUC or shHES1. DND41 show an increase in protein expression of Bbc3 in cells expressing both HES1 hairpins compared to cells expressing shLUC control (**Figure 4.8**).

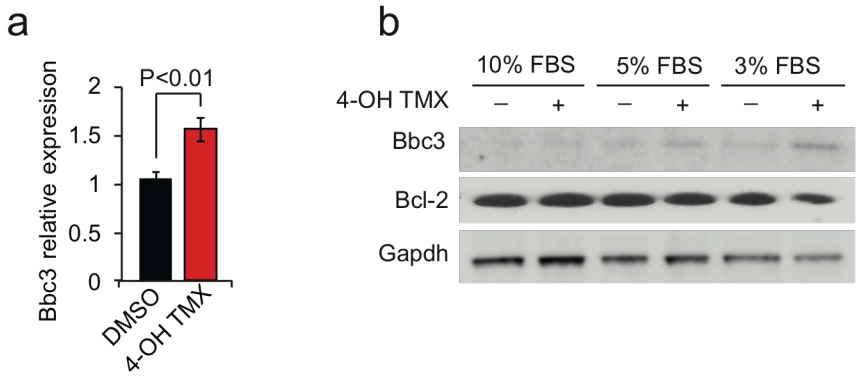

Figure 4.7. *Bbc3* upregulation after *Hes1* knockout in NOTCH1-induced T-ALL. (**a**) Quantitative RT-PCR of *Bbc3* expression in *Hes1* conditional knockout T-ALL (ΔE-NOTCH1 Rosa26 Cre-ERT2 *Hes1*$^{flox/flox}$) after treatment with vehicle only (ETOH) or 4-hydroxy tamoxifen (4-OH TMX) *in vitro*. (**b**) Western blot analysis of Bbc3 expression in *Hes1* conditional knockout leukemia cells grown in decreasing concentrations of serum and upon tamoxifen-induced *Hes1* deletion. Bar graphs indicate mean values and error bars represent s.d of biological triplicates. *P* values were calculated using the two-tailed Student's *t*-test.

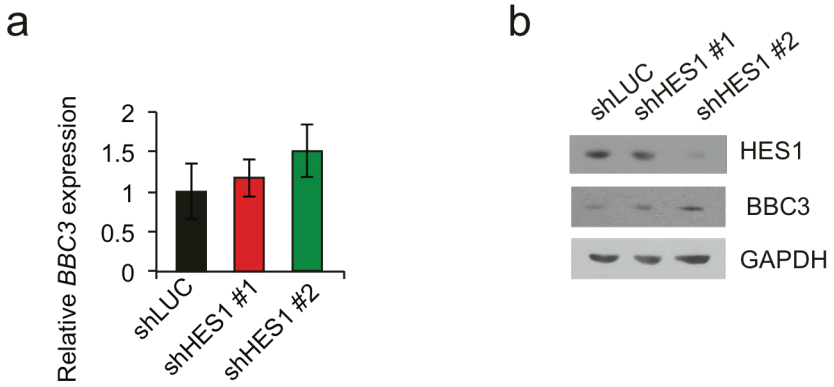

Figure 4.8. *Bbc3* upregulation after *HES1* inactivation in NOTCH1-induced T-ALL. (**a**) Quantitative RT-PCR of *BBC3* expression in DND41 cells expressing shLUC, shHES1#1, and shHES1#2. (**b**) Western blot analysis of BBC3 expression in DND41 cells infected in lentivirus expressing shLUC, shHES1#1, and shHES1#2. Bar graphs indicate mean values and error bars represent s.d. of biological triplicates. *P* values were calculated using the two-tailed Student's *t*-test.

HES1 is a bHLH repressor protein which functions by binding to specific N-BOX sequences in the promoter regions of its target genes. Analysis of the proximal regulatory sequences (+2 kb to -3kb) flanking the *BBC3* transcription initiation site identified ten N-box motif elements that could potentially mediate its transcriptional repression via direct HES1 binding (**Figure 4.9**). In the representative diagram we show the promoter region and the N-box motif elements. In addition, BBC3 is a direct target of TP53 and there are two binding site

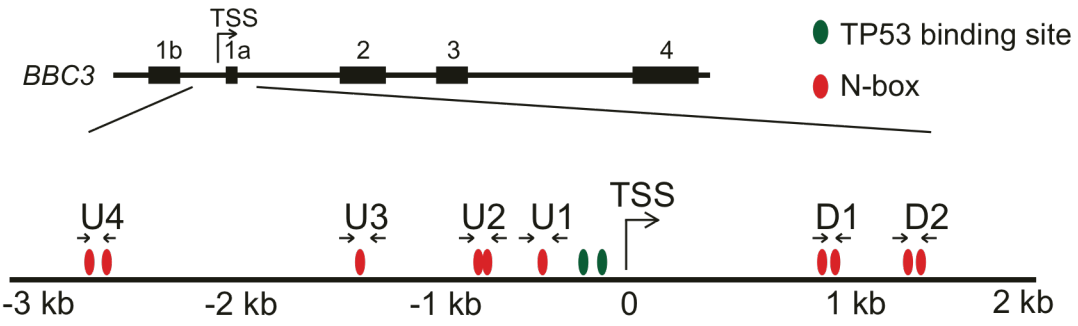

Figure 4.9. *BBC3* promoter with potential HES1 binding sites. Schematic representation of the *BBC3* proximal promoter indicating potential HES1 N-box binding sequences upstream (U) and downstream (D) of the transcription start site.

upstream of the TSS depicted by the green ovals. To identify which specific region HES1 may bind to in the promoter region of *BBC3,* we performed chromatin immunoprecipitation analysis on CUTLL1 cells using a HES1 antibody. The HES1 ChIP had a significant enrichment of HES1 binding to the -415 to -410 *BBC3* proximal promoter, a region containing a single canonical N-box site (U1) (**Figure 4.10**). Notably, this putative regulatory element located -410 bp from the *BBC3* transcription initiation site is in close proximity to two well characterized TP53 binding sites that mediate *BBC3* upregulation downstream of TP53 activation (Han, Flemington et al. 2001). To test this possibility, we analyzed the effect of HES1 expression on the activity of a –544 to –121 *BBC3* promoter construct in luciferase reporter assays. In these experiments,

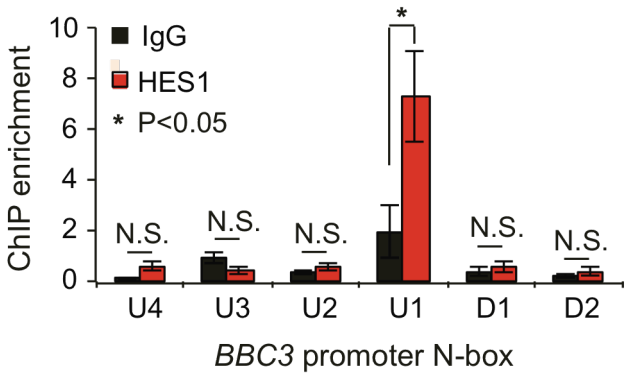

Figure 4.10. HES1 specifically binds to the N-box upstream of the *BBC3* transcription start site. Chromatin immunoprecipitation (ChIP) of HES1 binding sites in CUTLL1 cells analyzing the HES1 binding of 6 regions in the upstream and downstream proximal *BBC3* promoter. Bar graphs indicate mean values and error bars represent s.d. of biological triplicates. *P* values were calculated using the two-tailed Student's *t*-test.

transfection of HEK293 cells with the *BBC3* promoter construct in combination with a HES1 expression plasmid induced a 91% (~11 fold) downregulation of the *BBC3* reporter activity. To ensure HES1 was binding to the N-box sequence (U1) we created two mutant *BBC3* promoter plasmids, which either replaced the N-BOX with a scramble sequence (Scramble) or deleted the six base pairs (deleted). Alteration of the -410 *BBC3* N-box sequence by mutation or deletion abrogated the ability for HES1 to repress the *BBC3* promoter sequence (**Figure 4.11.a**). The combination of the HES1 ChIP and the *BBC3* luciferase reporter assay show that HES1 represses *BBC3* by directly binding to the -410 *BBC3* N-box sequence. Given that TP53 acts as a major driver of *BBC3* expression, we then analyzed the effects of HES1 on TP53-*BBC3* regulation. Consistent with previous reports (Han, Flemington et al. 2001), BBC3 reporter activity was induced upon transfection of TP53-expressing constructs. In contrast, co-expression of HES1 effectively abrogated TP53-induced *BBC3* upregulation (**Figure 4.11.b**).

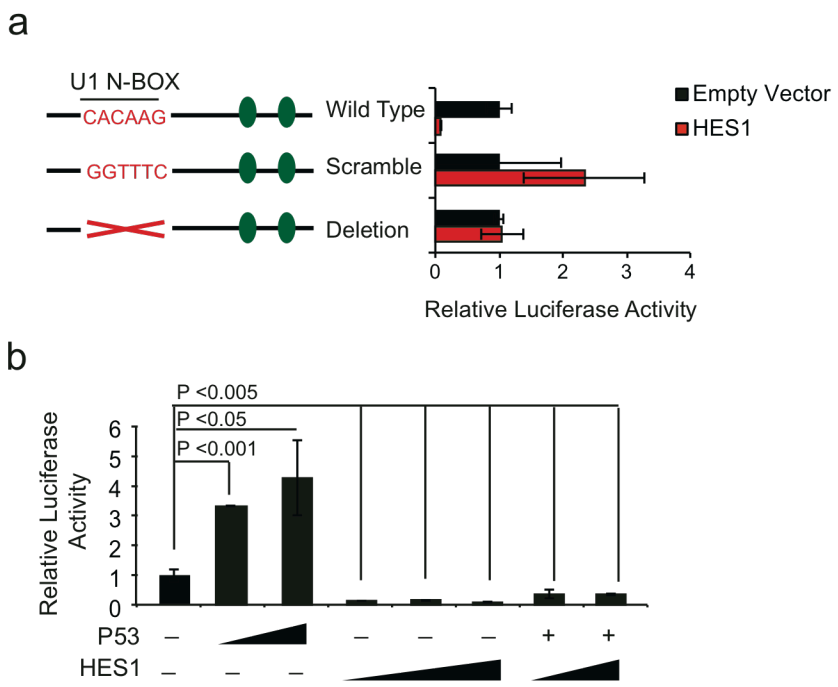

Figure 4.11. HES1 represses *BBC3* transcription. (**a**) Luciferase reporter activity in HEK 293T cells of a *BBC3* promoter construct (Wild Type), a *BBC3* promoter containing a scramble sequence in the N-box bound by HES1 (Scramble), and a *BBC3* promoter with the deletion of the N-box bound by HES1 (Deletion). (**b**) Luciferase reporter activity of the *BBC3* wild type reporter construct in response to increasing doses of TP53, increasing doses of HES1, and the combination of TP53 and HES1. Bar graphs indicate mean values and error bars represent s.d. *P* values were calculated using the two-tailed Student's *t*-test.

These findings suggest a role for HES1 in antagonizing TP53-mediated *BBC3* transcriptional upregulation in T-ALL. Overall, these results identify *BBC3* as a direct HES1 target gene and support a potentially dominant role for HES1-mediated repression in *BBC3* transcriptional regulation.

To functionally explore the significance of the Hes1-*Bbc3* transcriptional regulatory axis in leukemia cell survival we analyzed the effects of *Bbc3* depletion on *Hes1*-knockout induced apoptosis. We infected the *Hes1* conditional knockout NOTCH1-induced leukemia cell line with

lentiviruses driving the expression of two independent *Bbc3* shRNAs or a control inactive shRNA (shLUC). RT-PCR analysis show the effective downregulation of Bbc3 in both shBbc3 compared to control shLUC (**Figure 4.12.a**). Previously we established that low serum conditions amplified apoptosis induced by HES1 inactivation in NOTCH1-induced T-ALL.

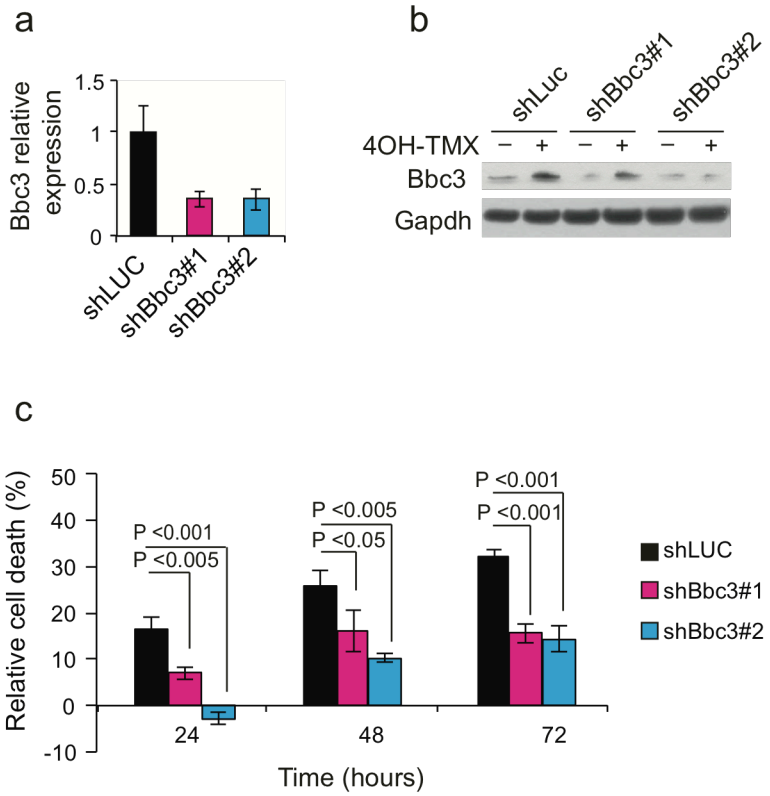

Figure 4.12. *Bbc3* inactivation after *Hes1* deletion in NOTCH1-induced T-ALL. (**a**) Quantitative RT-PCR of *BBC3* expression in CUTLL1 and DND41 cells expressing shLUC, shHES1#1, and shHES1#2. (**b**) Western blot analysis of BBC3 expression in CUTLL1 and DND41 cells infected in lentivirus expressing shLUC, shHES1#1, and shHES1#2. Bar graphs indicate mean values and error bars represent s.d of biological triplicates. *P* values were calculated using the two-tailed Student's *t*-test. (**c**) Relative quantification of apoptosis induced by *Hes1* deletion in control (shLUC) and Bbc3 knockdown (shBbc3) in *Hes1* conditional knockout T-ALL cells treated with 4-OH tamoxifen. Bar graphs indicate mean values and error bars represent s.d of biological triplicates. *P* values were calculated using the two-tailed Student's *t*-test.

Therefore, we cultured cells infected with either of the two shBbc3 hairpins or control shLUC under 3% FBS serum and treated with either 4-hydroxy tamoxifen or ethanol control and quantified cellular viability at 24 and 48 hours post treatment. Western blot analysis 24 hours after treatment show an increase in Bbc3 protein levels in the cells with *Hes1* deletion and expression of the control shLUC hairpin, but those cells infected with shBbc3 are silenced for Bbc3 expression (**Figure 4.12.b**). Consistent with our previous results, tamoxifen-induced Cre-mediated deletion of *Hes1* induced apoptosis in T-ALL lymphoblasts expressing a control shRNA (shLUC) (**Figure 3.12.b**). Notably, however, the apoptotic response triggered by *Hes1* deletion was significantly abrogated in T-ALL lymphoblasts with lentiviral expression of two independent *Bbc3* shRNAs (**Figure 3.12.c**). Taken together, these results identify HES1-mediated downregulation of *BBC3* expression as a critical mechanism promoting increased survival in NOTCH1-induced T-ALL.

Discussion

Loss of HES1 in both human and mouse NOTCH1-induced T-ALL cells leads to the upregulation of DNA damage and cell cycle regulators resulting in the induction of apoptosis in the transformed T lymphoblasts. Previously we described our efforts to capture the early cellular and transcriptional effects 24 hours after treatment with either tamoxifen or vehicle in *Hes1* $^{flox/flox\text{-}CreERT2}$ NOTCH1-induced T-ALL infiltrated mice. To our surprise, 24 hours did not capture the early effects of *Hes1* inactivation but instead demonstrated the consequences of tumor lysis syndrome. Here we describe our development of an immortal cell line from the cells derived from *Hes1* $^{flox/flox\text{-}CreERT2}$ NOTCH1-induced T-ALL tumor 1. The development of this cell line offered the opportunity to exploit the use of an *in vitro* system and capture various time points to annotate the gene expression changes leading to the induction of apoptosis after *Hes1* deletion. Mechanistically, we show that loss of *Hes1* in T-ALL triggers apoptosis via upregulation of *Bbc3*, a critical mediator of TP53 dependent DNA damage-induced apoptosis, as well as TP53-

independent cell death responses triggered by serum starvation and cytokine deprivation (Han, Flemington et al. 2001, Jeffers, Parganas et al. 2003, Wu, Heinrichs et al. 2005). The relevance of *Bbc3* downregulation as an effector of the oncogenic program controlled by the NOTCH1-HES1 pathway in T-ALL is highlighted by the ability of Bbc3 inactivation to rescue Hes1-knockout-induced apoptosis. Our results demonstrate a novel mechanism in which the NOTCH1-HES1 axis directly inhibits the expression of pro-apoptotic factors, especially under DNA damaging or stress induced conditions.

HES1 regulation of pro-apoptotic factor BBC3

One of the hallmarks of cancer is the ability to evade apoptosis, a cell death pathway activated by a diverse set of apoptotic stimuli leading to morphological changes including nuclear fragmentation, chromatin condensation, chromosomal DNA fragmentation, membrane blebbing, and cell shrinkage. The mechanisms underlying the initiation of apoptosis are dependent on the specific apoptotic stimuli, as DNA damage would involve different mediators than serum and cytokine starvation. However, the specific stimuli and mediators converge to either activate pro-apoptotic factors (BH1-3 and BH3 only) or inhibit anti-apoptotic factors (BH1-4) (Zhang, Hartig et al. 2005). These factors, all members of the Bcl-2 family, control the integrity of the mitochondria by regulating the release of cytochrome C that leads to the activation of the caspase pathway and cell death. The anti-apoptotic BH1-4 members (Bcl-2, Bcl-XL, Mcl-1, and A1/Bfl-1) localize to the outer membrane of the mitochondria and inhibit the function of the two pro-apoptotic BH1-3 members (Bax and Bak). Bax and Bak form a pore-like opening of the mitochondrial membrane allowing for the release of cytochrome C (Kuwana, Mackey et al. 2002). The BH3-only pro-apoptotic factors (Bad, Bid Bik, Bim, Noxa, and Puma) all function by promoting the function of Bax and Bak, or inhibiting the function of anti-apoptotic Bcl-2 members (Huang and Strasser 2000).

Proteins involved in recognizing apoptotic stimuli are often targeted for direct or indirect inhibition in malignant cells. For example, TP53 is the most commonly mutated gene among human cancers (Olivier, Hollstein et al. 2010). Under the event of irreparable DNA damage in non-malignant cells, TP53 is upregulated and directly binds to two adjacent binding sites of the *Puma (Bbc3)* promoter, leading to the transcription and translation of the Puma (Bbbc3) protein. Puma is a BH3 only pro-apoptotic factor, which directly activates Bax and Bak and also binds to and inhibits all the anti-apoptotic BH1-4 family members to induce apoptosis. Although the presence of TP53 mutations are found in over 50% of cancers, the *TP53* tumor suppressor gene is rarely lost in T-ALL (Kawamura, Ohnishi et al. 1999). Our reporter assays demonstrate a potential mechanism in which T lymphoblasts do not require the survival advantage of TP53 mutations. In this setting, we hypothesize HES1 exerts a dominant effect in the regulation of the *Puma* promoter, meaning HES1 repression overrides TP53 activation and therefore blunts the induction of *BBC3* expression and oncogenic stress-induced apoptosis during T-cell transformation. The ability for HES1 to blunt TP53 in T cell lymphoblasts is significant as BBC3 activates nearly all apoptotic activity induced by TP53 in hematopoietic cells in response to radiation and oncogenes (Jeffers, Parganas et al. 2003). In order to better understand the mechanisms involved in the HES1 repression of *Puma* in the presence of TP53 expression, we could set an experiment involving the luciferase reporter assay with the plasmids expressing the scramble and deleted N-box sequence of the *Puma* promoter. Here, the presence of both HES1 and TP53 should promote the expression of *Puma* given that HES1 cannot bind the *Puma* promoter due to the loss of the N-box sequence. However, if the TP53 induced expression is slightly blunted in the cells expressing both HES1 and TP53 compared to the cells only expressing TP53, then this could suggest that HES1 directly binds TP53 to inhibit the upregulation of *Puma.* Tandem affinity purification of cells under DNA stress and expressing wild type HES1 and wild type TP53 would show whether HES1 and TP53 are able to bind each other. This would not be the first instance showing the binding of HES1 to DNA damage factors,

as HES1 was shown to bind and interact with the Fanconi anemia complex to promote its nuclear translocation and protein complex stability (Tremblay, Huang et al. 2008). Furthermore, HDAC3 was recently shown to inhibit the TP53 activation of *BBC3* transcription in gastric cancer where NOTCH1 is implicated as a potential oncogene (Feng, Pan et al. 2013).

Although we are the first to demonstrate the promotion of tumor survival through HES1 repression of *Bbc3* in T-ALL, transcriptional downregulation of *Bbc3* is critically implicated in the pathogenesis of B-precursor leukemias driven by the TCF3-HLF fusion oncogene (Wu, Heinrichs et al. 2005). In these tumors TCF3-HLF functions as the transcriptional activator driving the expression of SLUG, a transcriptional repressor, which directly inhibits *Bbc3* expression, antagonizing TP53-induced apoptosis (Wu, Heinrichs et al. 2005). Notably, in these leukemias the TCF3-HLF oncoprotein usurps the Tp53-Slug-Bbc3 regulatory axis, a physiologic regulatory circuitry that normally protects hematopoietic progenitors from DNA damage-induced apoptosis (Inoue, Seidel et al. 2002). Perhaps similarly, BBC3 downregulation downstream of oncogenic NOTCH1-HES1 in T-ALL may represent the oncogenic counterpart of a physiologic regulatory circuitry that allows survival of T-cell progenitor cells. Indeed, NOTCH1 activation and consequent HES1-mediated downregulation of *BBC3* expression may promote the survival of normal thymocytes in the face of DNA double strand breaks generated during antigen receptor recombination. Moreover, HES1-mediated downregulation of *BBC3* may also facilitate the survival of T-ALL lymphoblasts in cytokine-poor microenvironments as they infiltrate peripheral tissues during disease progression. We predict that the repression of *BBC3* may be functioning to inhibit either p53-dependent or p53-independent apoptosis, as our experiments show a significant increase of apoptosis after *Hes1* deletion in DNA damaging (p53 dependent) and serum starvation (53-independent) conditions.

HES1 transcriptional regulation of tumor suppressor in T-ALL

Our identification of *BBC3* as a direct downstream target of HES1, shows the significant contribution of the NOTCH1-HES1 signaling axis towards the survival of T-ALL. However, taking a closer look into the differentially expressed genes shows there may be other pathways involved in providing the apoptotic stimuli to promote BBC3 activation. For example, growth arrest and DNA-damage inducible gamma (GADD45g) is a stress induced protein whose transcription levels increase following exposure to DNA damaging conditions. HES1 is already established as a direct negative regulator through the binding of the *GADD45g* promoter (Kobayashi, Mizuno et al. 2009). Also, GADD45g downregulation or hypermethylation of the gene are found in over 50% of cell lines and patients samples from hepatocellular carcinoma, pituitary adenomas, anaplastic thyroid cancer, non-Hodgkin lymphoma, Hodgkin's lymphoma, nasopharyngeal carcinoma, and cervical cancer (Hoffman and Liebermann 2013, Zhang, Yang et al. 2014). The high frequency of GADD45g downregulation or hypermethylation and the already known status as a HES1 direct target suggests that in T-ALL, GADD45g may also act as a tumor suppressor. Furthermore, gene expression of the genes downregulated after acute *Hes1* inactivation are enriched for cellular metabolic pathways, MYC targets, and pediatric cancer markers. The combination of gene expression changes induced by *Hes1* inactivation implicates HES1 as a global negative regulator of tumor suppressor activity in the maintenance of T-ALL.

Chapter 5
Therapeutic Targeting of the HES1 Transcriptional Network

Introduction

Over the past decades, the survival rates of T-ALL in both children and adults have dramatically increased thanks to the introduction of intensified combination chemotherapy. However, patients with primary resistant disease or those whose leukemia relapses after a transient response have few effective therapeutic options and most will not be cured. In addition, although the mortality rates have decreased over the past 70 years, the use of intensified combination chemotherapy have long term consequences and morbidities to individuals using these treatments, especially within the pediatric population. Children treated with chemotherapy for T-ALL are at increased risk for growth delays, thyroid dysfunction, infertility, hearing loss, chronic heart failure, cataracts, secondary cancers, lung damage, osteoporosis, peripheral neuropathy, and decreased cognitive function. The co-morbidities associated with chemotherapy treatment and the lack of treatment options for patients with resistant disease highlights the need to develop new highly effective therapies that specifically target aberrant pathways driving the pathogenesis of T-ALL.

The characterization of the aberrant genetic and molecular mechanisms in T-ALL has enabled the development of new potential therapies for the treatment of T-ALL. However, these treatment options are in the early phases of testing. For example, the NOTCH1 pathway, aberrantly activated in over 50% of patients, can be inhibited through the use of gamma-secretase inhibitors (GSI). GSIs inhibit the intracellular cleavage of the NOTCH1 transmembrane receptor, which releases the ICN1 into the cytoplasm, thus preventing ICN1 transcriptional activation of target genes. GSI treatment of human T-ALL cell lines results in the inhibition of proliferation, cell cycle arrest, and eventual induction of apoptosis (De Keersmaecker, Lahortiga et al. 2008). The promising pre-clinical antileukemic effects of GSI led

to the development of a phase I clinical trial for patients with T-ALL. Unfortunately, GSI treatment in patients showed limited anti-tumor activity and severe gastrointestinal toxicity (DeAngelo, Stone et al. 2006). Our establishment of HES1 as a major downstream effector of NOTCH1 driven pathways in chapter 3 and its direct inhibition of pro-apoptotic factor *BBC3* in chapter 4 offers a unique opportunity to target the NOTCH1-HES1 axis for the treatment of T-ALL.

Results

Identification of Hes1 antagonistic drugs

The central role of Hes1 as a critical mediator of NOTCH1 induced leukemia and its direct role in promoting leukemia cell survival suggest that abrogation of HES1 activity in leukemia lymphoblasts could be exploited therapeutically. However, and despite recent advances in targeting transcription factor complexes with small molecules and synthetic peptides, a direct HES1 inhibitor is not readily available. To overcome this obstacle we used a gene expression based approach to identify small molecules that antagonize the Hes1 transcriptional circuitry as candidate drugs for the treatment of NOTCH1 induced leukemia. Towards this goal, we interrogated the Connectivity Map (cMAP), a large collection of genome-wide transcriptional expression data derived from tumor cells treated with bioactive small molecules (Lamb, Crawford et al. 2006) for compounds eliciting gene expression signatures overlapping with those induced by Cre mediated inactivation of *Hes1* in the context of NOTCH1 induced T-ALL. Overlap of the top differentially expressed genes 36 hours after *in vitro Hes1* deletion in NOTCH1 induced T-ALL with the cMAP produced a list of pharmaceuticals ranked by significance, specificity, and enrichment of the top differentially expressed genes (**Figure 5.1.a**). The data output from the cMAP highlighted in red represents drug candidates that produce a similar gene expression signature as deletion of Hes1, on the other hand, drugs highlighted in blue show a gene expression similar to T-ALL cells expressing endogenous Hes1. In order to

identify potential anti-leukemic therapies, we focused our studies on those pharmaceutical drugs that produce similar gene expression changes as cells with *Hes1* inactivation (drugs highlighted in red), because loss of Hes1 results in the induction of apoptosis.

The top five compounds with gene expression signatures mimicking loss of HES1 (Hes1 signature antagonist drugs) include a PI3K inhibitor (quinostatin), a glucocorticoid (cortisone), a CPT1/CPT2 inhibitor and partial beta-blocker (perhexiline), a sodium channel cblocker (propafenone), and a calcium channel blocker (bepridil). Given the current use of PI3K-inhibitors in clinical trials (Akinleye, Avvaru et al. 2013, Roti and Stegmaier 2014), the established use of

a

Cmap Name	Enrichment	P-Value	Specificity
quinostatin	0.983	0.00052	0.0221
perhexiline	0.877	0.00034	0.0104
propafenone	0.854	0.00064	0.0067
cortisone	0.841	0.00787	0.0331
bepridil	0.833	0.00117	0.0222
deptropine	0.795	0.00346	0.0056
xylometazolin	0.748	0.00778	0
azacyclonol	0.686	0.00767	0.0381
troglitazone	0.428	0.00343	0.006
trimethobenza	-0.714	0.00411	0.0403
droperidol	-0.735	0.00985	0.0056
epivincamine	-0.751	0.00772	0.0151
sulfaphenazol	-0.782	0.00454	0.0099
dyclonine	-0.793	0.00372	0
decamethoniu	-0.814	0.00225	0.0059
flutamide	-0.821	0.00046	0
amrinone	-0.828	0.00165	0.0227
carmustine	-0.831	0.00967	0.027
rifampicin	-0.864	0.00062	0.0071
ciclopirox	-0.917	0.0001	0

b

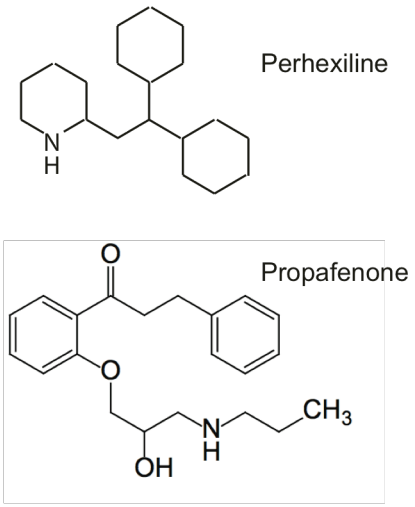

Figure 5.1. cMAP drugs with enrichment of the *Hes1* inactivation genetic signature. (**a**) Top Connectivity Map analysis hits for drugs with signatures overlapping that are induced by *Hes1* knockout in NOTCH1 induced T-ALL. (**b**) Chemical structure of perhexiline and propafenone.

glucocorticoids in the treatment of T-ALL (Obexer, Certa et al. 2001), and the established antileukemic effects of bepridil (Parekh, Advani et al. 1990, Parekh, Shallom et al. 1991), we were interested in establishing the antileukemic effects of perhexiline and propafenone.

Antileukemic effects of perhexiline and propafenone

The cross analysis of the *Hes1* inactivation genetic signature and the cMAP identified perhexiline and propafenone as a potential therapeutic agent for T-ALL based on their ability to elicit a gene expression signature resembling that induced by Hes1 inhibition (**Figure 5.1.b.**). Perhexiline is an inhibitor of mitochondrial carnitine palmitoyltransferase-1 in clinical use for treatment of cardiac ischemia (Kennedy, Unger et al. 1996), and propafenone is a class IC sodium channel blocker with weak β-blocker activity used for the treatment of atrial fibrillation and supraventricular tachycardia (Borowicz and Banach 2014). To test the potential anti-leukemic effects of perhexiline and propafenone we analyzed the effects of treatment with both drugs individually on a broad panel of T-ALL cell lines (HPB-ALL, DND41, JURKAT, CCRF-CEM, RPMI-8402, and CUTLL1) harboring activating mutations in *NOTCH1* (Weng, Ferrando et al. 2004, Palomero, Lim et al. 2006). Treatment with perhexiline induced strong antileukemic responses across all six T-ALL lines analyzed with an average IC50 of 8.43 μM (range 3.48-17.8 μM) at 72 hours (**Figure 5.2.a**). Treatment with propafenone induced a weaker antileukemic response with much variation between the six T-ALL lines analyzed. CUTLL1, HPB-ALL, and CCRF-CEM were all resistant to treatment with propafenone, in contrast DND41, RPMI-8402, and JURKAT cells had an average IC50 of 21.97 μM (range 13.0-30.2 μM) at 72 hours (**Figure 5.2.b**). From these preliminary experiments we decided to focus on perhexiline for future examination as a potential antileukemic therapy, given that 50% of the cell lines tested were resistant to high doses of propafenone treatment.

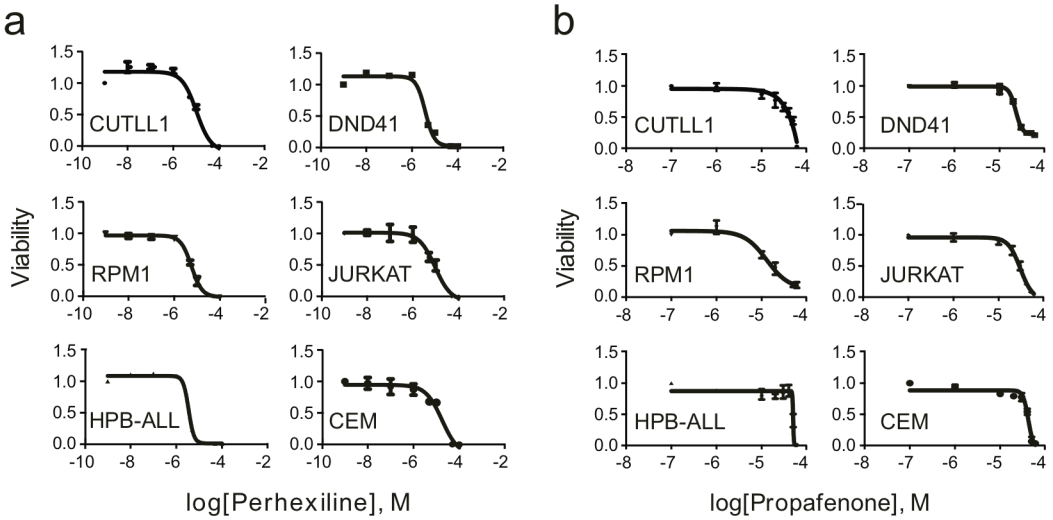

Figure 5.2. Perhexiline and propafenone antileukemic effects (**a**) Dose response cell viability curves of CUTLL1, DND41, HPB-ALL, RPMI 8402, JURKAT, and CCRF-CEM T-ALL cells treated with increasing concentrations of perhexiline. (**b**) Dose response cell viability curves of CUTLL1, DND41, HPB-ALL, RPMI 8402, JURKAT, and CCRF-CEM T-ALL cells treated with increasing concentrations of propafenone.

Next, we evaluated the effects of perhexiline treatment on primary human T-ALL patient samples. In order to successfully grow primary T-ALL cells in culture, one must support cells by co-culture with bone marrow MS5 stroma cells expressing the Delta-like 1 NOTCH1 ligand in the presence of human serum, cytokines, insulin, and glutamax. We treated cells with increasing doses of perhexiline for 72 hours and then analyzed cells through a flow cytometry-based cytotoxicity assay (Armstrong, Brunet de la Grange et al. 2009, Piovan, Yu et al. 2013). Treatment of perhexiline induced significant antileukemic effects in all five independent primary T- ALL samples tested (**Figure 5.3**).

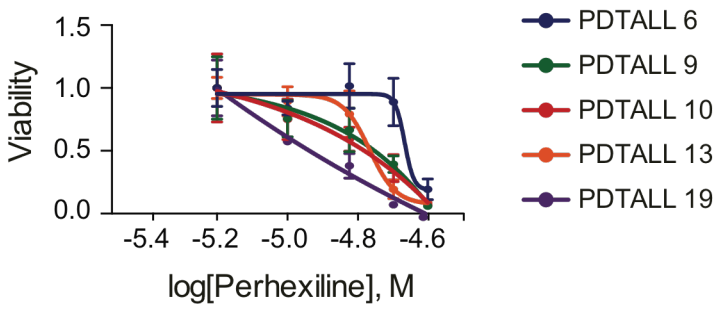

Figure 5.3. Antileukemic effects of perhexiline on primary patient samples. Dose response cell viability curves of 5 primary T-ALL samples treated with increasing concentrations of perhexiline ranging from 0 μM to 25 μM.

Antileukemic effects of perhexiline in NOTCH1 driven T-ALL

Perhexiline treatment on a broad panel of human T-ALL cell lines and human primary samples resulted in significant anti-leukemic effects *in vitro.* Thus, we next evaluated the efficacy of perhexiline treatment *in vivo* in C57BL/6 mice secondarily transplanted with primary murine NOTCH1-induced T-ALL cells expressing the luciferase gene. To generate NOTCH1-induced T-ALL tumors we performed retroviral infection of bone marrow cells with a mutated and oncogenic form of NOTCH1, HDΔPEST (L1601P HD domain mutation and deletion of the PEST domain), and transplanted infected cells into lethally irradiated recipients (Piovan, Yu et al. 2013). Once T-ALL developed, cells were infected with the luciferase gene and secondarily transplanted into a cohort of 12 mice. After tumor establishment we separated mice into two groups harboring comparable tumor burdens and treated with vehicle only (5% DMSO in water) and 53.68 mg kg^{-1} perhexiline for 5 consecutive days. We monitored the response to treatment with perhexiline or vehicle only in T-ALL-bearing mice by *in vivo* bioimaging on day 0, day 3, and day 6. In this experiment, *in vivo* bioimaging revealed rapid disease progression in mice treated with vehicle control. In contrast, perhexiline-treated animals showed significant antitumor

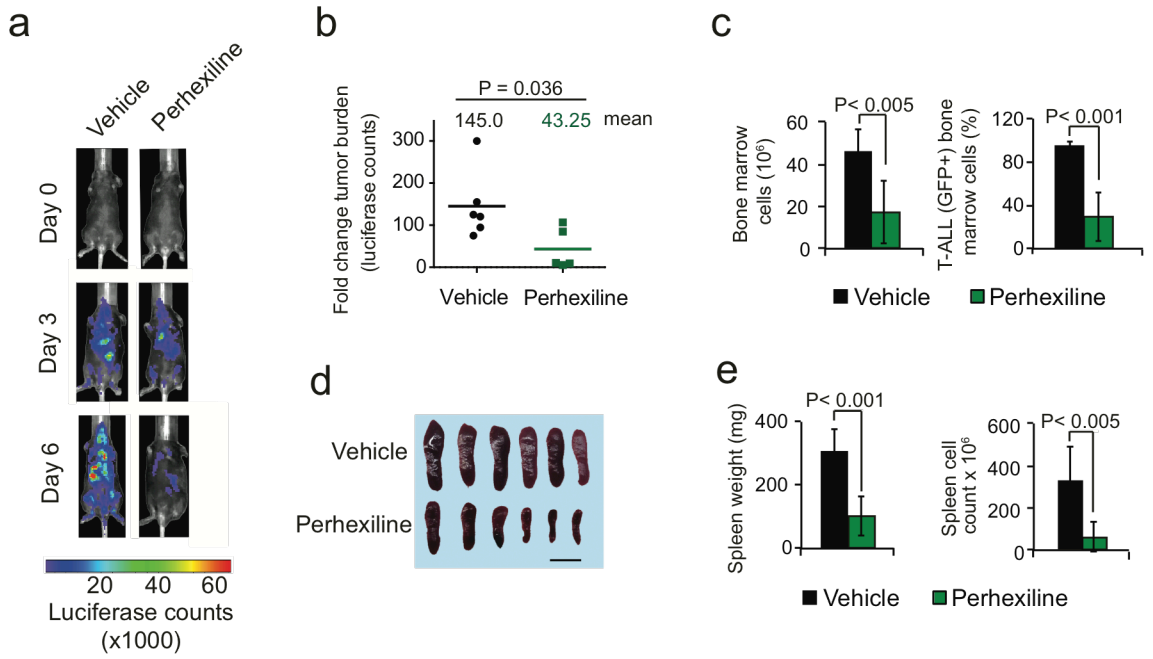

Figure 5.4. Antileukemic effects of perhexiline, a Hes1-signature modulator drug. (**a**) Representative images (**b**) and quantitative changes in tumor burden (**f**) assessed by luciferase in *vivo* bioimaging in NOTCH1-induced T-ALL bearing mice treated with vehicle only or perhexiline. (**c**) Quantitative analysis of cellularity and leukemia infiltration (assessed by GFP expression) in bone marrow from NOTCH1-induced T-ALL bearing mice treated with vehicle only or perhexiline. (**d**) Image of mouse spleens from NOTCH1-induced T-ALL bearing mice treated with vehicle only or perhexiline. (**e**) Quantification analysis of tumor burden by spleen weight and cellularity in NOTCH1-induced T-ALL bearing mice treated with vehicle only or perhexiline. (**a-e**) show data across 6 individual mice per treatment group from 1 representative experiment. Bar graphs in **c** and **e** indicate mean values and error bars represent s.d. *P* values in **b, c,** and **e** were calculated using the two-tailed Student's *t*-test.

responses after 5 days of treatment (**Figure 5.4.a**). Quantification between treatment groups reveals a 3.4 fold decrease in luciferase counts and therefore tumor burden in the perhexiline treated mice compared to vehicle treated mice (**Figure 5.4.b**). In addition, total cell counts and NOTCH1-GFP expressing cells showed a significant decrease of T-ALL infiltration of the bone marrow in mice treated with perhexiline (**Figure 5.4.c)**. Analysis of spleen revealed a marked reduction in spleen size and leukemia infiltration in perhexiline-treated animals compared with

controls (**Figure 5.4.d-e**). Overall these results support a therapeutic role for perhexiline as a Hes1-signature modulator drug in the treatment of NOTCH1-induced T-ALL.

Perhexiline treatment of human primary T-ALL

To test the efficacy of perhexiline treatment for human T-ALL, we established leukemia xenografts in NOD rag gamma (NRG) immunodeficient mice using primograft human T-ALL patient sample PDTALL9 that expresses aberrant *NOTCH1*. Mice transplanted with PDTALL9 were monitored for disease establishment, separated into two groups with similar tumor burdens, and treated with vehicle only (5%DMSO) and perhexiline. Although our initial protocol was to treat mice for 5 consecutive days with 53.68 mg kg^{-1} perhexiline or vehicle (5% DMSO) only, treatment with perhexiline resulted in extreme toxicity and only 3 days of treatment were possible. After 3 days of treatment, mice were sacrificed and analyzed for tumor burden (**Figure**

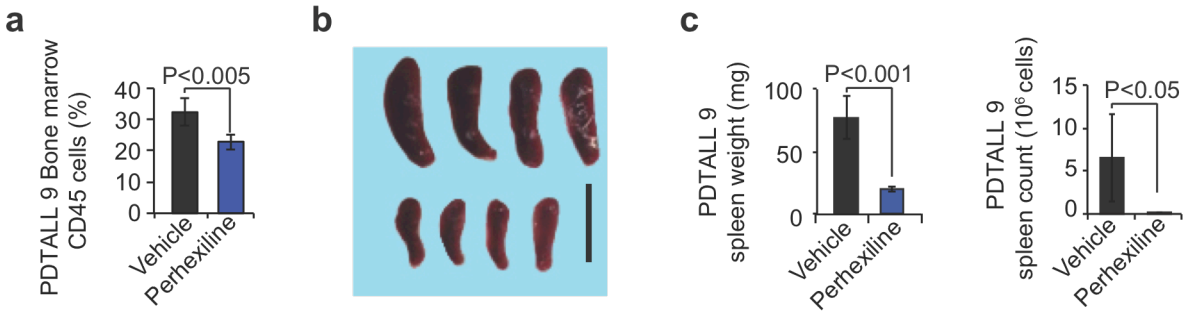

Figure 5.5. Perhexiline treatment of primary human T-ALL PDTALL9 xenograft. (**a**) Quantification of tumor burden by FACs analysis of CD45+ cells in the bone marrow of mice xenografted with PDTALL9 and treated for three days with vehicle only or perhexiline. (**b**) Image of spleen size of mice xenografted with PDTALL9 and treated for three days with vehicle only or perhexiline. (**c**). Quantification of spleen weight and cell counts in mice xenografted with PDTALL9 and treated for three days with vehicle only or perhexiline. Bar graphs in **a** and **c** indicate mean values and error bars represent s.d. *P* values in **a** and **c** were calculated using the two-tailed Student's *t*-test.

5.5). Quantification of bone marrow infiltration of CD45+ cells showed a significant decrease of tumor burden in mice treated with perhexiline (**Figure 5.5.a**). In addition, tumor burden quantified by spleen weight and cell count had significantly decreased in mice treated with perhexiline compared to vehicle treated controls (**Figure 5.5.b-c**).

The decrease of tumor burden seen in the bone marrow and spleen of mice infiltrated with a primary human T-ALL xenograft and treated with perhexiline highlights the therapeutic potential of this Hes1 antagonistic drug. Given the significant antileukemic effects seen in PDTALL9, we tested a second primary human tumor with *NOTCH1* mutations, PDTALL10. To this end, we transplanted PDTALL10 into a cohort of 12 NRG, confirmed disease progression by *in vivo* bioimaging, separated mice into two groups with similar tumor burdens and treated for 5 consecutive days with 40 mg kg^{-1} perhexiline or vehicle only (**Figure 5.6**). Mice were sacrificed after the five days of treatment and analyzed for tumor burden in the bone marrow and spleen. Quantification of bone marrow tumor burden by FACs analysis of CD45+ cells showed no significant difference between perhexiline treated and vehicle treated (**Figure 5.6**). However, the tumor load in the vehicle treated mice engrafted with PDTALL10 was only 7% compared to more that 30% in the vehicle treated mice engrafted with PDTALL9. Although there was not a significant change in bone marrow T-ALL burden, there was a significant decrease of spleen size and cell count in mice treated with perhexiline compared to vehicle treated mice (**Figure 5.6.b-c**). The difference in perhexiline anti-leukemic effects may be attributed to the timing of treatment initiation.

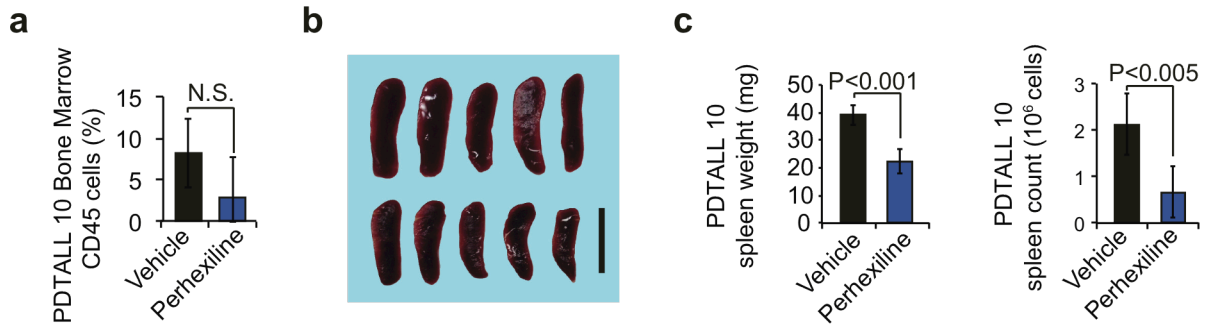

Figure 5.6. Perhexiline treatment in primary human T-ALL PDTALL10 xenograft. (**a**) Quantification of tumor burden by FACs analysis of CD45+ cells in the bone marrow of mice xenografted with PDTALL10 and treated for three days with vehicle only or perhexiline. (**b**) Image of spleen size of mice xenografted with PDTALL10 and treated for three days with vehicle only or perhexiline. (**c**). Quantification of spleen weight and cell counts in mice xenografted with PDTALL10 and treated for three days with vehicle only or perhexiline. Bar graphs in **a** and **c** indicate mean values and error bars represent s.d. *P* values in **a** and **c** were calculated using the two-tailed Student's *t*-test.

Discussion

The development of intensified combination chemotherapies for T-ALL has resulted in markedly improved survival rates in both children and adults with this disease (Pui, Robison et al. 2008). However, patients with primary resistant T-ALL, or those whose leukemia relapses after a transient response, have few effective therapeutic options and face a dismal prognosis (Goldberg, Silverman et al. 2003, Oudot, Auclerc et al. 2008), highlighting the need to develop more effective treatment options. Our identification of HES1 as a major mediator of T-ALL cell survival exposed the potential for targeting this pathway in the treatment of NOTCH1 induced T-ALL. Crossing our *Hes1* knockout gene expression signature with the cMAP database we identified potential HES1 signature modulator drugs. The presence of a PI3K inhibitor and a glucocorticoid attests to the significant role HES1 plays in the regulation of the genetic network

associated with tumor survival. Further analysis of the top antagonistic drugs identified perhexiline as a HES1-signature antagonist drug with remarkable single agent antileukemic activity *in vitro* and *in vivo.*

Antileukemic effects of perhexiline

The discovery of perhexiline may have a direct clinical impact, as perhexiline is already in clinical use for the treatment of cardiac ischemia and refractory angina in humans (Killalea and Krum 2001, Lee, Horowitz et al. 2004). Mechanistically, the anti-ischemic effects of perhexiline have been linked with inhibition of the CPT-1 and CPT-2 palmitoyltransferases, which results in the block of long-chain fatty acids into the mitochondria for oxidation and decrease of oxygen demand in the myocardium (Kennedy, Unger et al. 1996). The inhibitory effect in fatty acid metabolism categorizes perhexiline as a fatty acid oxidation inhibitor (FAOI) (Ashrafian, Horowitz et al. 2007). In addition, perhexiline may also inhibit voltage gated L type calcium and sodium channels resulting in modulation of myocardial electrical activity (Barry, Horowitz et al. 1985, Grima, Velly et al. 1988).

Alterations the cellular metabolism are often consequences of the mutations in cancer genes and aberrant signaling pathways in tumor cells. Malignant cells were noticed to have an increase in glucose and glutamine metabolism for the use of anabolic pathways including amino acid synthesis and fatty acid synthesis (DeBerardinis, Mancuso et al. , Vander Heiden, Locasale et al. 2010, Hitosugi, Zhou et al. 2012). The conversion of acetyl CoA to malonyl CoA initiates fatty acid synthesis (FAS), which is important for rapidly diving cells, such as cancer cells. Fatty acids are a source of energy when catabolized by fatty acid oxidation (FAO) also known as β-oxidation (Carracedo, Cantley et al. 2013). FAO shortens fatty acids to generate NADH and FADH, which can then enter the electron transport chain, and acetyl CoA, which enters the tricarboxylic acid cycle (TCA), to produce ATP. Lipid turnover, including synthesis and metabolism, have been shown to promote tumor growth and survival in melanoma, ovarian and

breast cancer (Nomura, Long et al. 2010). In acute myeloid leukemia, treatment of cells with an FAOI targeting CPT-1 sensitizes cells to apoptosis induction (Samudio, Harmancey et al. 2010). More specifically, FAOI treatment increases the cellular toxicity by facilitating Bak and Bax oligomerization resulting in the induction apoptosis. Perhaps through similar mechanisms, perhexiline induced inhibition of CPT-1 leads to the induction of apoptosis in T-ALL.

Notably NOTCH1 signaling has been linked with increased glucose metabolism during thymocyte development (Ciofani and Zuniga-Pflucker 2006) and regulation of anabolic pathways may play an important role in the response of T-ALL cells to anti-NOTCH1 therapies (Palomero, Sulis et al. 2007). In this context, the convergent antileukemic effects and transcriptional programs of perhexiline and HES1 inhibition in T-ALL could suggest a previously unrecognized role of perhexiline in the regulation of HES1 transcriptional complexes. It is also possible that the antileukemic effects of perhexiline do not involve direct HES1 inhibition, but instead may modulate other downstream effector pathways common to those triggered by HES1 inactivation. More specifically, perhexiline inhibits CPT-1, which if we suppose functions similarly to the FAOI tested in AML, then leads to the decrease in long-fatty acid chains transported into the membrane therefore increasing oxygen availability and inducing the Bax and Bak oligomerization and induction of apoptosis. This pathway is represented in the differentially expressed genes after *Hes1* inactivation, as GSEA across the C2 database showed an enrichment in pathways involved in lipid metabolism including SREBP cholesterol synthesis, and hypoxia, tying the CPT-1 inhibitory function of perhexiline to the HES1 genetic signature (**Figure 4.6**).

The potential use of perhexiline for the treatment of leukemia brings into question whether it may have synergistic effects with the current standard of chemotherapy. To explore this possibility, combination drug therapy and analysis of the anti-leukemic effects should be conducted first *in vitro* and then on primary human xenografts in the mice. This would be similar to the studies conducted using GSI with dexamethasone treatment, where treatment alone with

GSI showed mild-antileukemic effects but combination treatment lead to a significant reduction of tumor burden (Real, Tosello et al. 2009). In addition, a long-term treatment protocol should be established to see whether continuous treatment of perhexiline alone or in combination with other chemotherapeutics is able to eliminate T-ALL. A point of consideration may involve the route of administration for perhexiline, as IV administration produces the most toxic side effects. In addition, testing the dosage tolerated over a long-term treatment is especially important since accumulation of perhexiline in the blood stream can potentially lead to hepatotoxicity and neuropathies. However, perhexiline levels are readily monitored in patients, especially those with polymorphic CYP2D6, and only patients with plasma concentrations between 720 μg/L and 2680 μg/L on oral doses of perhexiline from 50-400mg/day show these potentially dangerous side effects. Therefore close monitoring and dose adjustment would be required for the treatment of perhexiline as an anti-leukemic agent.

Patients with primary resistant T-ALL, or those whose leukemia relapses after a transient response, have few effective therapeutic options and face a dismal prognosis, highlighting the need to develop more effective treatments. Our identification of HES1 as a major mediator of T-ALL cell survival and perhexiline as a HES1-signature antagonist drug with remarkable single agent antileukemic activity *in vitro* and *in vivo* may have a direct clinical impact, as perhexiline is already in clinical use for the treatment of cardiac ischemia and refractory angina in humans (Lee, Horowitz et al. 2004).

Chapter 6
Conclusions

"A scientist in his laboratory is not a mere technician: he is a child confronting natural phenomena that impress him as though they were fairy tales"

–Marie Curie

T-ALL is an aggressive hematological disease resulting from the malignant transformation of T-cell progenitors. NOTCH1 is the most prominent T-ALL specific oncogene, with over 60% of patients showing aberrant activation of the NOTCH1 signaling pathway (Weng, Ferrando et al. 2004). Constitutive activation of mutant NOTCH1 in T-ALL drives the transcriptional regulation of multiple direct and indirect targets promoting the cellular growth, metabolism, proliferations, and survival of T-ALL. Among the NOTCH1 targets, *HES1* functions as a critical factor mediating transcriptional repression of tumor suppressors *PTEN* and *CYLD* (Palomero, Sulis et al. 2007, Espinosa, Cathelin et al. 2010). Here we show the first comprehensive analysis of the cellular and transcriptions effects after HES1 loss in NOTCH1-induced T-ALL. Our results show a requirement of *HES1* in the survival of established T-ALL in both human and murine NOTCH1-driven T-ALL. Specifically, we show that *HES1* inactivation in two different NOTCH1 driven T-ALL human cell lines results in the induction of apoptosis. The requirement of HES1 in tumor survival was re-established when tamoxifen induced cre-mediated deletion of *Hes1* resulted in an increase in overall survival in mice infiltrated with T-ALL. Furthermore, acute deletion of *Hes1* in T-ALL revealed a significant decrease of tumor burden due to the induction of apoptosis of T-ALL cells.

Our transcriptional analysis of the downstream pathways regulated by HES1 in NOTCH-induced T-ALL implicates HES1 as a global negative regulator of tumor suppressor activity resulting in increased survival of transformed T lymphoblasts. Mechanistically, we show that the

induction of apoptosis in T-ALL cells after *Hes1* inactivation is initiated by the upregulation of *Bbc3*. BBC3 is a critical mediator of both TP53 dependent DNA damage-induced apoptosis and TP53-independent cell death responses triggered by serum starvation and cytokine deprivation (Han, Flemington et al. 2001, Jeffers, Parganas et al. 2003, Wu, Heinrichs et al. 2005). Our

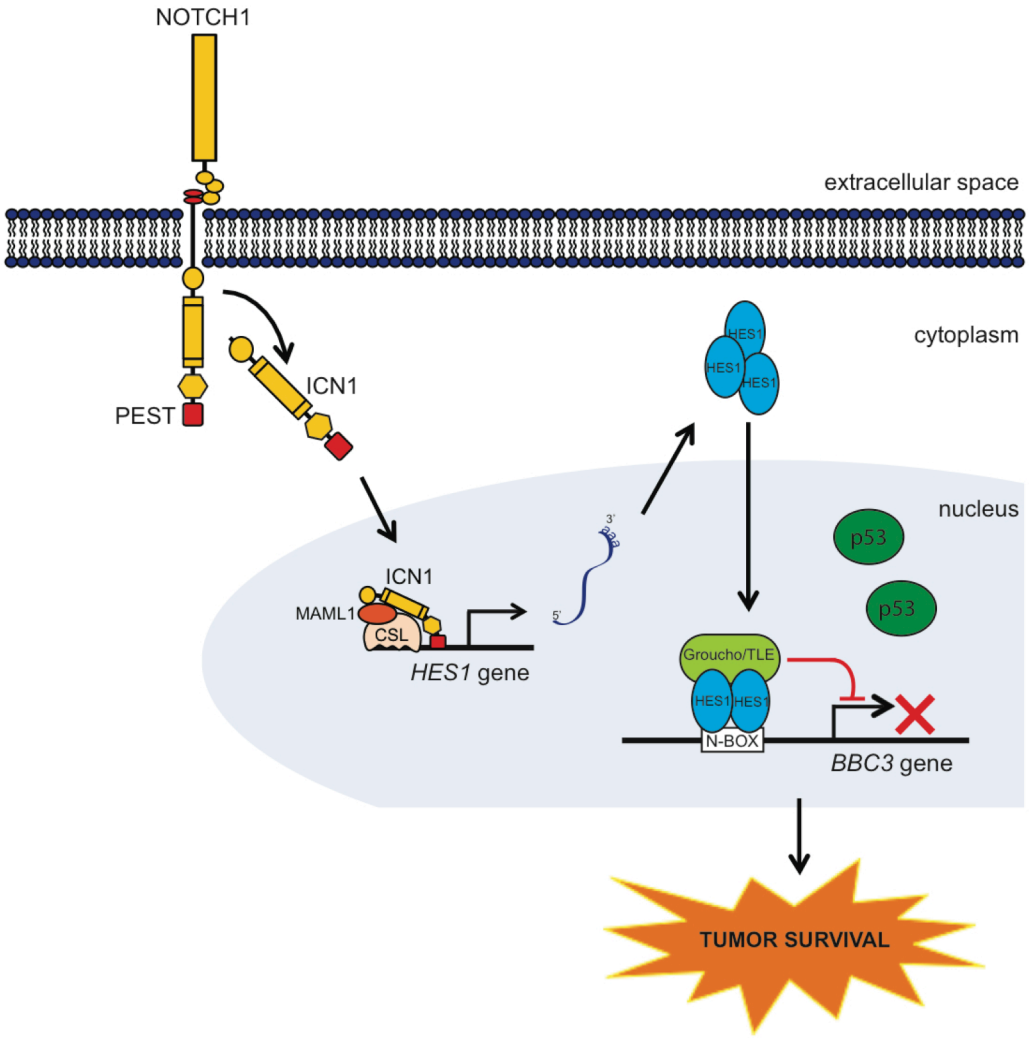

Figure 6.1 HES1 repression of *BBC3* in NOTCH1-induced T-ALL. Schematic representation of the NOTCH1-HES1 axis repression of pro-apoptotic factor *BBC3*. Briefly, aberrant NOTCH1 activation leads to the translocation of ICN1 into the nucleus, associates with the RBPJ/CSL protein, recruits MAML coactivators and actives expression of *HES1*. *HES1* upregulation results in the repression of *BBC3* by the direct HES1 binding to the N-box proximal of the transcription start site.

results indicate that under DNA damaging and serum deprivations environments, transformed T cells have an increased sensitivity to loss of *HES1,* resulting in immediate upregulation of *BBC3* and subsequent cellular death. The NOTCH1-HES1 axis regulation of *BBC3* was further highlighted by the ability of Bbc3 inactivation to rescue Hes1-knockout-induced apoptosis. In summary, these results demonstrate a novel mechanism in which the NOTCH1-HES1 axis directly inhibits the expression of pro-apoptotic factor, *BBC3*, especially under DNA damaging or stress induced conditions (**Figure 6.1**). We hypothesize that the loss of *HES1* under stressful conditions allows other tumor suppressors to activate the transcription of pro-apoptotic factor *BBC3.*

Although the emergence of intensified combination chemotherapy has increased survival rates in T-ALL, 25% of pediatric and over 50% of adult T-ALL patients fail induction remission or their disease relapses. These patients have few effective therapeutic options and face a poor prognosis, highlighting the necessity for the development of new-targeted effective treatments. Our identification of HES1 as a critical regulator of T-ALL survival exposed the potential for targeting this transcriptional pathway in the treatment of NOTCH1 induced T-ALL. We identified HES1 signature modulator drugs through the differentially expressed genes upon *HES1* inactivation across the cMAP database. Perhexiline, a HES1 signature modulator drug, was discovered to induce remarkable single agent antileukemic activity in NOTCH1 induced primary T-ALL. Although still preliminary, the use of perhexiline may have a direct clinical impact, as perhexiline is already in clinical use for the treatment of cardiac ischemia and refractory angina in humans (Killalea and Krum 2001, Lee, Horowitz et al. 2004).

Overall our results highlight a central role for HES1 and BBC3 in the control of NOTCH1-induced leukemia cell survival and identify perhexiline as a highly active antileukemic drug for the treatment of T-ALL.

REFERENCES

Adolfsson, J., O. J. Borge, D. Bryder, K. Theilgaard-Monch, I. Astrand-Grundstrom, E. Sitnicka, Y. Sasaki and S. E. Jacobsen (2001). "Upregulation of Flt3 expression within the bone marrow Lin(-)Sca1(+)c-kit(+) stem cell compartment is accompanied by loss of self-renewal capacity." Immunity **15**(4): 659-669.

Agrawal, A. and D. G. Schatz (1997). "RAG1 and RAG2 form a stable postcleavage synaptic complex with DNA containing signal ends in V(D)J recombination." Cell **89**(1): 43-53.

Aifantis, I., E. Raetz and S. Buonamici (2008). "Molecular pathogenesis of T-cell leukaemia and lymphoma." Nat Rev Immunol **8**(5): 380-390.

Akashi, K., M. Kondo, U. von Freeden-Jeffry, R. Murray and I. L. Weissman (1997). "Bcl-2 rescues T lymphopoiesis in interleukin-7 receptor-deficient mice." Cell **89**(7): 1033-1041.

Akashi, K., D. Traver, T. Miyamoto and I. L. Weissman (2000). "A clonogenic common myeloid progenitor that gives rise to all myeloid lineages." Nature **404**(6774): 193-197.

Akinleye, A., P. Avvaru, M. Furqan, Y. Song and D. Liu (2013). "Phosphatidylinositol 3-kinase (PI3K) inhibitors as cancer therapeutics." J Hematol Oncol **6**(1): 88.

Anderson, G. and E. J. Jenkinson (2001). "Lymphostromal interactions in thymic development and function." Nat Rev Immunol **1**(1): 31-40.

Apelqvist, A., H. Li, L. Sommer, P. Beatus, D. J. Anderson, T. Honjo, M. Hrabe de Angelis, U. Lendahl and H. Edlund (1999). "Notch signalling controls pancreatic cell differentiation." Nature **400**(6747): 877-881.

Aplan, P. D., D. P. Lombardi, A. M. Ginsberg, J. Cossman, V. L. Bertness and I. R. Kirsch (1990). "Disruption of the human SCL locus by "illegitimate" V-(D)-J recombinase activity." Science **250**(4986): 1426-1429.

Armstrong, F., P. Brunet de la Grange, B. Gerby, M. C. Rouyez, J. Calvo, M. Fontenay, N. Boissel, H. Dombret, A. Baruchel, J. Landman-Parker, P. H. Romeo, P. Ballerini and F. Pflumio (2009). "NOTCH is a key regulator of human T-cell acute leukemia initiating cell activity." Blood **113**(8): 1730-1740.

Arstila, T. P., A. Casrouge, V. Baron, J. Even, J. Kanellopoulos and P. Kourilsky (1999). "A direct estimate of the human alphabeta T cell receptor diversity." Science **286**(5441): 958-961.

Ashrafian, H., J. D. Horowitz and M. P. Frenneaux (2007). "Perhexiline." Cardiovasc Drug Rev **25**(1): 76-97.

Asnafi, V., I. Radford-Weiss, N. Dastugue, C. Bayle, D. Leboeuf, C. Charrin, R. Garand, M. Lafage-Pochitaloff, E. Delabesse, A. Buzyn, X. Troussard and E. Macintyre (2003). "CALM-AF10 is a common fusion transcript in T-ALL and is specific to the TCRgammadelta lineage." Blood **102**(3): 1000-1006.

Asselin, B. L., M. Devidas, C. Wang, J. Pullen, M. J. Borowitz, R. Hutchison, S. E. Lipshultz and B. M. Camitta (2011). "Effectiveness of high-dose methotrexate in T-cell lymphoblastic leukemia and advanced-stage lymphoblastic lymphoma: a randomized study by the Children's Oncology Group (POG 9404)." Blood **118**(4): 874-883.

Aster, J. C., W. S. Pear and S. C. Blacklow (2008). "Notch signaling in leukemia." Annu Rev Pathol **3**: 587-613.

Aster, J. C., E. S. Robertson, R. P. Hasserjian, J. R. Turner, E. Kieff and J. Sklar (1997). "Oncogenic forms of NOTCH1 lacking either the primary binding site for RBP-Jkappa or nuclear localization sequences retain the ability to associate with RBP-Jkappa and activate transcription." J Biol Chem **272**(17): 11336-11343.

Attarbaschi, A., G. Mann, R. Panzer-Grumayer, S. Rottgers, M. Steiner, M. Konig, E. Csinady, M. N. Dworzak, M. Seidel, D. Janousek, A. Moricke, C. Reichelt, J. Harbott, M. Schrappe, H. Gadner and O. A. Haas (2008). "Minimal residual disease values discriminate between low and high relapse risk in children with B-cell precursor acute lymphoblastic leukemia and an intrachromosomal amplification of chromosome 21: the Austrian and German acute lymphoblastic leukemia Berlin-Frankfurt-Munster (ALL-BFM) trials." J Clin Oncol **26**(18): 3046-3050.

Baek, J. H., J. Hatakeyama, S. Sakamoto, T. Ohtsuka and R. Kageyama (2006). "Persistent and high levels of Hes1 expression regulate boundary formation in the developing central nervous system." Development **133**(13): 2467-2476.

Balgobind, B. V., P. Van Vlierberghe, A. M. van den Ouweland, H. B. Beverloo, J. N. Terlouw-Kromosoeto, E. R. van Wering, D. Reinhardt, M. Horstmann, G. J. Kaspers, R. Pieters, C. M. Zwaan, M. M. Van den Heuvel-Eibrink and J. P. Meijerink (2008). "Leukemia-associated NF1 inactivation in patients with pediatric T-ALL and AML lacking evidence for neurofibromatosis." Blood **111**(8): 4322-4328.

Bar-Eli, M., H. Ahuja, A. Foti and M. J. Cline (1989). "N-RAS mutations in T-cell acute lymphocytic leukaemia: analysis by direct sequencing detects a novel mutation." Br J Haematol **72**(1): 36-39.

Begley, C. G., P. D. Aplan, M. P. Davey, K. Nakahara, K. Tchorz, J. Kurtzberg, M. S. Hershfield, B. F. Haynes, D. I. Cohen, T. A. Waldmann and et al. (1989). "Chromosomal translocation in a human leukemic stem-cell line disrupts the T-cell antigen receptor delta-chain diversity region and results in a previously unreported fusion transcript." Proc Natl Acad Sci U S A **86**(6): 2031-2035.

Bell, J. J. and A. Bhandoola (2008). "The earliest thymic progenitors for T cells possess myeloid lineage potential." Nature **452**(7188): 764-767.

Bernard, O., P. Guglielmi, P. Jonveaux, D. Cherif, S. Gisselbrecht, M. Mauchauffe, R. Berger, C. J. Larsen and D. Mathieu-Mahul (1990). "Two distinct mechanisms for the SCL gene activation in the t(1;14) translocation of T-cell leukemias." Genes Chromosomes Cancer **1**(3): 194-208.

Bernard, O. A., M. Busson-LeConiat, P. Ballerini, M. Mauchauffe, V. Della Valle, R. Monni, F. Nguyen Khac, T. Mercher, V. Penard-Lacronique, P. Pasturaud, L. Gressin, R. Heilig, M. T.

Daniel, M. Lessard and R. Berger (2001). "A new recurrent and specific cryptic translocation, t(5;14)(q35;q32), is associated with expression of the Hox11L2 gene in T acute lymphoblastic leukemia." Leukemia **15**(10): 1495-1504.

Beverly, L. J., D. W. Felsher and A. J. Capobianco (2005). "Suppression of p53 by Notch in lymphomagenesis: implications for initiation and regression." Cancer Res **65**(16): 7159-7168.

Bhandoola, A., H. von Boehmer, H. T. Petrie and J. C. Zuniga-Pflucker (2007). "Commitment and developmental potential of extrathymic and intrathymic T cell precursors: plenty to choose from." Immunity **26**(6): 678-689.

Boehm, T., L. Foroni, Y. Kaneko, M. F. Perutz and T. H. Rabbitts (1991). "The rhombotin family of cysteine-rich LIM-domain oncogenes: distinct members are involved in T-cell translocations to human chromosomes 11p15 and 11p13." Proc Natl Acad Sci U S A **88**(10): 4367-4371.

Borowicz, K. K. and M. Banach (2014). "Antiarrhythmic drugs and epilepsy." Pharmacol Rep **66**(4): 545-551.

Buonamici, S., T. Trimarchi, M. G. Ruocco, L. Reavie, S. Cathelin, B. G. Mar, A. Klinakis, Y. Lukyanov, J. C. Tseng, F. Sen, E. Gehrie, M. Li, E. Newcomb, J. Zavadil, D. Meruelo, M. Lipp, S. Ibrahim, A. Efstratiadis, D. Zagzag, J. S. Bromberg, M. L. Dustin and I. Aifantis (2009). "CCR7 signalling as an essential regulator of CNS infiltration in T-cell leukaemia." Nature **459**(7249): 1000-1004.

Burtrum, D. B., S. Kim, E. C. Dudley, A. C. Hayday and H. T. Petrie (1996). "TCR gene recombination and alpha beta-gamma delta lineage divergence: productive TCR-beta rearrangement is neither exclusive nor preclusive of gamma delta cell development." J Immunol **157**(10): 4293-4296.

Carr, E. L., A. Kelman, G. S. Wu, R. Gopaul, E. Senkevitch, A. Aghvanyan, A. M. Turay and K. A. Frauwirth (2010). "Glutamine uptake and metabolism are coordinately regulated by ERK/MAPK during T lymphocyte activation." J Immunol **185**(2): 1037-1044.

Carracedo, A., L. C. Cantley and P. P. Pandolfi (2013). "Cancer metabolism: fatty acid oxidation in the limelight." Nat Rev Cancer **13**(4): 227-232.

Ceredig, R. and T. Rolink (2002). "A positive look at double-negative thymocytes." Nat Rev Immunol **2**(11): 888-897.

Chen, C., Y. C. Chang, C. L. Liu, T. P. Liu, K. J. Chang and I. C. Guo (2007). "Leptin induces proliferation and anti-apoptosis in human hepatocarcinoma cells by up-regulating cyclin D1 and down-regulating Bax via a Janus kinase 2-linked pathway." Endocr Relat Cancer **14**(2): 513-529.

Chen, Q., J. T. Cheng, L. H. Tasi, N. Schneider, G. Buchanan, A. Carroll, W. Crist, B. Ozanne, M. J. Siciliano and R. Baer (1990). "The tal gene undergoes chromosome translocation in T cell leukemia and potentially encodes a helix-loop-helix protein." Embo J **9**(2): 415-424.

Chervinsky, D. S., S. N. Sait, N. J. Nowak, T. B. Shows and P. D. Aplan (1995). "Complex MLL rearrangement in a patient with T-cell acute lymphoblastic leukemia." Genes Chromosomes Cancer **14**(1): 76-84.

Christensen, J. L. and I. L. Weissman (2001). "Flk-2 is a marker in hematopoietic stem cell differentiation: a simple method to isolate long-term stem cells." Proc Natl Acad Sci U S A **98**(25): 14541-14546.

Ciofani, M., T. M. Schmitt, A. Ciofani, A. M. Michie, N. Cuburu, A. Aublin, J. L. Maryanski and J. C. Zuniga-Pflucker (2004). "Obligatory role for cooperative signaling by pre-TCR and Notch during thymocyte differentiation." J Immunol **172**(9): 5230-5239.

Ciofani, M. and J. C. Zuniga-Pflucker (2005). "Notch promotes survival of pre-T cells at the beta-selection checkpoint by regulating cellular metabolism." Nat Immunol **6**(9): 881-888.

Ciofani, M. and J. C. Zuniga-Pflucker (2006). "A survival guide to early T cell development." Immunol Res **34**(2): 117-132.

Clappier, E., S. Collette, N. Grardel, S. Girard, L. Suarez, G. Brunie, S. Kaltenbach, K. Yakouben, F. Mazingue, A. Robert, P. Boutard, D. Plantaz, P. Rohrlich, P. van Vlierberghe, C. Preudhomme, J. Otten, F. Speleman, N. Dastugue, S. Suciu, Y. Benoit, Y. Bertrand, H. Cave and C. L. G. Eortc (2010). "NOTCH1 and FBXW7 mutations have a favorable impact on early response to treatment, but not on outcome, in children with T-cell acute lymphoblastic leukemia (T-ALL) treated on EORTC trials 58881 and 58951." Leukemia **24**(12): 2023-2031.

Clappier, E., W. Cuccuini, J. M. Cayuela, D. Vecchione, A. Baruchel, H. Dombret, F. Sigaux and J. Soulier (2006). "Cyclin D2 dysregulation by chromosomal translocations to TCR loci in T-cell acute lymphoblastic leukemias." Leukemia **20**(1): 82-86.

Clappier, E., W. Cuccuini, A. Kalota, A. Crinquette, J. M. Cayuela, W. A. Dik, A. W. Langerak, B. Montpellier, B. Nadel, P. Walrafen, O. Delattre, A. Aurias, T. Leblanc, H. Dombret, A. M. Gewirtz, A. Baruchel, F. Sigaux and J. Soulier (2007). "The C-MYB locus is involved in chromosomal translocation and genomic duplications in human T-cell acute leukemia (T-ALL), the translocation defining a new T-ALL subtype in very young children." Blood **110**(4): 1251-1261.

Conter, V., C. R. Bartram, M. G. Valsecchi, A. Schrauder, R. Panzer-Grumayer, A. Moricke, M. Arico, M. Zimmermann, G. Mann, G. De Rossi, M. Stanulla, F. Locatelli, G. Basso, F. Niggli, E. Barisone, G. Henze, W. D. Ludwig, O. A. Haas, G. Cazzaniga, R. Koehler, D. Silvestri, J. Bradtke, R. Parasole, R. Beier, J. J. van Dongen, A. Biondi and M. Schrappe (2010). "Molecular response to treatment redefines all prognostic factors in children and adolescents with B-cell precursor acute lymphoblastic leukemia: results in 3184 patients of the AIEOP-BFM ALL 2000 study." Blood **115**(16): 3206-3214.

Crosnier, C., N. Vargesson, S. Gschmeissner, L. Ariza-McNaughton, A. Morrison and J. Lewis (2005). "Delta-Notch signalling controls commitment to a secretory fate in the zebrafish intestine." Development **132**(5): 1093-1104.

Cuevas, I. C., A. L. Slocum, P. Jun, J. F. Costello, A. W. Bollen, G. J. Riggins, M. W. McDermott and A. Lal (2005). "Meningioma transcript profiles reveal deregulated Notch signaling pathway." Cancer Res **65**(12): 5070-5075.

Davies, C., L. A. Hogarth, P. A. Dietrich, P. S. Bachmann, K. L. Mackenzie, A. G. Hall and R. B. Lock (2011). "p53-independent epigenetic repression of the p21(WAF1) gene in T-cell acute lymphoblastic leukemia." J Biol Chem **286**(43): 37639-37650.

Dawson, S. R., D. L. Turner, H. Weintraub and S. M. Parkhurst (1995). "Specificity for the hairy/enhancer of split basic helix-loop-helix (bHLH) proteins maps outside the bHLH domain and suggests two separable modes of transcriptional repression." Mol Cell Biol **15**(12): 6923-6931.

De Keersmaecker, K., C. Graux, M. D. Odero, N. Mentens, R. Somers, J. Maertens, I. Wlodarska, P. Vandenberghe, A. Hagemeijer, P. Marynen and J. Cools (2005). "Fusion of EML1 to ABL1 in T-cell acute lymphoblastic leukemia with cryptic t(9;14)(q34;q32)." Blood **105**(12): 4849-4852.

De Keersmaecker, K., I. Lahortiga, N. Mentens, C. Folens, L. Van Neste, S. Bekaert, P. Vandenberghe, M. D. Odero, P. Marynen and J. Cools (2008). "In vitro validation of gamma-secretase inhibitors alone or in combination with other anti-cancer drugs for the treatment of T-cell acute lymphoblastic leukemia." Haematologica **93**(4): 533-542.

De Keersmaecker, K., P. J. Real, G. D. Gatta, T. Palomero, M. L. Sulis, V. Tosello, P. Van Vlierberghe, K. Barnes, M. Castillo, X. Sole, M. Hadler, J. Lenz, P. D. Aplan, M. Kelliher, B. L. Kee, P. P. Pandolfi, D. Kappes, F. Gounari, H. Petrie, J. Van der Meulen, F. Speleman, E. Paietta, J. Racevskis, P. H. Wiernik, J. M. Rowe, J. Soulier, D. Avran, H. Cave, N. Dastugue, S. Raimondi, J. P. Meijerink, C. Cordon-Cardo, A. Califano and A. A. Ferrando (2010). "The TLX1 oncogene drives aneuploidy in T cell transformation." Nat Med **16**(11): 1321-1327.

De Obaldia, M. E., J. J. Bell, X. Wang, C. Harly, Y. Yashiro-Ohtani, J. H. DeLong, D. A. Zlotoff, D. A. Sultana, W. S. Pear and A. Bhandoola (2013). "T cell development requires constraint of the myeloid regulator C/EBP-alpha by the Notch target and transcriptional repressor Hes1." Nat Immunol **14**(12): 1277-1284.

DeAngelo, D. J., R. M. Stone, M. L. Heaney, S. D. Nimer, R. L. Paquette, R. B. Klisovic, M. A. Caligiuri, M. R. Cooper, J. M. Lecerf, M. D. Karol, S. Sheng, N. Holford, P. T. Curtin, B. J. Druker and M. C. Heinrich (2006). "Phase 1 clinical results with tandutinib (MLN518), a novel FLT3 antagonist, in patients with acute myelogenous leukemia or high-risk myelodysplastic syndrome: safety, pharmacokinetics, and pharmacodynamics." Blood **108**(12): 3674-3681.

DeBerardinis, R. J., A. Mancuso, E. Daikhin, I. Nissim, M. Yudkoff, S. Wehrli and C. B. Thompson (2007). "Beyond aerobic glycolysis: transformed cells can engage in glutamine metabolism that exceeds the requirement for protein and nucleotide synthesis." Proc Natl Acad Sci U S A **104**(49): 19345-19350.

Della Gatta, G., T. Palomero, A. Perez-Garcia, A. Ambesi-Impiombato, M. Bansal, Z. W. Carpenter, K. De Keersmaecker, X. Sole, L. Xu, E. Paietta, J. Racevskis, P. H. Wiernik, J. M. Rowe, J. P. Meijerink, A. Califano and A. A. Ferrando (2012). "Reverse engineering of TLX oncogenic transcriptional networks identifies RUNX1 as tumor suppressor in T-ALL." Nat Med **18**(3): 436-440.

Delves, P. J. and I. M. Roitt (2000). "The immune system. First of two parts." N Engl J Med **343**(1): 37-49.

Delves, P. J. and I. M. Roitt (2000). "The immune system. Second of two parts." N Engl J Med **343**(2): 108-117.

DeVita, V. T., Jr. and E. Chu (2008). "A history of cancer chemotherapy." Cancer Res **68**(21): 8643-8653.

Dohda, T., A. Maljukova, L. Liu, M. Heyman, D. Grander, D. Brodin, O. Sangfelt and U. Lendahl (2007). "Notch signaling induces SKP2 expression and promotes reduction of p27Kip1 in T-cell acute lymphoblastic leukemia cell lines." Exp Cell Res **313**(14): 3141-3152.

Dube, I. D., S. Kamel-Reid, C. C. Yuan, M. Lu, X. Wu, G. Corpus, S. C. Raimondi, W. M. Crist, A. J. Carroll, J. Minowada and et al. (1991). "A novel human homeobox gene lies at the chromosome 10 breakpoint in lymphoid neoplasias with chromosomal translocation t(10;14)." Blood **78**(11): 2996-3003.

Ellisen, L. W., J. Bird, D. C. West, A. L. Soreng, T. C. Reynolds, S. D. Smith and J. Sklar (1991). "TAN-1, the human homolog of the Drosophila notch gene, is broken by chromosomal translocations in T lymphoblastic neoplasms." Cell **66**(4): 649-661.

Erikson, J., L. Finger, L. Sun, A. ar-Rushdi, K. Nishikura, J. Minowada, J. Finan, B. S. Emanuel, P. C. Nowell and C. M. Croce (1986). "Deregulation of c-myc by translocation of the alpha-locus of the T-cell receptor in T-cell leukemias." Science **232**(4752): 884-886.

Espinosa, L., S. Cathelin, T. D'Altri, T. Trimarchi, A. Statnikov, J. Guiu, V. Rodilla, J. Ingles-Esteve, J. Nomdedeu, B. Bellosillo, C. Besses, O. Abdel-Wahab, N. Kucine, S. C. Sun, G. Song, C. C. Mullighan, R. L. Levine, K. Rajewsky, I. Aifantis and A. Bigas (2010). "The Notch/Hes1 pathway sustains NF-kappaB activation through CYLD repression in T cell leukemia." Cancer Cell **18**(3): 268-281.

Fan, X., W. Matsui, L. Khaki, D. Stearns, J. Chun, Y. M. Li and C. G. Eberhart (2006). "Notch pathway inhibition depletes stem-like cells and blocks engraftment in embryonal brain tumors." Cancer Res **66**(15): 7445-7452.

Farnie, G., R. B. Clarke, K. Spence, N. Pinnock, K. Brennan, N. G. Anderson and N. J. Bundred (2007). "Novel cell culture technique for primary ductal carcinoma in situ: role of Notch and epidermal growth factor receptor signaling pathways." J Natl Cancer Inst **99**(8): 616-627.

Fehling, H. J., A. Krotkova, C. Saint-Ruf and H. von Boehmer (1995). "Crucial role of the pre-T-cell receptor alpha gene in development of alpha beta but not gamma delta T cells." Nature **375**(6534): 795-798.

Feng, L., M. Pan, J. Sun, H. Lu, Q. Shen, S. Zhang, T. Jiang, L. Liu, W. Jin, Y. Chen, X. Wang and H. Jin (2013). "Histone deacetylase 3 inhibits expression of PUMA in gastric cancer cells." J Mol Med (Berl) **91**(1): 49-58.

Feng, Y., G. T. Bommer, J. Zhao, M. Green, E. Sands, Y. Zhai, K. Brown, A. Burberry, K. R. Cho and E. R. Fearon (2011). "Mutant KRAS promotes hyperplasia and alters differentiation in the colon epithelium but does not expand the presumptive stem cell pool." Gastroenterology **141**(3): 1003-1013 e1001-1010.

Ferrando, A. A., D. S. Neuberg, J. Staunton, M. L. Loh, C. Huard, S. C. Raimondi, F. G. Behm, C. H. Pui, J. R. Downing, D. G. Gilliland, E. S. Lander, T. R. Golub and A. T. Look (2002). "Gene expression signatures define novel oncogenic pathways in T cell acute lymphoblastic leukemia." Cancer Cell **1**(1): 75-87.

Feyerabend, T. B., G. Terszowski, A. Tietz, C. Blum, H. Luche, A. Gossler, N. W. Gale, F. Radtke, H. J. Fehling and H. R. Rodewald (2009). "Deletion of Notch1 converts pro-T cells to dendritic cells and promotes thymic B cells by cell-extrinsic and cell-intrinsic mechanisms." Immunity **30**(1): 67-79.

Finkin, S., Y. Aylon, S. Anzi, M. Oren and E. Shaulian (2008). "Fbw7 regulates the activity of endoreduplication mediators and the p53 pathway to prevent drug-induced polyploidy." Oncogene **27**(32): 4411-4421.

Flex, E., V. Petrangeli, L. Stella, S. Chiaretti, T. Hornakova, L. Knoops, C. Ariola, V. Fodale, E. Clappier, F. Paoloni, S. Martinelli, A. Fragale, M. Sanchez, S. Tavolaro, M. Messina, G. Cazzaniga, A. Camera, G. Pizzolo, A. Tornesello, M. Vignetti, A. Battistini, H. Cave, B. D. Gelb, J. C. Renauld, A. Biondi, S. N. Constantinescu, R. Foa and M. Tartaglia (2008). "Somatically acquired JAK1 mutations in adult acute lymphoblastic leukemia." J Exp Med **205**(4): 751-758.

Fogelstrand, L., A. Staffas, C. Wasslavik, H. Sjogren, S. Soderhall, B. M. Frost, E. Forestier, S. Degerman, M. Behrendtz, J. Heldrup, K. Karrman, B. Johansson, M. Heyman, J. Abrahamsson and L. Palmqvist (2014). "Prognostic implications of mutations in NOTCH1 and FBXW7 in childhood T-ALL treated according to the NOPHO ALL-1992 and ALL-2000 protocols." Pediatr Blood Cancer **61**(3): 424-430.

Gaiano, N., J. S. Nye and G. Fishell (2000). "Radial glial identity is promoted by Notch1 signaling in the murine forebrain." Neuron **26**(2): 395-404.

Gao, C., S. G. Liu, R. D. Zhang, W. J. Li, X. X. Zhao, L. Cui, M. Y. Wu, H. Y. Zheng and Z. G. Li (2014). "NOTCH1 mutations are associated with favourable long-term prognosis in paediatric T-cell acute lymphoblastic leukaemia: a retrospective study of patients treated on BCH-2003 and CCLG-2008 protocol in China." Br J Haematol **166**(2): 221-228.

Gao, F., Y. Zhang, S. Wang, Y. Liu, L. Zheng, J. Yang, W. Huang, Y. Ye, W. Luo and D. Xiao (2014). "Hes1 is involved in the self-renewal and tumourigenicity of stem-like cancer cells in colon cancer." Sci Rep **4**: 3963.

Gaynon, P. S., A. L. Angiolillo, W. L. Carroll, J. B. Nachman, M. E. Trigg, H. N. Sather, S. P. Hunger, M. Devidas and G. Children's Oncology (2010). "Long-term results of the children's cancer group studies for childhood acute lymphoblastic leukemia 1983-2002: a Children's Oncology Group Report." Leukemia **24**(2): 285-297.

Geest, C. R. and P. J. Coffer (2009). "MAPK signaling pathways in the regulation of hematopoiesis." J Leukoc Biol **86**(2): 237-250.

Gilbert, L. A., M. A. Horlbeck, B. Adamson, J. E. Villalta, Y. Chen, E. H. Whitehead, C. Guimaraes, B. Panning, H. L. Ploegh, M. C. Bassik, L. S. Qi, M. Kampmann and J. S. Weissman (2014). "Genome-Scale CRISPR-Mediated Control of Gene Repression and Activation." Cell.

Giovannini, C., L. Gramantieri, M. Minguzzi, F. Fornari, P. Chieco, G. L. Grazi and L. Bolondi (2012). "CDKN1C/P57 is regulated by the Notch target gene Hes1 and induces senescence in human hepatocellular carcinoma." Am J Pathol **181**(2): 413-422.

Godfrey, D. I., J. Kennedy, T. Suda and A. Zlotnik (1993). "A developmental pathway involving four phenotypically and functionally distinct subsets of CD3-CD4-CD8- triple-negative adult mouse thymocytes defined by CD44 and CD25 expression." J Immunol **150**(10): 4244-4252.

Goldberg, J. M., L. B. Silverman, D. E. Levy, V. K. Dalton, R. D. Gelber, L. Lehmann, H. J. Cohen, S. E. Sallan and B. L. Asselin (2003). "Childhood T-cell acute lymphoblastic leukemia: the Dana-Farber Cancer Institute acute lymphoblastic leukemia consortium experience." J Clin Oncol **21**(19): 3616-3622.

Gonzalez-Garcia, S., M. Garcia-Peydro, E. Martin-Gayo, E. Ballestar, M. Esteller, R. Bornstein, J. L. de la Pompa, A. A. Ferrando and M. L. Toribio (2009). "CSL-MAML-dependent Notch1 signaling controls T lineage-specific IL-7R{alpha} gene expression in early human thymopoiesis and leukemia." J Exp Med **206**(4): 779-791.

Gounari, F., I. Aifantis, K. Khazaie, S. Hoeflinger, N. Harada, M. M. Taketo and H. von Boehmer (2001). "Somatic activation of beta-catenin bypasses pre-TCR signaling and TCR selection in thymocyte development." Nat Immunol **2**(9): 863-869.

Grabher, C., H. von Boehmer and A. T. Look (2006). "Notch 1 activation in the molecular pathogenesis of T-cell acute lymphoblastic leukaemia." Nat Rev Cancer **6**(5): 347-359.

Graux, C., J. Cools, C. Melotte, H. Quentmeier, A. Ferrando, R. Levine, J. R. Vermeesch, M. Stul, B. Dutta, N. Boeckx, A. Bosly, P. Heimann, A. Uyttebroeck, N. Mentens, R. Somers, R. A. MacLeod, H. G. Drexler, A. T. Look, D. G. Gilliland, L. Michaux, P. Vandenberghe, I. Wlodarska, P. Marynen and A. Hagemeijer (2004). "Fusion of NUP214 to ABL1 on amplified episomes in T-cell acute lymphoblastic leukemia." Nat Genet **36**(10): 1084-1089.

Grbavec, D. and S. Stifani (1996). "Molecular interaction between TLE1 and the carboxyl-terminal domain of HES-1 containing the WRPW motif." Biochem Biophys Res Commun **223**(3): 701-705.

Greenwald, I. (1998). "LIN-12/Notch signaling: lessons from worms and flies." Genes Dev **12**(12): 1751-1762.

Gutierrez, A., T. Sanda, W. Ma, J. Zhang, R. Grebliunaite, S. Dahlberg, D. Neuberg, A. Protopopov, S. S. Winter, R. S. Larson, M. J. Borowitz, L. B. Silverman, L. Chin, S. P. Hunger, C. Jamieson, S. E. Sallan and A. T. Look (2010). "Inactivation of LEF1 in T-cell acute lymphoblastic leukemia." Blood **115**(14): 2845-2851.

Hallahan, A. R., J. I. Pritchard, S. Hansen, M. Benson, J. Stoeck, B. A. Hatton, T. L. Russell, R. G. Ellenbogen, I. D. Bernstein, P. A. Beachy and J. M. Olson (2004). "The SmoA1 mouse model reveals that notch signaling is critical for the growth and survival of sonic hedgehog-induced medulloblastomas." Cancer Res **64**(21): 7794-7800.

Han, J., C. Flemington, A. B. Houghton, Z. Gu, G. P. Zambetti, R. J. Lutz, L. Zhu and T. Chittenden (2001). "Expression of bbc3, a pro-apoptotic BH3-only gene, is regulated by diverse cell death and survival signals." Proc Natl Acad Sci U S A **98**(20): 11318-11323.

Hartman, J., P. Muller, J. S. Foster, J. Wimalasena, J. A. Gustafsson and A. Strom (2004). "HES-1 inhibits 17beta-estradiol and heregulin-beta1-mediated upregulation of E2F-1." Oncogene **23**(54): 8826-8833.

Hatano, M., C. W. Roberts, M. Minden, W. M. Crist and S. J. Korsmeyer (1991). "Deregulation of a homeobox gene, HOX11, by the t(10;14) in T cell leukemia." Science **253**(5015): 79-82.

Hebert, J., J. M. Cayuela, J. Berkeley and F. Sigaux (1994). "Candidate tumor-suppressor genes MTS1 (p16INK4A) and MTS2 (p15INK4B) display frequent homozygous deletions in primary cells from T- but not from B-cell lineage acute lymphoblastic leukemias." Blood **84**(12): 4038-4044.

Heinzel, K., C. Benz, V. C. Martins, I. D. Haidl and C. C. Bleul (2007). "Bone marrow-derived hemopoietic precursors commit to the T cell lineage only after arrival in the thymic microenvironment." J Immunol **178**(2): 858-868.

Herranz, D., A. Ambesi-Impiombato, T. Palomero, S. A. Schnell, L. Belver, A. A. Wendorff, L. Xu, M. Castillo-Martin, D. Llobet-Navas, C. Cordon-Cardo, E. Clappier, J. Soulier and A. A. Ferrando (2014). "A NOTCH1-driven MYC enhancer promotes T cell development, transformation and acute lymphoblastic leukemia." Nat Med **20**(10): 1130-1137.

Hirata, H., S. Yoshiura, T. Ohtsuka, Y. Bessho, T. Harada, K. Yoshikawa and R. Kageyama (2002). "Oscillatory expression of the bHLH factor Hes1 regulated by a negative feedback loop." Science **298**(5594): 840-843.

Hitosugi, T., L. Zhou, S. Elf, J. Fan, H. B. Kang, J. H. Seo, C. Shan, Q. Dai, L. Zhang, J. Xie, T. L. Gu, P. Jin, M. Aleckovic, G. LeRoy, Y. Kang, J. A. Sudderth, R. J. DeBerardinis, C. H. Luan, G. Z. Chen, S. Muller, D. M. Shin, T. K. Owonikoko, S. Lonial, M. L. Arellano, H. J. Khoury, F. R. Khuri, B. H. Lee, K. Ye, T. J. Boggon, S. Kang, C. He and J. Chen (2012). "Phosphoglycerate mutase 1 coordinates glycolysis and biosynthesis to promote tumor growth." Cancer Cell **22**(5): 585-600.

Ho, I. C., T. S. Tai and S. Y. Pai (2009). "GATA3 and the T-cell lineage: essential functions before and after T-helper-2-cell differentiation." Nat Rev Immunol **9**(2): 125-135.

Hoffman, B. and D. A. Liebermann (2013). "Gadd45 in modulation of solid tumors and leukemia." Adv Exp Med Biol **793**: 21-33.

Hopfer, O., D. Zwahlen, M. F. Fey and S. Aebi (2005). "The Notch pathway in ovarian carcinomas and adenomas." Br J Cancer **93**(6): 709-718.

Howard, S. C., D. P. Jones and C. H. Pui (2011). "The tumor lysis syndrome." N Engl J Med **364**(19): 1844-1854.

Hozumi, K., N. Negishi, I. Tsuchiya, N. Abe, K. Hirano, D. Suzuki, M. Yamamoto, J. D. Engel and S. Habu (2008). "Notch signaling is necessary for GATA3 function in the initiation of T cell development." Eur J Immunol **38**(4): 977-985.

Huang, D. C. and A. Strasser (2000). "BH3-Only proteins-essential initiators of apoptotic cell death." Cell **103**(6): 839-842.

Huang, Q., A. Raya, P. DeJesus, S. H. Chao, K. C. Quon, J. S. Caldwell, S. K. Chanda, J. C. Izpisua-Belmonte and P. G. Schultz (2004). "Identification of p53 regulators by genome-wide functional analysis." Proc Natl Acad Sci U S A **101**(10): 3456-3461.

Huesmann, M., B. Scott, P. Kisielow and H. von Boehmer (1991). "Kinetics and efficacy of positive selection in the thymus of normal and T cell receptor transgenic mice." Cell **66**(3): 533-540.

Hunault, M., J. L. Harousseau, M. Delain, M. Truchan-Graczyk, J. Y. Cahn, F. Witz, T. Lamy, B. Pignon, J. P. Jouet, R. Garidi, D. Caillot, C. Berthou, D. Guyotat, A. Sadoun, J. J. Sotto, B. Lioure, P. Casassus, P. Solal-Celigny, L. Stalnikiewicz, B. Audhuy, O. Blanchet, L. Baranger, M. C. Bene, N. Ifrah and G. Group (2004). "Better outcome of adult acute lymphoblastic leukemia after early genoidentical allogeneic bone marrow transplantation (BMT) than after late high-dose therapy and autologous BMT: a GOELAMS trial." Blood **104**(10): 3028-3037.

Hussey, D. J., M. Nicola, S. Moore, G. B. Peters and A. Dobrovic (1999). "The (4;11)(q21;p15) translocation fuses the NUP98 and RAP1GDS1 genes and is recurrent in T-cell acute lymphocytic leukemia." Blood **94**(6): 2072-2079.

Ikawa, T., H. Kawamoto, A. W. Goldrath and C. Murre (2006). "E proteins and Notch signaling cooperate to promote T cell lineage specification and commitment." J Exp Med **203**(5): 1329-1342.

Imayoshi, I., T. Shimogori, T. Ohtsuka and R. Kageyama (2008). "Hes genes and neurogenin regulate non-neural versus neural fate specification in the dorsal telencephalic midline." Development **135**(15): 2531-2541.

Inlay, M. A., D. Bhattacharya, D. Sahoo, T. Serwold, J. Seita, H. Karsunky, S. K. Plevritis, D. L. Dill and I. L. Weissman (2009). "Ly6d marks the earliest stage of B-cell specification and identifies the branchpoint between B-cell and T-cell development." Genes Dev **23**(20): 2376-2381.

Jamieson, B. D., D. C. Douek, S. Killian, L. E. Hultin, D. D. Scripture-Adams, J. V. Giorgi, D. Marelli, R. A. Koup and J. A. Zack (1999). "Generation of functional thymocytes in the human adult." Immunity **10**(5): 569-575.

Jarriault, S., C. Brou, F. Logeat, E. H. Schroeter, R. Kopan and A. Israel (1995). "Signalling downstream of activated mammalian Notch." Nature **377**(6547): 355-358.

Jarriault, S., O. Le Bail, E. Hirsinger, O. Pourquie, F. Logeat, C. F. Strong, C. Brou, N. G. Seidah and A. Isra l (1998). "Delta-1 activation of notch-1 signaling results in HES-1 transactivation." Mol Cell Biol **18**(12): 7423-7431.

Jeffers, J. R., E. Parganas, Y. Lee, C. Yang, J. Wang, J. Brennan, K. H. MacLean, J. Han, T. Chittenden, J. N. Ihle, P. J. McKinnon, J. L. Cleveland and G. P. Zambetti (2003). "Puma is an essential mediator of p53-dependent and -independent apoptotic pathways." Cancer Cell **4**(4): 321-328.

Johnson, J. E., S. J. Birren, T. Saito and D. J. Anderson (1992). "DNA binding and transcriptional regulatory activity of mammalian achaete-scute homologous (MASH) proteins revealed by interaction with a muscle-specific enhancer." Proc Natl Acad Sci U S A **89**(8): 3596-3600.

Joshi, I., L. M. Minter, J. Telfer, R. M. Demarest, A. J. Capobianco, J. C. Aster, P. Sicinski, A. Fauq, T. E. Golde and B. A. Osborne (2009). "Notch signaling mediates G1/S cell-cycle progression in T cells via cyclin D3 and its dependent kinases." Blood **113**(8): 1689-1698.

Jotta, P. Y., M. A. Ganazza, A. Silva, M. B. Viana, M. J. da Silva, L. J. Zambaldi, J. T. Barata, S. R. Brandalise and J. A. Yunes (2010). "Negative prognostic impact of PTEN mutation in pediatric T-cell acute lymphoblastic leukemia." Leukemia **24**(1): 239-242.

Kadish, J. L. and R. S. Basch (1976). "Hematopoietic thymocyte precursors. I. Assay and kinetics of the appearance of progeny." J Exp Med **143**(5): 1082-1099.

Kageyama, R. and T. Ohtsuka (1999). "The Notch-Hes pathway in mammalian neural development." Cell Res **9**(3): 179-188.

Kageyama, R., T. Ohtsuka and T. Kobayashi (2007). "The Hes gene family: repressors and oscillators that orchestrate embryogenesis." Development **134**(7): 1243-1251.

Kamakura, S., K. Oishi, T. Yoshimatsu, M. Nakafuku, N. Masuyama and Y. Gotoh (2004). "Hes binding to STAT3 mediates crosstalk between Notch and JAK-STAT signalling." Nat Cell Biol **6**(6): 547-554.

Kamstrup, M. R., L. M. Gjerdrum, E. Biskup, B. T. Lauenborg, E. Ralfkiaer, A. Woetmann, N. Odum and R. Gniadecki (2010). "Notch1 as a potential therapeutic target in cutaneous T-cell lymphoma." Blood **116**(14): 2504-2512.

Kang, S. A., J. H. Seol and J. Kim (2005). "The conserved WRPW motif of Hes6 mediates proteasomal degradation." Biochem Biophys Res Commun **332**(1): 33-36.

Kannan, S., W. Fang, G. Song, C. G. Mullighan, R. Hammitt, J. McMurray and P. A. Zweidler-McKay (2011). "Notch/HES1-mediated PARP1 activation: a cell type-specific mechanism for tumor suppression." Blood **117**(10): 2891-2900.

Kastan, M. B. and J. Bartek (2004). "Cell-cycle checkpoints and cancer." Nature **432**(7015): 316-323.

Kathrein, K. L., S. Chari and S. Winandy (2008). "Ikaros directly represses the notch target gene Hes1 in a leukemia T cell line: implications for CD4 regulation." J Biol Chem **283**(16): 10476-10484.

Kennedy, J. A., S. A. Unger and J. D. Horowitz (1996). "Inhibition of carnitine palmitoyltransferase-1 in rat heart and liver by perhexiline and amiodarone." Biochem Pharmacol **52**(2): 273-280.

Kennedy, M. A., R. Gonzalez-Sarmiento, U. R. Kees, F. Lampert, N. Dear, T. Boehm and T. H. Rabbitts (1991). "HOX11, a homeobox-containing T-cell oncogene on human chromosome 10q24." Proc Natl Acad Sci U S A **88**(20): 8900-8904.

Khor, B. and B. P. Sleckman (2005). "Intra- and inter-allelic ordering of T cell receptor beta chain gene assembly." Eur J Immunol **35**(3): 964-970.

Kiel, M. J., O. H. Yilmaz, T. Iwashita, O. H. Yilmaz, C. Terhorst and S. J. Morrison (2005). "SLAM family receptors distinguish hematopoietic stem and progenitor cells and reveal endothelial niches for stem cells." Cell **121**(7): 1109-1121.

Kim, H. K. and G. Siu (1998). "The notch pathway intermediate HES-1 silences CD4 gene expression." Mol Cell Biol **18**(12): 7166-7175.

Kitagawa, K., Y. Hiramatsu, C. Uchida, T. Isobe, T. Hattori, T. Oda, K. Shibata, S. Nakamura, A. Kikuchi and M. Kitagawa (2009). "Fbw7 promotes ubiquitin-dependent degradation of c-Myb: involvement of GSK3-mediated phosphorylation of Thr-572 in mouse c-Myb." Oncogene **28**(25): 2393-2405.

Klein, L., M. Hinterberger, G. Wirnsberger and B. Kyewski (2009). "Antigen presentation in the thymus for positive selection and central tolerance induction." Nat Rev Immunol **9**(12): 833-844.

Kleppe, M., I. Lahortiga, T. El Chaar, K. De Keersmaecker, N. Mentens, C. Graux, K. Van Roosbroeck, A. A. Ferrando, A. W. Langerak, J. P. Meijerink, F. Sigaux, T. Haferlach, I. Wlodarska, P. Vandenberghe, J. Soulier and J. Cools (2010). "Deletion of the protein tyrosine phosphatase gene PTPN2 in T-cell acute lymphoblastic leukemia." Nat Genet **42**(6): 530-535.

Kobayashi, T., H. Mizuno, I. Imayoshi, C. Furusawa, K. Shirahige and R. Kageyama (2009). "The cyclic gene Hes1 contributes to diverse differentiation responses of embryonic stem cells." Genes Dev **23**(16): 1870-1875.

Koch, U., E. Fiorini, R. Benedito, V. Besseyrias, K. Schuster-Gossler, M. Pierres, N. R. Manley, A. Duarte, H. R. Macdonald and F. Radtke (2008). "Delta-like 4 is the essential, nonredundant ligand for Notch1 during thymic T cell lineage commitment." J Exp Med **205**(11): 2515-2523.

Koch, U. and F. Radtke (2011). "Mechanisms of T cell development and transformation." Annu Rev Cell Dev Biol **27**: 539-562.

Kodama, Y., M. Hijikata, R. Kageyama, K. Shimotohno and T. Chiba (2004). "The role of notch signaling in the development of intrahepatic bile ducts." Gastroenterology **127**(6): 1775-1786.

Kondo, M., I. L. Weissman and K. Akashi (1997). "Identification of clonogenic common lymphoid progenitors in mouse bone marrow." Cell **91**(5): 661-672.

Konishi, J., K. S. Kawaguchi, H. Vo, N. Haruki, A. Gonzalez, D. P. Carbone and T. P. Dang (2007). "Gamma-secretase inhibitor prevents Notch3 activation and reduces proliferation in human lung cancers." Cancer Res **67**(17): 8051-8057.

Kopan, R., E. H. Schroeter, H. Weintraub and J. S. Nye (1996). "Signal transduction by activated mNotch: importance of proteolytic processing and its regulation by the extracellular domain." Proc Natl Acad Sci U S A **93**(4): 1683-1688.

Kox, C., M. Zimmermann, M. Stanulla, S. Leible, M. Schrappe, W. D. Ludwig, R. Koehler, G. Tolle, O. R. Bandapalli, S. Breit, M. U. Muckenthaler and A. E. Kulozik (2010). "The favorable effect of activating NOTCH1 receptor mutations on long-term outcome in T-ALL patients treated on the ALL-BFM 2000 protocol can be separated from FBXW7 loss of function." Leukemia **24**(12): 2005-2013.

Kunisato, A., S. Chiba, E. Nakagami-Yamaguchi, K. Kumano, T. Saito, S. Masuda, T. Yamaguchi, M. Osawa, R. Kageyama, H. Nakauchi, M. Nishikawa and H. Hirai (2003). "HES-1 preserves purified hematopoietic stem cells ex vivo and accumulates side population cells in vivo." Blood **101**(5): 1777-1783.

Kuwana, T., M. R. Mackey, G. Perkins, M. H. Ellisman, M. Latterich, R. Schneiter, D. R. Green and D. D. Newmeyer (2002). "Bid, Bax, and lipids cooperate to form supramolecular openings in the outer mitochondrial membrane." Cell **111**(3): 331-342.

Lacronique, V., A. Boureux, V. D. Valle, H. Poirel, C. T. Quang, M. Mauchauffe, C. Berthou, M. Lessard, R. Berger, J. Ghysdael and O. A. Bernard (1997). "A TEL-JAK2 fusion protein with constitutive kinase activity in human leukemia." Science **278**(5341): 1309-1312.

Lai, A. Y. and M. Kondo (2007). "Identification of a bone marrow precursor of the earliest thymocytes in adult mouse." Proc Natl Acad Sci U S A **104**(15): 6311-6316.

Lamb, J., E. D. Crawford, D. Peck, J. W. Modell, I. C. Blat, M. J. Wrobel, J. Lerner, J. P. Brunet, A. Subramanian, K. N. Ross, M. Reich, H. Hieronymus, G. Wei, S. A. Armstrong, S. J. Haggarty, P. A. Clemons, R. Wei, S. A. Carr, E. S. Lander and T. R. Golub (2006). "The Connectivity Map: using gene-expression signatures to connect small molecules, genes, and disease." Science **313**(5795): 1929-1935.

Lauritsen, J. P., G. W. Wong, S. Y. Lee, J. M. Lefebvre, M. Ciofani, M. Rhodes, D. J. Kappes, J. C. Zuniga-Pflucker and D. L. Wiest (2009). "Marked induction of the helix-loop-helix protein Id3 promotes the gammadelta T cell fate and renders their functional maturation Notch independent." Immunity **31**(4): 565-575.

Lee, J. B., T. E. Werbowetski-Ogilvie, J. H. Lee, B. A. McIntyre, A. Schnerch, S. H. Hong, I. H. Park, G. Q. Daley, I. D. Bernstein and M. Bhatia (2013). "Notch-HES1 signaling axis controls hemato-endothelial fate decisions of human embryonic and induced pluripotent stem cells." Blood **122**(7): 1162-1173.

Lee, S. H., H. S. Hong, Z. X. Liu, R. H. Kim, M. K. Kang, N. H. Park and K. H. Shin (2012). "TNFalpha enhances cancer stem cell-like phenotype via Notch-Hes1 activation in oral squamous cell carcinoma cells." Biochem Biophys Res Commun **424**(1): 58-64.

Lewis, H. D., M. Leveridge, P. R. Strack, C. D. Haldon, J. O'Neil, H. Kim, A. Madin, J. C. Hannam, A. T. Look, N. Kohl, G. Draetta, T. Harrison, J. A. Kerby, M. S. Shearman and D. Beher (2007). "Apoptosis in T cell acute lymphoblastic leukemia cells after cell cycle arrest induced by pharmacological inhibition of notch signaling." Chem Biol **14**(2): 209-219.

Li, J., A. M. Pauley, R. L. Myers, R. Shuang, J. R. Brashler, R. Yan, A. E. Buhl, C. Ruble and M. E. Gurney (2002). "SEL-10 interacts with presenilin 1, facilitates its ubiquitination, and alters A-beta peptide production." J Neurochem **82**(6): 1540-1548.

Lind, E. F., S. E. Prockop, H. E. Porritt and H. T. Petrie (2001). "Mapping precursor movement through the postnatal thymus reveals specific microenvironments supporting defined stages of early lymphoid development." J Exp Med **194**(2): 127-134.

Lindahl, A., A. Nilsson and O. G. Isaksson (1987). "Effects of growth hormone and insulin-like growth factor-I on colony formation of rabbit epiphyseal chondrocytes at different stages of maturation." J Endocrinol **115**(2): 263-271.

Malecki, M. J., C. Sanchez-Irizarry, J. L. Mitchell, G. Histen, M. L. Xu, J. C. Aster and S. C. Blacklow (2006). "Leukemia-associated mutations within the NOTCH1 heterodimerization domain fall into at least two distinct mechanistic classes." Mol Cell Biol **26**(12): 4642-4651.

Malyukova, A., T. Dohda, N. von der Lehr, S. Akhoondi, M. Corcoran, M. Heyman, C. Spruck, D. Grander, U. Lendahl and O. Sangfelt (2007). "The tumor suppressor gene hCDC4 is frequently mutated in human T-cell acute lymphoblastic leukemia with functional consequences for Notch signaling." Cancer Res **67**(12): 5611-5616.

Maniati, E., M. Bossard, N. Cook, J. B. Candido, N. Emami-Shahri, S. A. Nedospasov, F. R. Balkwill, D. A. Tuveson and T. Hagemann (2011). "Crosstalk between the canonical NF-kappaB and Notch signaling pathways inhibits Ppargamma expression and promotes pancreatic cancer progression in mice." J Clin Invest **121**(12): 4685-4699.

Mansson, R., A. Hultquist, S. Luc, L. Yang, K. Anderson, S. Kharazi, S. Al-Hashmi, K. Liuba, L. Thoren, J. Adolfsson, N. Buza-Vidas, H. Qian, S. Soneji, T. Enver, M. Sigvardsson and S. E. Jacobsen (2007). "Molecular evidence for hierarchical transcriptional lineage priming in fetal and adult stem cells and multipotent progenitors." Immunity **26**(4): 407-419.

Margolin, A. A., T. Palomero, P. Sumazin, A. Califano, A. A. Ferrando and G. Stolovitzky (2009). "ChIP-on-chip significance analysis reveals large-scale binding and regulation by human transcription factor oncogenes." Proc Natl Acad Sci U S A **106**(1): 244-249.

McGuire, E. A., R. D. Hockett, K. M. Pollock, M. F. Bartholdi, S. J. O'Brien and S. J. Korsmeyer (1989). "The t(11;14)(p15;q11) in a T-cell acute lymphoblastic leukemia cell line activates multiple transcripts, including Ttg-1, a gene encoding a potential zinc finger protein." Mol Cell Biol **9**(5): 2124-2132.

Meerbrey, K. L., G. Hu, J. D. Kessler, K. Roarty, M. Z. Li, J. E. Fang, J. I. Herschkowitz, A. E. Burrows, A. Ciccia, T. Sun, E. M. Schmitt, R. J. Bernardi, X. Fu, C. S. Bland, T. A. Cooper, R. Schiff, J. M. Rosen, T. F. Westbrook and S. J. Elledge (2011). "The pINDUCER lentiviral toolkit for inducible RNA interference in vitro and in vivo." Proc Natl Acad Sci U S A **108**(9): 3665-3670.

Mellentin, J. D., S. D. Smith and M. L. Cleary (1989). "lyl-1, a novel gene altered by chromosomal translocation in T cell leukemia, codes for a protein with a helix-loop-helix DNA binding motif." Cell **58**(1): 77-83.

Milano, J., J. McKay, C. Dagenais, L. Foster-Brown, F. Pognan, R. Gadient, R. T. Jacobs, A. Zacco, B. Greenberg and P. J. Ciaccio (2004). "Modulation of notch processing by gamma-secretase inhibitors causes intestinal goblet cell metaplasia and induction of genes known to specify gut secretory lineage differentiation." Toxicol Sci **82**(1): 341-358.

Moellering, R. E., M. Cornejo, T. N. Davis, C. Del Bianco, J. C. Aster, S. C. Blacklow, A. L. Kung, D. G. Gilliland, G. L. Verdine and J. E. Bradner (2009). "Direct inhibition of the NOTCH transcription factor complex." Nature **462**(7270): 182-188.

Mohty, M. and J. F. Apperley (2010). "Long-term physiological side effects after allogeneic bone marrow transplantation." Hematology Am Soc Hematol Educ Program **2010**: 229-236.

Moricke, A., M. Zimmermann, A. Reiter, G. Henze, A. Schrauder, H. Gadner, W. D. Ludwig, J. Ritter, J. Harbott, G. Mann, T. Klingebiel, F. Zintl, C. Niemeyer, B. Kremens, F. Niggli, D. Niethammer, K. Welte, M. Stanulla, E. Odenwald, H. Riehm and M. Schrappe (2010). "Long-term results of five consecutive trials in childhood acute lymphoblastic leukemia performed by the ALL-BFM study group from 1981 to 2000." Leukemia **24**(2): 265-284.

Morrison, S. J. and I. L. Weissman (1994). "The long-term repopulating subset of hematopoietic stem cells is deterministic and isolatable by phenotype." Immunity **1**(8): 661-673.

Murata, K., M. Hattori, N. Hirai, Y. Shinozuka, H. Hirata, R. Kageyama, T. Sakai and N. Minato (2005). "Hes1 directly controls cell proliferation through the transcriptional repression of p27Kip1." Mol Cell Biol **25**(10): 4262-4271.

Nachman, J. B., H. N. Sather, M. G. Sensel, M. E. Trigg, J. M. Cherlow, J. N. Lukens, L. Wolff, F. M. Uckun and P. S. Gaynon (1998). "Augmented post-induction therapy for children with high-risk acute lymphoblastic leukemia and a slow response to initial therapy." N Engl J Med **338**(23): 1663-1671.

Nagel, S., M. Kaufmann, H. G. Drexler and R. A. MacLeod (2003). "The cardiac homeobox gene NKX2-5 is deregulated by juxtaposition with BCL11B in pediatric T-ALL cell lines via a novel t(5;14)(q35.1;q32.2)." Cancer Res **63**(17): 5329-5334.

Nakashima, K., M. Yanagisawa, H. Arakawa, N. Kimura, T. Hisatsune, M. Kawabata, K. Miyazono and T. Taga (1999). "Synergistic signaling in fetal brain by STAT3-Smad1 complex bridged by p300." Science **284**(5413): 479-482.

Nateri, A. S., L. Riera-Sans, C. Da Costa and A. Behrens (2004). "The ubiquitin ligase SCFFbw7 antagonizes apoptotic JNK signaling." Science **303**(5662): 1374-1378.

Ng, S. Y., T. Yoshida, J. Zhang and K. Georgopoulos (2009). "Genome-wide lineage-specific transcriptional networks underscore Ikaros-dependent lymphoid priming in hematopoietic stem cells." Immunity **30**(4): 493-507.

Nomura, D. K., J. Z. Long, S. Niessen, H. S. Hoover, S. W. Ng and B. F. Cravatt (2010). "Monoacylglycerol lipase regulates a fatty acid network that promotes cancer pathogenesis." Cell **140**(1): 49-61.

Ntziachristos, P., A. Tsirigos, P. Van Vlierberghe, J. Nedjic, T. Trimarchi, M. S. Flaherty, D. Ferres-Marco, V. da Ros, Z. Tang, J. Siegle, P. Asp, M. Hadler, I. Rigo, K. De Keersmaecker, J. Patel, T. Huynh, F. Utro, S. Poglio, J. B. Samon, E. Paietta, J. Racevskis, J. M. Rowe, R. Rabadan, R. L. Levine, S. Brown, F. Pflumio, M. Dominguez, A. Ferrando and I. Aifantis (2012). "Genetic inactivation of the polycomb repressive complex 2 in T cell acute lymphoblastic leukemia." Nat Med **18**(2): 298-301.

O'Neil, J., J. Grim, P. Strack, S. Rao, D. Tibbitts, C. Winter, J. Hardwick, M. Welcker, J. P. Meijerink, R. Pieters, G. Draetta, R. Sears, B. E. Clurman and A. T. Look (2007). "FBW7 mutations in leukemic cells mediate NOTCH pathway activation and resistance to gamma-secretase inhibitors." J Exp Med **204**(8): 1813-1824.

Obexer, P., U. Certa, R. Kofler and A. Helmberg (2001). "Expression profiling of glucocorticoid-treated T-ALL cell lines: rapid repression of multiple genes involved in RNA-, protein- and nucleotide synthesis." Oncogene **20**(32): 4324-4336.

Ogden, C. A., J. D. Pound, B. K. Batth, S. Owens, I. Johannessen, K. Wood and C. D. Gregory (2005). "Enhanced apoptotic cell clearance capacity and B cell survival factor production by IL-10-activated macrophages: implications for Burkitt's lymphoma." J Immunol **174**(5): 3015-3023.

Ohsako, S., J. Hyer, G. Panganiban, I. Oliver and M. Caudy (1994). "Hairy function as a DNA-binding helix-loop-helix repressor of Drosophila sensory organ formation." Genes Dev **8**(22): 2743-2755.

Ohtsuka, T., M. Ishibashi, G. Gradwohl, S. Nakanishi, F. Guillemot and R. Kageyama (1999). "Hes1 and Hes5 as notch effectors in mammalian neuronal differentiation." EMBO J **18**(8): 2196-2207.

Ohtsuka, T., M. Sakamoto, F. Guillemot and R. Kageyama (2001). "Roles of the basic helix-loop-helix genes Hes1 and Hes5 in expansion of neural stem cells of the developing brain." J Biol Chem **276**(32): 30467-30474.

Orkin, S. H. and L. I. Zon (2008). "Hematopoiesis: an evolving paradigm for stem cell biology." Cell **132**(4): 631-644.

Otsubo, K., H. Kanegane, M. Eguchi, M. Eguchi-Ishimae, K. Tamura, K. Nomura, A. Abe, E. Ishii and T. Miyawaki (2010). "ETV6-ARNT fusion in a patient with childhood T lymphoblastic leukemia." Cancer Genet Cytogenet **202**(1): 22-26.

Oudot, C., M. F. Auclerc, V. Levy, R. Porcher, C. Piguet, Y. Perel, V. Gandemer, M. Debre, C. Vermylen, B. Pautard, C. Berger, C. Schmitt, T. Leblanc, J. M. Cayuela, G. Socie, G. Michel, G. Leverger and A. Baruchel (2008). "Prognostic factors for leukemic induction failure in children with acute lymphoblastic leukemia and outcome after salvage therapy: the FRALLE 93 study." J Clin Oncol **26**(9): 1496-1503.

Paganin, M. and A. Ferrando (2011). "Molecular pathogenesis and targeted therapies for NOTCH1-induced T-cell acute lymphoblastic leukemia." Blood Rev **25**(2): 83-90.

Paietta, E., A. A. Ferrando, D. Neuberg, J. M. Bennett, J. Racevskis, H. Lazarus, G. Dewald, J. M. Rowe, P. H. Wiernik, M. S. Tallman and A. T. Look (2004). "Activating FLT3 mutations in CD117/KIT(+) T-cell acute lymphoblastic leukemias." Blood **104**(2): 558-560.

Palomero, T., K. C. Barnes, P. J. Real, J. L. Glade Bender, M. L. Sulis, V. V. Murty, A. I. Colovai, M. Balbin and A. A. Ferrando (2006). "CUTLL1, a novel human T-cell lymphoma cell line with t(7;9) rearrangement, aberrant NOTCH1 activation and high sensitivity to gamma-secretase inhibitors." Leukemia **20**(7): 1279-1287.

Palomero, T., M. Dominguez and A. A. Ferrando (2008). "The role of the PTEN/AKT Pathway in NOTCH1-induced leukemia." Cell Cycle **7**(8): 965-970.

Palomero, T. and A. A. Ferrando (2009). "Genomic tools for dissecting oncogenic transcriptional networks in human leukemia." Leukemia **23**(7): 1236-1242.

Palomero, T., W. K. Lim, D. T. Odom, M. L. Sulis, P. J. Real, A. Margolin, K. C. Barnes, J. O'Neil, D. Neuberg, A. P. Weng, J. C. Aster, F. Sigaux, J. Soulier, A. T. Look, R. A. Young, A. Califano and A. A. Ferrando (2006). "NOTCH1 directly regulates c-MYC and activates a feed-forward-loop transcriptional network promoting leukemic cell growth." Proc Natl Acad Sci U S A **103**(48): 18261-18266.

Palomero, T., M. L. Sulis, M. Cortina, P. J. Real, K. Barnes, M. Ciofani, E. Caparros, J. Buteau, K. Brown, S. L. Perkins, G. Bhagat, A. M. Agarwal, G. Basso, M. Castillo, S. Nagase, C. Cordon-Cardo, R. Parsons, J. C. Zuniga-Pflucker, M. Dominguez and A. A. Ferrando (2007). "Mutational loss of PTEN induces resistance to NOTCH1 inhibition in T-cell leukemia." Nat Med **13**(10): 1203-1210.

Parekh, H., S. Advani and M. Chitnis (1990). "Bepridil enhances adriamycin-induced DNA biosynthesis inhibition in human myeloid leukemia cells." Sel Cancer Ther **6**(4): 183-191.

Parekh, H. K., J. M. Shallom, S. H. Advani and M. P. Chitnis (1991). "Response of human chronic myeloid leukemia cells to mitoxantrone cytotoxicity: potentiation by bepridil, a calcium channel antagonist." Neoplasma **38**(6): 575-581.

Parkin, J. and B. Cohen (2001). "An overview of the immune system." Lancet **357**(9270): 1777-1789.

Pearse, G. (2006). "Normal structure, function and histology of the thymus." Toxicol Pathol **34**(5): 504-514.

Peschon, J. J., P. J. Morrissey, K. H. Grabstein, F. J. Ramsdell, E. Maraskovsky, B. C. Gliniak, L. S. Park, S. F. Ziegler, D. E. Williams, C. B. Ware, J. D. Meyer and B. L. Davison (1994). "Early lymphocyte expansion is severely impaired in interleukin 7 receptor-deficient mice." J Exp Med **180**(5): 1955-1960.

Pession, A., M. G. Valsecchi, G. Masera, W. A. Kamps, E. Magyarosy, C. Rizzari, E. R. van Wering, L. Lo Nigro, A. van der Does, F. Locatelli, G. Basso and M. Arico (2005). "Long-term results of a randomized trial on extended use of high dose L-asparaginase for standard risk childhood acute lymphoblastic leukemia." J Clin Oncol **23**(28): 7161-7167.

Petrie, H. T. (2002). "Role of thymic organ structure and stromal composition in steady-state postnatal T-cell production." Immunol Rev **189**: 8-19.

Petrie, H. T. and J. C. Zuniga-Pflucker (2007). "Zoned out: functional mapping of stromal signaling microenvironments in the thymus." Annu Rev Immunol **25**: 649-679.

Porritt, H. E., K. Gordon and H. T. Petrie (2003). "Kinetics of steady-state differentiation and mapping of intrathymic-signaling environments by stem cell transplantation in nonirradiated mice." J Exp Med **198**(6): 957-962.

Pui, C. H. (2001). "Risk assessment in acute lymphoblastic leukemia: beyond leukemia cell characteristics." J Pediatr Hematol Oncol **23**(7): 405-408.

Pui, C. H. (2010). "Recent research advances in childhood acute lymphoblastic leukemia." J Formos Med Assoc **109**(11): 777-787.

Pui, C. H., D. Campana and W. E. Evans (2001). "Childhood acute lymphoblastic leukaemia--current status and future perspectives." Lancet Oncol **2**(10): 597-607.

Pui, C. H. and W. E. Evans (2006). "Treatment of acute lymphoblastic leukemia." N Engl J Med **354**(2): 166-178.

Pui, C. H. and W. E. Evans (2013). "A 50-year journey to cure childhood acute lymphoblastic leukemia." Semin Hematol **50**(3): 185-196.

Pui, C. H., D. Pei, J. T. Sandlund, R. C. Ribeiro, J. E. Rubnitz, S. C. Raimondi, M. Onciu, D. Campana, L. E. Kun, S. Jeha, C. Cheng, S. C. Howard, M. L. Metzger, D. Bhojwani, J. R. Downing, W. E. Evans and M. V. Relling (2010). "Long-term results of St Jude Total Therapy Studies 11, 12, 13A, 13B, and 14 for childhood acute lymphoblastic leukemia." Leukemia **24**(2): 371-382.

Pui, C. H., M. V. Relling and J. R. Downing (2004). "Acute lymphoblastic leukemia." N Engl J Med **350**(15): 1535-1548.

Pui, C. H., L. L. Robison and A. T. Look (2008). "Acute lymphoblastic leukaemia." Lancet **371**(9617): 1030-1043.

Pui, J. C., D. Allman, L. Xu, S. DeRocco, F. G. Karnell, S. Bakkour, J. Y. Lee, T. Kadesch, R. R. Hardy, J. C. Aster and W. S. Pear (1999). "Notch1 expression in early lymphopoiesis influences B versus T lineage determination." Immunity **11**(3): 299-308.

Radtke, F., A. Wilson, S. J. Mancini and H. R. MacDonald (2004). "Notch regulation of lymphocyte development and function." Nat Immunol **5**(3): 247-253.

Real, P. J., V. Tosello, T. Palomero, M. Castillo, E. Hernando, E. de Stanchina, M. L. Sulis, K. Barnes, C. Sawai, I. Homminga, J. Meijerink, I. Aifantis, G. Basso, C. Cordon-Cardo, W. Ai and A. Ferrando (2009). "Gamma-secretase inhibitors reverse glucocorticoid resistance in T cell acute lymphoblastic leukemia." Nat Med **15**(1): 50-58.

Reizis, B. and P. Leder (2002). "Direct induction of T lymphocyte-specific gene expression by the mammalian Notch signaling pathway." Genes Dev **16**(3): 295-300.

Richards, S., C. H. Pui, P. Gayon and G. Childhood Acute Lymphoblastic Leukemia Collaborative (2013). "Systematic review and meta-analysis of randomized trials of central nervous system directed therapy for childhood acute lymphoblastic leukemia." Pediatr Blood Cancer **60**(2): 185-195.

Roti, G. and K. Stegmaier (2014). "New Approaches to Target T-ALL." Front Oncol **4**: 170.

Royer-Pokora, B., U. Loos and W. D. Ludwig (1991). "TTG-2, a new gene encoding a cysteine-rich protein with the LIM motif, is overexpressed in acute T-cell leukaemia with the t(11;14)(p13;q11)." Oncogene **6**(10): 1887-1893.

Rubnitz, J. E., F. G. Behm, A. M. Curcio-Brint, R. P. Pinheiro, A. J. Carroll, S. C. Raimondi, S. A. Shurtleff and J. R. Downing (1996). "Molecular analysis of t(11;19) breakpoints in childhood acute leukemias." Blood **87**(11): 4804-4808.

Rubnitz, J. E., B. M. Camitta, H. Mahmoud, S. C. Raimondi, A. J. Carroll, M. J. Borowitz, J. J. Shuster, M. P. Link, D. J. Pullen, J. R. Downing, F. G. Behm and C. H. Pui (1999). "Childhood acute lymphoblastic leukemia with the MLL-ENL fusion and t(11;19)(q23;p13.3) translocation." J Clin Oncol **17**(1): 191-196.

Sade, H., S. Krishna and A. Sarin (2004). "The anti-apoptotic effect of Notch-1 requires p56lck-dependent, Akt/PKB-mediated signaling in T cells." J Biol Chem **279**(4): 2937-2944.

Sallusto, F., D. Lenig, R. Forster, M. Lipp and A. Lanzavecchia (1999). "Two subsets of memory T lymphocytes with distinct homing potentials and effector functions." Nature **401**(6754): 708-712.

Samudio, I., R. Harmancey, M. Fiegl, H. Kantarjian, M. Konopleva, B. Korchin, K. Kaluarachchi, W. Bornmann, S. Duvvuri, H. Taegtmeyer and M. Andreeff (2010). "Pharmacologic inhibition of fatty acid oxidation sensitizes human leukemia cells to apoptosis induction." J Clin Invest **120**(1): 142-156.

Sander, J. D. and J. K. Joung (2014). "CRISPR-Cas systems for editing, regulating and targeting genomes." Nat Biotechnol **32**(4): 347-355.

Sang, L., H. A. Coller and J. M. Roberts (2008). "Control of the reversibility of cellular quiescence by the transcriptional repressor HES1." Science **321**(5892): 1095-1100.

Sang, L., J. M. Roberts and H. A. Coller (2010). "Hijacking HES1: how tumors co-opt the anti-differentiation strategies of quiescent cells." Trends Mol Med **16**(1): 17-26.

Sasai, Y., R. Kageyama, Y. Tagawa, R. Shigemoto and S. Nakanishi (1992). "Two mammalian helix-loop-helix factors structurally related to Drosophila hairy and Enhancer of split." Genes Dev **6**(12B): 2620-2634.

Schatz, D. G., M. A. Oettinger and M. S. Schlissel (1992). "V(D)J recombination: molecular biology and regulation." Annu Rev Immunol **10**: 359-383.

Schmitt, T. M., M. Ciofani, H. T. Petrie and J. C. Zuniga-Pflucker (2004). "Maintenance of T cell specification and differentiation requires recurrent notch receptor-ligand interactions." J Exp Med **200**(4): 469-479.

Shah, D. K. and J. C. Zuniga-Pflucker (2014). "An overview of the intrathymic intricacies of T cell development." J Immunol **192**(9): 4017-4023.

Shima, E. A., M. M. Le Beau, T. W. McKeithan, J. Minowada, L. C. Showe, T. W. Mak, M. D. Minden, J. D. Rowley and M. O. Diaz (1986). "Gene encoding the alpha chain of the T-cell receptor is moved immediately downstream of c-myc in a chromosomal 8;14 translocation in a cell line from a human T-cell leukemia." Proc Natl Acad Sci U S A **83**(10): 3439-3443.

Shin, H. M., L. M. Minter, O. H. Cho, S. Gottipati, A. H. Fauq, T. E. Golde, G. E. Sonenshein and B. A. Osborne (2006). "Notch1 augments NF-kappaB activity by facilitating its nuclear retention." EMBO J **25**(1): 129-138.

Sicinska, E., I. Aifantis, L. Le Cam, W. Swat, C. Borowski, Q. Yu, A. A. Ferrando, S. D. Levin, Y. Geng, H. von Boehmer and P. Sicinski (2003). "Requirement for cyclin D3 in lymphocyte development and T cell leukemias." Cancer Cell **4**(6): 451-461.

Silverman, L. B., L. Declerck, R. D. Gelber, V. K. Dalton, B. L. Asselin, R. D. Barr, L. A. Clavell, C. A. Hurwitz, A. Moghrabi, Y. Samson, M. A. Schorin, J. M. Lipton, H. J. Cohen and S. E. Sallan (2000). "Results of Dana-Farber Cancer Institute Consortium protocols for children with newly diagnosed acute lymphoblastic leukemia (1981-1995)." Leukemia **14**(12): 2247-2256.

Silverman, L. B., R. D. Gelber, V. K. Dalton, B. L. Asselin, R. D. Barr, L. A. Clavell, C. A. Hurwitz, A. Moghrabi, Y. Samson, M. A. Schorin, S. Arkin, L. Declerck, H. J. Cohen and S. E. Sallan (2001). "Improved outcome for children with acute lymphoblastic leukemia: results of Dana-Farber Consortium Protocol 91-01." Blood **97**(5): 1211-1218.

Silverman, L. B., K. E. Stevenson, J. E. O'Brien, B. L. Asselin, R. D. Barr, L. Clavell, P. D. Cole, K. M. Kelly, C. Laverdiere, B. Michon, M. A. Schorin, C. L. Schwartz, E. W. O'Holleran, D. S. Neuberg, H. J. Cohen and S. E. Sallan (2010). "Long-term results of Dana-Farber Cancer Institute ALL Consortium protocols for children with newly diagnosed acute lymphoblastic leukemia (1985-2000)." Leukemia **24**(2): 320-334.

Simon, C., J. Chagraoui, J. Krosl, P. Gendron, B. Wilhelm, S. Lemieux, G. Boucher, P. Chagnon, S. Drouin, R. Lambert, C. Rondeau, A. Bilodeau, S. Lavallee, M. Sauvageau, J. Hebert and G. Sauvageau (2012). "A key role for EZH2 and associated genes in mouse and human adult T-cell acute leukemia." Genes Dev **26**(7): 651-656.

Sitnicka, E. (2009). "From the bone marrow to the thymus: the road map of early stages of T-cell development." Crit Rev Immunol **29**(6): 487-530.

Soulier, J., E. Clappier, J. M. Cayuela, A. Regnault, M. Garcia-Peydro, H. Dombret, A. Baruchel, M. L. Toribio and F. Sigaux (2005). "HOXA genes are included in genetic and biologic networks defining human acute T-cell leukemia (T-ALL)." Blood **106**(1): 274-286.

Spangrude, G. J. and R. Scollay (1990). "Differentiation of hematopoietic stem cells in irradiated mouse thymic lobes. Kinetics and phenotype of progeny." J Immunol **145**(11): 3661-3668.

Subramanian, A., P. Tamayo, V. K. Mootha, S. Mukherjee, B. L. Ebert, M. A. Gillette, A. Paulovich, S. L. Pomeroy, T. R. Golub, E. S. Lander and J. P. Mesirov (2005). "Gene set enrichment analysis: a knowledge-based approach for interpreting genome-wide expression profiles." Proc Natl Acad Sci U S A **102**(43): 15545-15550.

Sulis, M. L., O. Williams, T. Palomero, V. Tosello, S. Pallikuppam, P. J. Real, K. Barnes, L. Zuurbier, J. P. Meijerink and A. A. Ferrando (2008). "NOTCH1 extracellular juxtamembrane expansion mutations in T-ALL." Blood **112**(3): 733-740.

Sundqvist, A., M. T. Bengoechea-Alonso, X. Ye, V. Lukiyanchuk, J. Jin, J. W. Harper and J. Ericsson (2005). "Control of lipid metabolism by phosphorylation-dependent degradation of the SREBP family of transcription factors by SCF(Fbw7)." Cell Metab **1**(6): 379-391.

Surh, C. D. and J. Sprent (1994). "T-cell apoptosis detected in situ during positive and negative selection in the thymus." Nature **372**(6501): 100-103.

Swain, S. L., L. M. Bradley, M. Croft, S. Tonkonogy, G. Atkins, A. D. Weinberg, D. D. Duncan, S. M. Hedrick, R. W. Dutton and G. Huston (1991). "Helper T-cell subsets: phenotype, function and the role of lymphokines in regulating their development." Immunol Rev **123**: 115-144.

Taelman, V., R. Van Wayenbergh, M. Solter, B. Pichon, T. Pieler, D. Christophe and E. J. Bellefroid (2004). "Sequences downstream of the bHLH domain of the Xenopus hairy-related transcription factor-1 act as an extended dimerization domain that contributes to the selection of the partners." Dev Biol **276**(1): 47-63.

Takatsuka, K., J. Hatakeyama, Y. Bessho and R. Kageyama (2004). "Roles of the bHLH gene Hes1 in retinal morphogenesis." Brain Res **1004**(1-2): 148-155.

Tan, M., Y. Zhao, S. J. Kim, M. Liu, L. Jia, T. L. Saunders, Y. Zhu and Y. Sun (2011). "SAG/RBX2/ROC2 E3 ubiquitin ligase is essential for vascular and neural development by targeting NF1 for degradation." Dev Cell **21**(6): 1062-1076.

Tanigaki, K. and T. Honjo (2007). "Regulation of lymphocyte development by Notch signaling." Nat Immunol **8**(5): 451-456.

Tarantola, A., I. Quatresous, M. Ledrans, L. Lassel, E. Krastinova, H. Cordel, N. Lapidus, M. Debruyne, J. D. Poveda, M. Boude-Chevalier, I. Schuffenecker, H. Zeller, M. Grandadam, H. Tolou and C. Paquet (2009). "[Imported cases of dengue fever diagnosed in metropolitan France, from January 2001 to December 2006]." Med Mal Infect **39**(1): 41-47.

Thomas, X., J. M. Boiron, F. Huguet, H. Dombret, K. Bradstock, N. Vey, T. Kovacsovics, A. Delannoy, N. Fegueux, P. Fenaux, A. Stamatoullas, J. P. Vernant, O. Tournilhac, A. Buzyn, O. Reman, C. Charrin, C. Boucheix, J. Gabert, V. Lheritier and D. Fiere (2004). "Outcome of treatment in adults with acute lymphoblastic leukemia: analysis of the LALA-94 trial." J Clin Oncol **22**(20): 4075-4086.

Thompson, B. J., S. Buonamici, M. L. Sulis, T. Palomero, T. Vilimas, G. Basso, A. Ferrando and I. Aifantis (2007). "The SCFFBW7 ubiquitin ligase complex as a tumor suppressor in T cell leukemia." J Exp Med **204**(8): 1825-1835.

Tomita, K., M. Hattori, E. Nakamura, S. Nakanishi, N. Minato and R. Kageyama (1999). "The bHLH gene Hes1 is essential for expansion of early T cell precursors." Genes Dev **13**(9): 1203-1210.

Tomita, K., K. Moriyoshi, S. Nakanishi, F. Guillemot and R. Kageyama (2000). "Mammalian achaete-scute and atonal homologs regulate neuronal versus glial fate determination in the central nervous system." EMBO J **19**(20): 5460-5472.

Tosello, V., M. R. Mansour, K. Barnes, M. Paganin, M. L. Sulis, S. Jenkinson, C. G. Allen, R. E. Gale, D. C. Linch, T. Palomero, P. Real, V. Murty, X. Yao, S. M. Richards, A. Goldstone, J. Rowe, G. Basso, P. H. Wiernik, E. Paietta, R. Pieters, M. Horstmann, J. P. Meijerink and A. A. Ferrando (2009). "WT1 mutations in T-ALL." Blood **114**(5): 1038-1045.

Tremblay, C. S., F. F. Huang, O. Habi, C. C. Huard, C. Godin, G. Levesque and M. Carreau (2008). "HES1 is a novel interactor of the Fanconi anemia core complex." Blood **112**(5): 2062-2070.

Tycko, B., S. D. Smith and J. Sklar (1991). "Chromosomal translocations joining LCK and TCRB loci in human T cell leukemia." J Exp Med **174**(4): 867-873.

Van der Velden, V. H., L. Corral, M. G. Valsecchi, M. W. Jansen, P. De Lorenzo, G. Cazzaniga, E. R. Panzer-Grumayer, M. Schrappe, A. Schrauder, C. Meyer, R. Marschalek, L. L. Nigro, M. Metzler, G. Basso, G. Mann, M. L. Den Boer, A. Biondi, R. Pieters, J. J. Van Dongen and G. Interfant-99 Study (2009). "Prognostic significance of minimal residual disease in infants with acute lymphoblastic leukemia treated within the Interfant-99 protocol." Leukemia **23**(6): 1073-1079.

van Es, J. H., M. E. van Gijn, O. Riccio, M. van den Born, M. Vooijs, H. Begthel, M. Cozijnsen, S. Robine, D. J. Winton, F. Radtke and H. Clevers (2005). "Notch/gamma-secretase inhibition turns proliferative cells in intestinal crypts and adenomas into goblet cells." Nature **435**(7044): 959-963.

Van Limbergen, H., H. B. Beverloo, E. van Drunen, A. Janssens, K. Hahlen, B. Poppe, N. Van Roy, P. Marynen, A. De Paepe, R. Slater and F. Speleman (2001). "Molecular cytogenetic and clinical findings in ETV6/ABL1-positive leukemia." Genes Chromosomes Cancer **30**(3): 274-282.

Van Vlierberghe, P. and A. Ferrando (2012). "The molecular basis of T cell acute lymphoblastic leukemia." J Clin Invest **122**(10): 3398-3406.

Van Vlierberghe, P., J. P. Meijerink, R. W. Stam, W. van der Smissen, E. R. van Wering, H. B. Beverloo and R. Pieters (2005). "Activating FLT3 mutations in CD4+/CD8- pediatric T-cell acute lymphoblastic leukemias." Blood **106**(13): 4414-4415.

Van Vlierberghe, P., T. Palomero, H. Khiabanian, J. Van der Meulen, M. Castillo, N. Van Roy, B. De Moerloose, J. Philippe, S. Gonzalez-Garcia, M. L. Toribio, T. Taghon, L. Zuurbier, B. Cauwelier, C. J. Harrison, C. Schwab, M. Pisecker, S. Strehl, A. W. Langerak, J. Gecz, E. Sonneveld, R. Pieters, E. Paietta, J. M. Rowe, P. H. Wiernik, Y. Benoit, J. Soulier, B. Poppe, X. Yao, C. Cordon-Cardo, J. Meijerink, R. Rabadan, F. Speleman and A. Ferrando (2010). "PHF6 mutations in T-cell acute lymphoblastic leukemia." Nat Genet **42**(4): 338-342.

Van Vlierberghe, P., M. van Grotel, H. B. Beverloo, C. Lee, T. Helgason, J. Buijs-Gladdines, M. Passier, E. R. van Wering, A. J. Veerman, W. A. Kamps, J. P. Meijerink and R. Pieters (2006). "The cryptic chromosomal deletion del(11)(p12p13) as a new activation mechanism of LMO2 in pediatric T-cell acute lymphoblastic leukemia." Blood **108**(10): 3520-3529.

Van Vlierberghe, P., M. van Grotel, J. Tchinda, C. Lee, H. B. Beverloo, P. J. van der Spek, A. Stubbs, J. Cools, K. Nagata, M. Fornerod, J. Buijs-Gladdines, M. Horstmann, E. R. van Wering, J. Soulier, R. Pieters and J. P. Meijerink (2008). "The recurrent SET-NUP214 fusion as a new HOXA activation mechanism in pediatric T-cell acute lymphoblastic leukemia." Blood **111**(9): 4668-4680.

Vander Heiden, M. G., J. W. Locasale, K. D. Swanson, H. Sharfi, G. J. Heffron, D. Amador-Noguez, H. R. Christofk, G. Wagner, J. D. Rabinowitz, J. M. Asara and L. C. Cantley (2010). "Evidence for an alternative glycolytic pathway in rapidly proliferating cells." Science **329**(5998): 1492-1499.

Vermes, I., C. Haanen, H. Steffens-Nakken and C. Reutelingsperger (1995). "A novel assay for apoptosis. Flow cytometric detection of phosphatidylserine expression on early apoptotic cells using fluorescein labelled Annexin V." J Immunol Methods **184**(1): 39-51.

von Boehmer, H. (2005). "Unique features of the pre-T-cell receptor alpha-chain: not just a surrogate." Nat Rev Immunol **5**(7): 571-577.

von Freeden-Jeffry, U., P. Vieira, L. A. Lucian, T. McNeil, S. E. Burdach and R. Murray (1995). "Lymphopenia in interleukin (IL)-7 gene-deleted mice identifies IL-7 as a nonredundant cytokine." J Exp Med **181**(4): 1519-1526.

Wada, H., K. Masuda, R. Satoh, K. Kakugawa, T. Ikawa, Y. Katsura and H. Kawamoto (2008). "Adult T-cell progenitors retain myeloid potential." Nature **452**(7188): 768-772.

Wang, J., S. N. Jani-Sait, E. A. Escalon, A. J. Carroll, P. J. de Jong, I. R. Kirsch and P. D. Aplan (2000). "The t(14;21)(q11.2;q22) chromosomal translocation associated with T-cell acute lymphoblastic leukemia activates the BHLHB1 gene." Proc Natl Acad Sci U S A **97**(7): 3497-3502.

Weerkamp, F., M. R. Baert, B. A. Naber, E. E. Koster, E. F. de Haas, K. R. Atkuri, J. J. van Dongen, L. A. Herzenberg and F. J. Staal (2006). "Wnt signaling in the thymus is regulated by differential expression of intracellular signaling molecules." Proc Natl Acad Sci U S A **103**(9): 3322-3326.

Welcker, M. and B. E. Clurman (2008). "FBW7 ubiquitin ligase: a tumour suppressor at the crossroads of cell division, growth and differentiation." Nat Rev Cancer **8**(2): 83-93.

Wendorff, A. A., U. Koch, F. T. Wunderlich, S. Wirth, C. Dubey, J. C. Bruning, H. R. MacDonald and F. Radtke (2010). "Hes1 is a critical but context-dependent mediator of canonical Notch signaling in lymphocyte development and transformation." Immunity **33**(5): 671-684.

Weng, A. P., A. A. Ferrando, W. Lee, J. P. t. Morris, L. B. Silverman, C. Sanchez-Irizarry, S. C. Blacklow, A. T. Look and J. C. Aster (2004). "Activating mutations of NOTCH1 in human T cell acute lymphoblastic leukemia." Science **306**(5694): 269-271.

Wilson, A., H. R. MacDonald and F. Radtke (2001). "Notch 1-deficient common lymphoid precursors adopt a B cell fate in the thymus." J Exp Med **194**(7): 1003-1012.

Wong, G. W., G. C. Knowles, T. W. Mak, A. A. Ferrando and J. C. Zuniga-Pflucker (2012). "HES1 opposes a PTEN-dependent check on survival, differentiation, and proliferation of TCRbeta-selected mouse thymocytes." Blood **120**(7): 1439-1448.

Wu, Y., C. Cain-Hom, L. Choy, T. J. Hagenbeek, G. P. de Leon, Y. Chen, D. Finkle, R. Venook, X. Wu, J. Ridgway, D. Schahin-Reed, G. J. Dow, A. Shelton, S. Stawicki, R. J. Watts, J. Zhang, R. Choy, P. Howard, L. Kadyk, M. Yan, J. Zha, C. A. Callahan, S. G. Hymowitz and C. W. Siebel (2010). "Therapeutic antibody targeting of individual Notch receptors." Nature **464**(7291): 1052-1057.

Xia, Y., L. Brown, C. Y. Yang, J. T. Tsan, M. J. Siciliano, R. Espinosa, III, M. M. Le Beau and R. J. Baer (1991). "TAL2, a helix-loop-helix gene activated by the (7;9)(q34;q32) translocation in human T-cell leukemia." Proc Natl Acad Sci U S A **88**(24): 11416-11420.

Yamashita, M., R. Shinnakasu, H. Asou, M. Kimura, A. Hasegawa, K. Hashimoto, N. Hatano, M. Ogata and T. Nakayama (2005). "Ras-ERK MAPK cascade regulates GATA3 stability and Th2 differentiation through ubiquitin-proteasome pathway." J Biol Chem **280**(33): 29409-29419.

Yang, Q., J. Jeremiah Bell and A. Bhandoola (2010). "T-cell lineage determination." Immunol Rev **238**(1): 12-22.

Zhang, G., V. Gurtu, S. R. Kain and G. Yan (1997). "Early detection of apoptosis using a fluorescent conjugate of annexin V." Biotechniques **23**(3): 525-531.

Zhang, J., L. Ding, L. Holmfeldt, G. Wu, S. L. Heatley, D. Payne-Turner, J. Easton, X. Chen, J. Wang, M. Rusch, C. Lu, S. C. Chen, L. Wei, J. R. Collins-Underwood, J. Ma, K. G. Roberts, S. B. Pounds, A. Ulyanov, J. Becksfort, P. Gupta, R. Huether, R. W. Kriwacki, M. Parker, D. J. McGoldrick, D. Zhao, D. Alford, S. Espy, K. C. Bobba, G. Song, D. Pei, C. Cheng, S. Roberts, M. I. Barbato, D. Campana, E. Coustan-Smith, S. A. Shurtleff, S. C. Raimondi, M. Kleppe, J. Cools, K. A. Shimano, M. L. Hermiston, S. Doulatov, K. Eppert, E. Laurenti, F. Notta, J. E. Dick, G. Basso, S. P. Hunger, M. L. Loh, M. Devidas, B. Wood, S. Winter, K. P. Dunsmore, R. S. Fulton, L. L. Fulton, X. Hong, C. C. Harris, D. J. Dooling, K. Ochoa, K. J. Johnson, J. C. Obenauer, W. E. Evans, C. H. Pui, C. W. Naeve, T. J. Ley, E. R. Mardis, R. K. Wilson, J. R. Downing and C. G. Mullighan (2012). "The genetic basis of early T-cell precursor acute lymphoblastic leukaemia." Nature **481**(7380): 157-163.

Zhang, L., Z. Yang, A. Ma, Y. Qu, S. Xia, D. Xu, C. Ge, B. Qiu, Q. Xia, J. Li and Y. Liu (2014). "Growth arrest and DNA damage 45G down-regulation contributes to Janus kinase/signal transducer and activator of transcription 3 activation and cellular senescence evasion in hepatocellular carcinoma." Hepatology **59**(1): 178-189.

Zhang, N., H. Hartig, I. Dzhagalov, D. Draper and Y. W. He (2005). "The role of apoptosis in the development and function of T lymphocytes." Cell Res **15**(10): 749-769.

Zuurbier, L., I. Homminga, V. Calvert, M. L. te Winkel, J. G. Buijs-Gladdines, C. Kooi, W. K. Smits, E. Sonneveld, A. J. Veerman, W. A. Kamps, M. Horstmann, E. F. Petricoin, 3rd, R. Pieters and J. P. Meijerink (2010). "NOTCH1 and/or FBXW7 mutations predict for initial good prednisone response but not for improved outcome in pediatric T-cell acute lymphoblastic leukemia patients treated on DCOG or COALL protocols." Leukemia **24**(12): 2014-2022.